THE PHYSICO-CHEMICAL INVESTIGATION OF INTERFACIAL PROPERTIES IN NATURAL FIBER/VINYL ESTER BIOCOMPOSITES

A Dissertation
Submitted to the Graduate Faculty
of the
North Dakota State University
of Agriculture and Applied Science

By

Shanshan Huo

In Partial Fulfillment of the Requirements
for the Degree of
DOCTOR OF PHILOSOPHY

Major Program:
Mechanical Engineering

March 2012

Fargo, North Dakota

North Dakota State University
Graduate School

Title

The Physico-chemical Investigation of Interfacial Properties in

Natural Fiber/Vinyl Ester Biocomposites

By

Shanshan Huo

The Supervisory Committee certifies that this ***disquisition*** complies with North Dakota State University's regulations and meets the accepted standards for the degree of

DOCTOR OF PHILOSOPHY

SUPERVISORY COMMITTEE:

Dr. Chad A. Ulven

Chair

Dr. Ghodrat Karami

Dr. Xinnan Wang

Dr. Dean C. Webster

Approved:

04/30/2012

Date

Dr. Alan R. Kallmeyer

Department Chair

ABSTRACT

Bast fibers are one of most widely used types of cellulosic natural fibers. Flax fibers, a specific type of bast fiber, have historically been used as reinforcements in composites because they offer competitive advantages, including environmental and economic benefits, over mineral-based reinforcing materials. However, the poor interfacial properties due to the hydrophilicity of flax fibers and the hydrophobicity of most polymer matrices reduce the mechanical performance of flax thermoset composites. On the other hand, the structure of flax fiber is more complex than synthetic fibers, which causes most of traditional mechanical tests from the transverse direction to evaluate the interfacial properties of flax composites are not valid. In this study, the physical and chemical properties of flax fibers, vinyl ester resin and their composites are investigated. A comprehensive understanding of flax fiber, vinyl ester systems and their composites has been established.

Surface modifications to the flax fiber and chemical manipulations on vinyl ester systems have been studied to improve the interfacial properties of flax/vinyl ester biocomposites. A new chemical manipulation method for vinyl ester system has been invented. The specific interlaminar shear strength of alkaline treated flax/VE with 1.5% AR shows approximately 149% increase than untreated flax/VE composites. NaOH/Ethanol treated flax/VE with AR shows 33% higher in specific flexural modulus and 73% better in specific flexural strength than untreated flax/VE composites. In addition, AR modified alkaline treated flax composites performs approximately 75% better in specific tensile modulus and 201% higher in specific tensile strength than untreated flax/VE composites. Flax/VE composite with high elastic modulus, which is higher than their theoretically predicted elastic modulus, was achieved. The effects of thermal properties of flax fibers and vinyl ester resin systems on the interfacial properties of their biocomposites were also studied. The theory of modifying the thermal properties of flax and vinyl ester to improve the

interfacial adhesion has been proved by the study of the thermal residual stresses in their composites by XRD techniques.

ACKNOWLEDGEMENTS

I joined NDSU in August of 2007. With immense gratitude I would like to thank all the people with whom I spent the past five years.

I sincerely thank my wonderful advisor—Dr. Chad A. Ulven—one of the most important people in my life. He accepted my will to work in his group. He supported me constantly as much as he could in research and always encouraged me to be confident. I really wish that I could create the words that no one else used before to express my greatest thanks to him.

I would like to thank my other committee members, Dr. Ghodrat Karami, Dr. Xinnan Wang, and Dr. Dean C. Webster, for their assistance, guidance and time contributions to this committee, and efforts for reading and advising this dissertation.

I must thank Dr. Micheal A. Fuqua, who was working with me closely in Dr. Ulven's composite group. He helped me a lot in both courses' study and research work. I also thank all the members in this composite group. I appreciate the receiving, giving and sharing in this team, no matter of just some random thoughts, which might initiate a new idea. I would like to thank Dr. Angel Ugrinov for helping me in XRD measurements. Special thanks must be given to Dr. Danny E. Akin and Dr. David S. Himmelsbach. I learned so much from them not only about knowledge, but about how to be a good researcher.

I would like to dedicate this doctoral dissertation to my parents: Xiaodong Huo and Ruihua Lan. It would be doubtful that I could complete this process without their constant love, understanding, and support. The honor of this successful completion of my Ph.D. not only belongs to me, but also belongs to both of you.

TABLE OF CONTENTS

LIST OF TABLES

LIST OF FIGURES

Figure Page

LIST OF APPENDIX TABLES

LIST OF APPENDIX FIGURES

CHAPTER 1. INTRODUCTION

Bast fibers as reinforcements in polymer matrix composites offer a competitive advantage in terms of specific mechanical properties and the potential of biodegradability after service life over mineral-based reinforcing materials, e.g. glass fibers. Interest in using cellulosic fibers as reinforcements in biocomposites is increasing as these types of fibers are being extensively utilized in many automotive applications, including door panels, seat backs, interior dash and trim components as well as underbody shields and covers. The idea of using bast fibers composites in automotive industry is not a new one. In 1941, Henry Ford introduced the first composites in vehicles using hemp and wheat straw fibers as reinforcements. Since then different types of natural fibers have been utilized in many others industries, including garden furniture, consumer industry, aeronautic industry, and so on. BMW Group incorporated approximate 10,000 tons of natural fibers into its vehicles in 2004 [1]. The consumption of the natural fibers composites in European Union was more than 300,000 tons within automotive, construction, furniture, E-mobile, and consumer industries in 2010 [2], which is three-fold times than the prediction in 2005 [3]. Their use has been influenced by several eco-design factors, such as increased environmental and health concerns, social and economic impacts, which can reduce the energy consumption and support a desire for lighter-weight structures [4].

Natural fiber reinforced composites offer many environmental and economic benefits as compared to synthetic fibers. However, there are several questions which should be well studied before the natural fibers composites can be widely accepted. It is imperative to fully understand the controllability of the fibers' properties, the processing technology, the interfacial properties between fibers and matrix, moisture stability and flame retardant properties of the composites, and so on.

1.1. Importance of Interface in Composites

The interface between a reinforcing fiber and matrix is depicted in Fig. 1.1 (a). In the interface region, the interaction between fibers and matrices can be chemical, mechanical (interlocking), physical (van der Waals bond) or the combination thereof [5]. Interfacial properties dedicate the mechanical performance of polymer composites and therefore play an essential role. In a composite, loads are applied to the matrix and transferred to the fibers through both the ends of fiber and the cylindrical surface of the fiber (Fig. 1.1 (b)) [6]. The interfacial adhesion between the fiber and the matrix determines the quality of load transfer in a composite. Therefore, a better interfacial bonding indicates a composite will possess better mechanical properties, such as interlaminar shear strength, delamination resistance, fatigue and corrosion resistance.

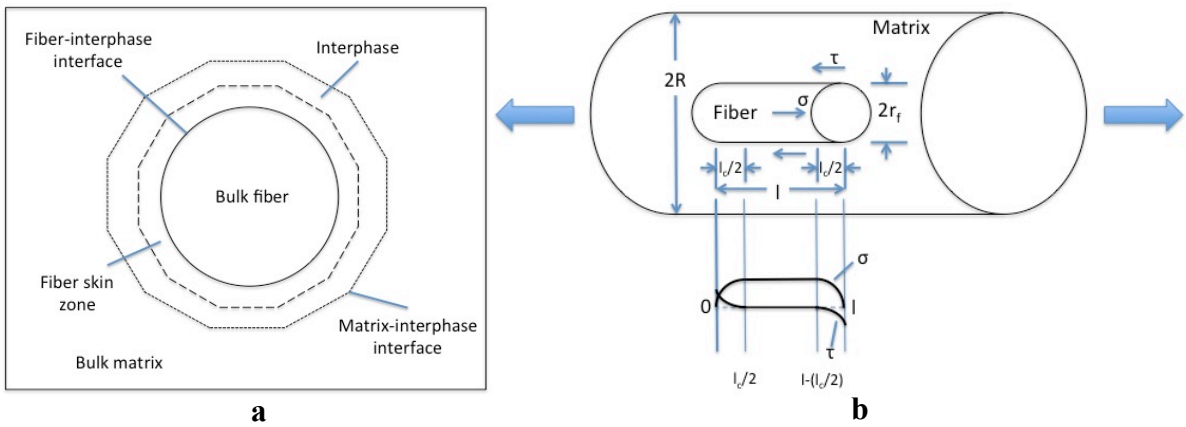

Figure 1.1 Interface in a composite (a) [5] and the tensile load transfer in the interface (b) [6].

There are several experimental methods which can be investigated to evaluate interfacial shear strength, interfacial tensile strength, debonding energy, frictional forces, the degree of interfacial adhesion and the bonding condition. These mechanical tests include fiber pull-out, fiber push-out, critical fiber length, short beam shear, fiber indentation, micro-debonding, transverse tension, polarized light microscopy and dynamic mechanical analysis [5]. Most of the mechanical tests to assess the interfacial properties are based on synthetic fiber reinforced composites, where the structure and geometry of the synthetic fibers are

uniform. However, there are significant differences in structure, geometry and constituents between synthetic fibers and natural fibers. Natural fibers have very complex structure which contain several types of natural polymer and are considered to be naturally occurring composites themselves. There are several interfaces which exist inside a natural fiber and some of the traditional mechanical tests for measuring the interfacial properties actually evaluate the combined results from both the interface in the composite and the interface inside the fiber, such as transverse tension. Thus in this study, only basic mechanical tests will be investigated, including short beam shear and fiber bundle pull-out, to assess the interfacial properties of flax composites. In addition, tensile and flexural tests in longitudinal direction will be used to evaluate the efficiency of load transfer inside the flax composites and to evaluate whether any of the treatments used to improve interfacial properties have an adverse effect on these general mechanical properties.

On the other hand, the surface properties of reinforcing fibers do show strong effects on the interfacial properties of the composites. Therefore, different surface treatments have been well studied in synthetic fibers in the past to improve the interfacial properties of their composites. The techniques traditionally used to characterize the fiber surface are used to predict the interfacial adhesion between fibers and matrices. These experimental methods include electron spectroscopy for chemical analysis (ESCA), X-ray photoelectron spectroscopy (XPS), Fourier transform infrared analysis (FTIR), dynamic contact angles, scanning tunneling microscopy (STM), scanning electron microscopy (SEM) and thermal desorption [5]. In this study, different surface modifications on flax fibers and matrix manipulations are investigated to improve the interfacial adhesion between flax and vinyl ester (VE) matrix. In addition, the effects of thermal residual stresses on the interfacial properties of the flax composites are evaluated by X-ray diffraction (XRD) assisted with aluminum powders.

1.2. Flax Fiber as the Reinforcement

Bast fibers are one of the major types of cellulosic fibers, which have a long and storied past. The earliest usage of bast fibers was 30,000 years ago in Upper Paleolithic Age [7]. Prehistoric hunter-gatherers twisted wild flax fibers and made cords to haft stone tools, weave baskets, or sew garments. Bast fibers have been widely used in textiles thousands of years ago in Egypt and China.

Flax grown for fiber (linen) and grown for seed oil (linseed) has been planted in temperate regions, such as Netherlands, France, Spain, Russia, Belgium, China, India, Argentina, Canada, and United States. Linen flax is the oldest textile known and an important rule for the modern textile industry. The Flax Council of Canada (FCC) website provides comprehensive details of linseed flax. The plant can grow between 80 and 150 cm in about 80 to 110 days, of which 75% of the plant's height can be used to produce fiber [3]. The physical properties of flax fibers are related to the components and internal structure of fibers.

1.2.1. Structure of Flax Fibers

A flax fiber consists of 70-85% cellulose, 11-20% hemicelluloses, 2-12% pectin, and about 2% lignin [8,9] with several minor extractives, such as fat, wax, protein, tannins, dyes, inorganic salts, etc. These constituents vary depending on the source of the fibers, growing conditions, plant age, and digestion processes [10]. The content of cellulose governs the properties of the fibers and dictates the performance of their composites. The non-cellulosic components are all amorphous polymers and reduce the strength and modulus of the cellulosic fibers [11]. Moreover, these constituents show a negative influence on cellulosic fiber reinforced composites.

Cellulose is a linear hydrophilic glucan polymer of D-glucopyranose units (Fig. 1.2), which are linked together by β-(1-4)-glucosidic bonds [12]. A large amount of hydroxyl

groups are attached on the aromatic rings, which cause cellulose to be hydrophilic. The existance of OH groups in cellulose also leads to plenty of hydrogen bonds. Due to these hydrogen bonds and van der Waals forces, part of the cellulose molecules align together, highly ordered, and form crystalline regions. Meanwhile, the rest of molecules with a less ordered arrangement constitute the amorphous part. The superamolecular structure of cellulose determines its chemical and physical properties. The degree of polymerization (DP) is the key factor, which varies with the type of natural fiber: ramie has 6500 DP; cotton has 7000 DP; flax has 8000 DP [10]. There are two forms cellulose existing in nature (cellulose I): cellulose I_α and celloluse I_β [13]. Cellulose I_α only exists in some green algae [14,15] and cellulose I_β exists in various species from plants to animals. Cellulose in different plant fibers has the same structure: cellulose I_β. Cellulose I_β crystallizes in monoclinic sphenodic structures with two chains in a parallel fashion [16,17]. Cellulose I can be transformed into cellulose II, cellulose III, or cellulose IV by different chemical or thermal treatments. In addition, these different forms of cellulose can be transformed back to cellulose I by treatments. Cellulose II is also a monoclinic structure, but its two chains are arranged in an antiparallel fashion. Cellulose II is more thermal stable than cellulose I [18]. However, cellulose I shows better mechanical properties.

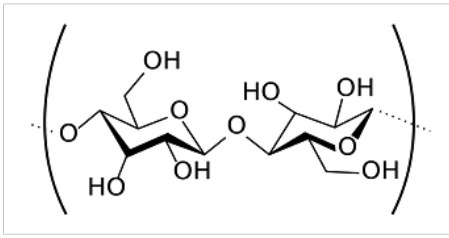

Figure 1.2 The molecular structure of cellulose.

Flax fibers are actually fiber bundles, which are complied by several single fibers. A single fiber (elementary fiber) can be considered as hollow composites: cellulose fibrils are the reinforcements; hemicellulose, lignin, and other amorphous components are matrices to

hold these fibrils together. There are several distinct layers in a single fiber (Fig. 1.3) [19] the center lumen, secondary wall (S3, S2, and S1), and primary wall from inside to outside. The primary wall is the first layer deposited containing hemicelluloses and cellulose during the cell growth encircling the secondary walls [20]. The secondary cell wall consists mainly of helically wound cellulose microfibrils. These microfibrils are made up of 30 to 100 cellulose molecules, with a diameter of about 10-30 nm, and provide mechanical strength to the fiber. S2 layer is thicker than S1 and S3 layers and contributes approximately 70% of the whole fiber's Young's modulus [10]. The microfibrillar angle between the fiber axis and the microfibril depends on the species, which is approximately 10° for flax. The spiral angel and S2 determine the mechanical properties of the fiber. The outer layer, middle lamella, is constituted of pectin and lignin to compile and bound fiber bundles together to form the plant fibers. The existence of pectin and lignin reduce the mechanical properties of the fiber, which also affect the interfacial properties between fibers and matrices. On the other hand, matrix systems are usually much more hydrophobic. The inherent lack of compatibility between cellulosic fibers and polymeric matrices leads to poor dispersion of the flax fibers and to poor adhesion between the fibers and the matrices.

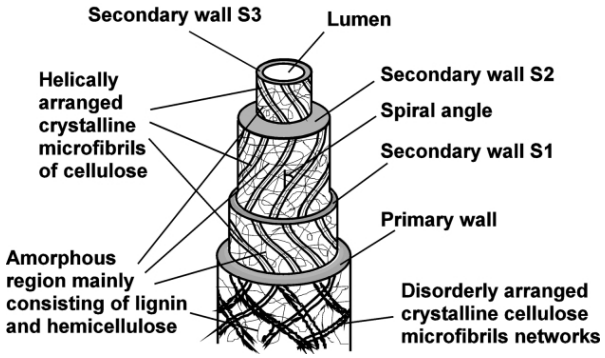

Figure 1.3 The structure of a long plant fiber cell [19].

In Table 1.1 the ranges in mechanical performance of unidirectional flax thermoset are listed. These long flax fibers have been cleaned well, mechanically handled, and some of

them have been spun into yarns, which are easy to process into composites and increase the mechanical performance of their composites. In addition, different thermoset resins and different processing procedures were involved, which affect the properties of these flax fiber composites. However, the interfacial bonding plays an important role in the physical and mechanical properties of these flax fiber composites.

Table 1.1 Unidirectional Flax Reinforced Thermoset Mechanical Performance [21]

Composite	Tensile		Flexural		Interlaminar Shear Strength (MPa)	V_f (%)
	Modulus (GPa)	Strength (MPa)	Modulus (GPa)	Strength (MPa)		
Flax/Polyester	14	140~143	15~17	170~198	22	28~31
Flax/Epoxy	15	160	16	168~190	30	25~30
Flax/Vinyl ester	14~24	143~248	-	95~135	10.5~21	34~37

1.2.2. Surface Modified Flax Fibers/VE Composites

To improve the interfacial properties of flax composites, different physical, chemical, or physico-chemical modifications are applied to the flax fibers. The physical methods, such as mechanical separation, stretching and rolling, solvent extraction, electric discharge, thermal treatment, steam explosion, and so on, can partially change the structural surface properties of flax fiber. Chemical modifications include alkaline treatment, coupling agents, bleaching, enzyme, peroxide, at et., to reduce non-cellulose components, decrease the hydrophilicity of flax fiber and improve chemical bonding between flax fiber and polymer matrices. Hydrothermal treatment and steam explosion with chemical solutions are two typical physico-chemical treatments applied to flax fibers to produce small, clean and fine fibers or fibrils, which increase the contact area between fiber and matrix.

In a preliminary study [22], different types of physical and chemical modifications (including: hot water washing, NaOH treatment, 10% VE tetrahydrofuran (THF) coating, acetic anhydride treatment, acrylic acid treatment, silane treatment, and bleaching) on European linen flax were investigated to analyze their effects on the interfacial properties of unidirectional flax/VE composites. The comparisons of mechanical performance among

untreated and treated flax/VE composites and unidirectional E-glass/VE composites were discussed.

Dissolution, coating, or a combination of both can occur during surface treatments. Specifically, hot water treatment causes dissolution. With hot water treatment in the preliminary study [22], the ash and protein substances were washed away from the surface of flax fiber to improve the adhesion between flax fiber and vinyl ester matrix. The NaOH/ethanol treatment also showed the same effect as the hot water treatment. In addition, alkaline treatment degrades lignin, and alters parts of the structure of cellulose lattices, but the hot water treatment does not cause either effect.

The acetic anhydride treatment is a type of acetylation reaction, which can reduce the hydrophilicity of the flax fiber. In this study, acetic anhydride was reacted with hydroxyl group (–OH) of flax fiber, which results in the formation of acetate, thus increasing the hydrophobicity, as showed in Formula 1.1. This treatment promotes a pseudo coating on the surface of flax fiber.

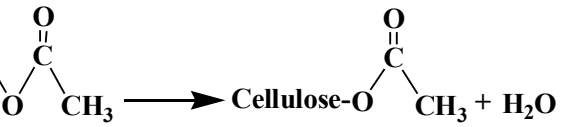

(1.1)

During the acetylation, cellulose will start to hydrolyze when pH is lower than 5.5, which will decrease the weight of flax fiber (Formula 1.2). The product of hydrolyzation can react with acetic anhydride to form acetate that has very low molecular weight.

$$(C_6H_{10}O_5)_n + nH_2O \longrightarrow nC_6H_{12}O_6 \quad (1.2)$$

The acrylic acid treatment is the combination of dissolution and coating, which involves dewaxing, delignification, bleaching and copolymerization. Several types of chemical reactions are equally probable during the surface treatment. The first method is grafting. Cellulose can react with acrylic acid to form acrylate, which reduces the

hydrophilicity of cellulose and forms water as the byproduct. The reaction between acrylic acid and cellulose is showed as Formula 1.3:

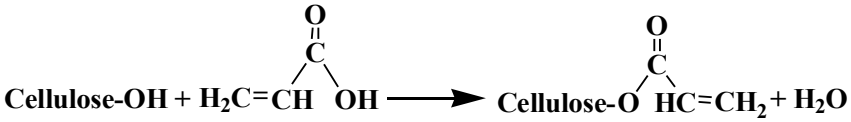

(1.3)

Meanwhile, another parallel reaction can occur during the first step. If the concentration of acrylic acid is too high, acrylic acid can polymerize to form oligomer, as shown in Formula 1.4. Oligomer also can react with celluloses, which can increase the length of the branch and water is the byproduct (Formula 1.5). Both reactions will increase the amount of water.

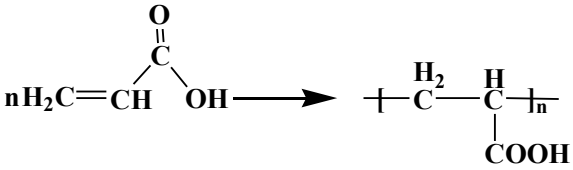

(1.4)

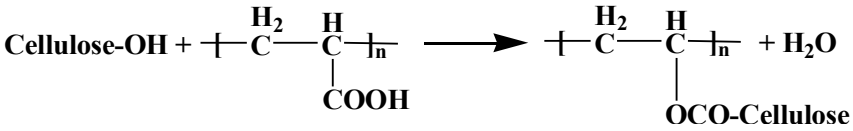

(1.5)

During evaporation of the unreacted acrylic acid and water there may be several kinds of chemical left: flax fiber without any grafting, flax fiber grafted acrylate, oligomers, and products from hydrolysis. There might be some residual hydrogen bonds in the treated flax fiber (Formula 1.6). FTIR can be used to detect the functional groups and verify the chemical reactions. The carbon double bonds of acrylic acid can also polymerize with vinyl ester resin when vinyl ester resin is infused during the processing composites panel. Silane treatment is similar with the acetic anhydride treatment, which also includes coating. In addition, the grafted silane increases the mechanical interlocking between the flax fiber and the vinyl ester matrix.

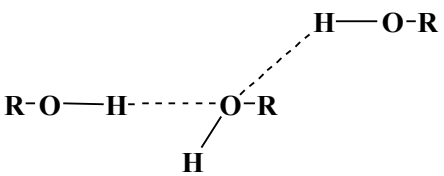

(1.6)

Vinyl-ester-resin treatment treatment involves coating, which has no chemical reactions between vinyl ester resin and flax fiber. In this treatment, toluene solution was chosen first as it is a common solvent, which cannot break down flax fiber. Nevertheless, the polarity of toluene is much lower than THF, which is not helpful to disperse flax fiber. In the THF solution, flax fiber and vinyl ester resin were expected to have a higher degree of contact. The coated vinyl ester resin can increase the wettability between flax and VE during the composites' process.

Bleaching treatment is a traditional treatment for wood fibers, which reduces pectin and lignin. In this study, linseed flax fiber contents 16% lignin, which affects the properties of flax fiber and its composite significantly. The bleaching principle of sodium chlorite is still not clear in the literature. One assumption [23], which is accepted by many scientists, is that oxygen is the key to break down lignin. The other assumption [23] is Cl_2 which oxides lignin. However, the bleaching of sodium chlorite will not break down small amount of flax fiber within a reasonable cost compared to hydrogen peroxide.

The results of the surface treatments on the specific interlaminar shear strength and the comparisons among flax/VE composites and E-glass/VE composites are shown in Fig. 1.4. The physical methods applied to the flax fibers were the hot water washing and the 10% vinyl ester resin coating. The chemical methods included: alkaline treatment (NaOH), coupling agents (acetic anhydride, acrylic acid, and silane treatment), and bleaching treatment ($NaClO_2$). Compared with the untreated Flax/VE composites, all of the surface treatments investigated increased the specific interlaminar shear strength (ILSS) of the composites to a certain degree, which indicates that all the treatments improve the interfacial adhesion between flax fibers and VE matrix. Physical methods increase the mechanical interlocking between fibers and matrix. Chemical modifications build bridges by forming chemical bonds between fibers and matrix to improve the interfacial properties of the

composites. Moreover, most surface treatments show higher specific ILSS than E-glass/VE composites, except hot water washing and acetic anhydride treatment. However, different treatments affect other mechanical properties of their composites in different way. Moreover, the time-efficiency and the cost of these treatments are issues, which should be considered.

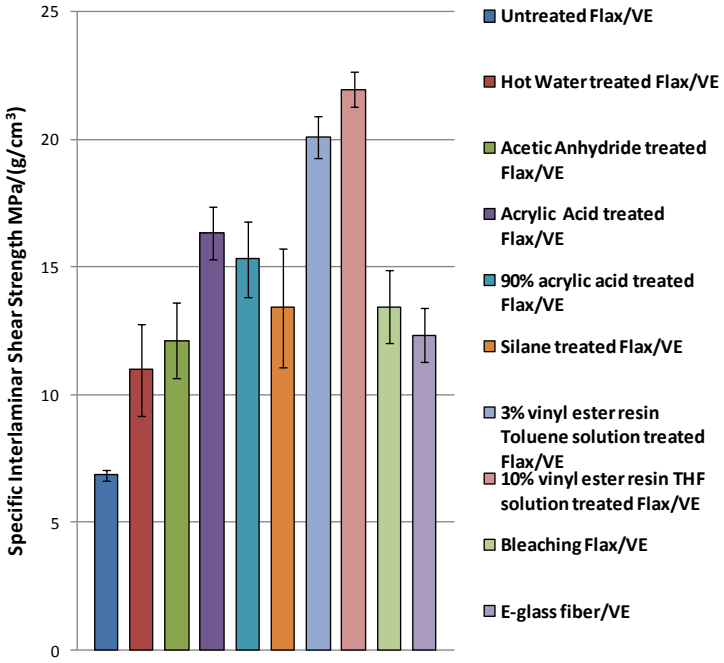

Figure 1.4 Specific interlaminar shear strength comparisons among untreated and treated European flax/VE composites and E-glass/VE composites [22].

The mechanical properties of flax fiber/VE composites depend on the mechanical properties of flax fiber, the mechanical properties of the VE matrix, and the efficiency of load transfer. The specific tensile modulus and the specific flexural modulus of the flax/VE composites are shown in Fig. 1.5 and Fig. 1.6. It is clear that most of the physical and chemical treatments show negative effects on the mechanical moduli of the flax/VE composites, which are related to the structural variation of the flax fibers. This is due to the effects of chemicals in the treatments. For the physical methods, the solvent THF is a polar solvent, which can dissolve different type of hydrophobic and hydrophilic chemicals. The

carbon chain of flax fibers can relax and free-walk in THF solution, as well as the carbon of VE resin and acrylic resin. VE resin or AR is able to fill up the apparent surface flaws in flax fiber and results in better adhesion [18]. However, some coiled fibrils in flax fibers are loosened and exposed in THF solution during treatments [19]. These fibrils can contribute to uncoiling when a bending force is applied, which leads to the reduction in interfacial stress transfer. Moreover, the swelling and partial removal of non-cellulosic chemicals in flax fibers decreases the resistance of microfibrils to stretching [24].

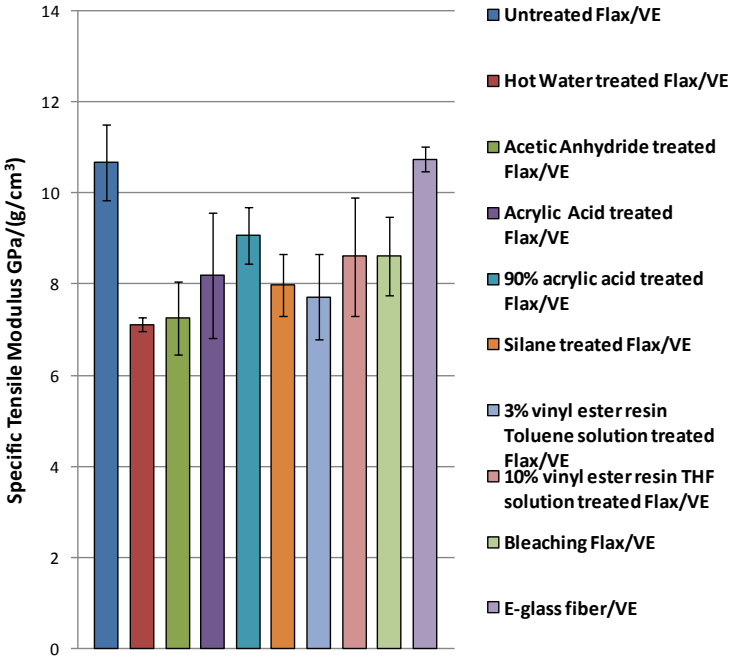

Figure 1.5 Specific tensile modulus comparisons among untreated and treated flax/VE composites and E-glass/VE composites [22].

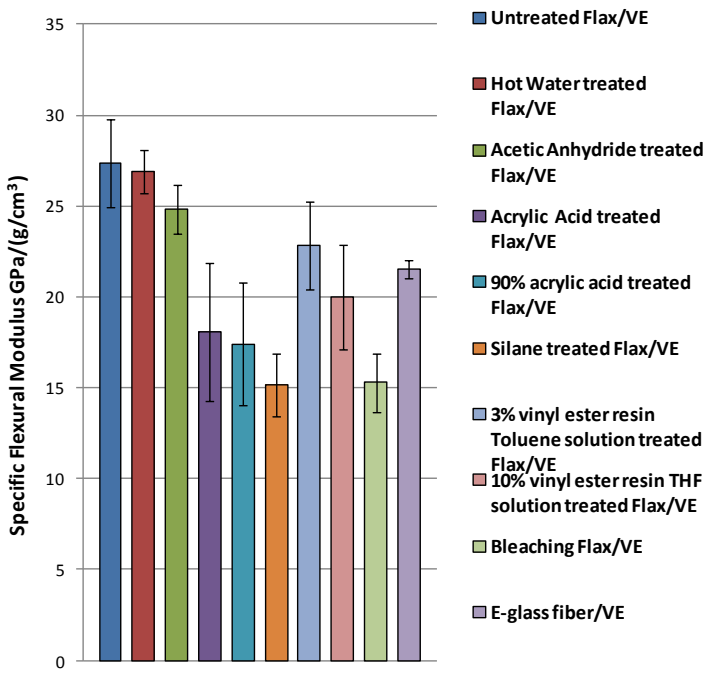

Figure 1.6 Specific flexural modulus comparisons among untreated and treated flax/VE composites and E-glass/VE composites [22].

Different physical or chemical treatments on flax fibers can remove non-cellulose chemicals to improve the interfacial bonding between flax and VE. However, these treatments also introduce some damage to the fiber structure, which reduce the mechanical performance of flax/VE composites. Moreover, some of the physical or chemical treatments increase the total cost of flax/VE composites, and some of the chemical treatments are not environmentally friendly or can generate polluted by-products. Thus, a easy processing, cost-saving and eco-friendly method to improve the interfacial properties of flax/VE composites needs to be developed and thus because the focus of this dissertation.

1.3. Vinyl Ester System

Surface treatments clean the fibers, increase the contact areas between fibers and matrices, or introduce chemical bonds between fibers and polymer matrices to improve the interfacial properties of the flax composites. On the other hand, the polymer matrix can also

be modified to improve the adhesion between fibers and matrices. In terms of liquid molding resins, the mechanical properties and cost of vinyl ester (VE) are intermediate to those of polyester or epoxy. VE offers better resistance to moisture absorption and hydrolytic attack than polyesters [24], which is because of fewer ester groups in the VE structure. These ester groups are readily hydrolyzed, leading to a significant moisture uptake in the cured composites [25].

VE resins are oligomers with unsaturated terminal sites, which generated by the reaction between bisphenol-A and unsaturated carboxylic acid. Bisphenol-A is based epoxy oligomers and unsaturated carboxylic acids can be acrylic or methacrylic acid. In order to control the viscosity of VE resin system, styrene as a diluent is added [26,27]. Vinyl groups of styrene and the end acrylic or methacrylic groups of VE resin can crosslink to form a network by the free-radical copolymerization. The cure process of VE, which determines the mechanical properties of the final product, is influenced by reaction conditions, which include concentration of the monomers, initiators, and temperature [28]. Moreover, the curing process of VE is an exothermic reaction and for very thick VE bulks the exothermic temperature can be as high as 193ºC [29].

The kinetics of curing vinyl ester has been studied using different techniques, such as FTIR, C^{13} NMR, DSC curing behavior, DMA, and TMA. The structure of VE network is considered to be heterogeneous, which has been proved by TEM [30] and AFM [31]. During the curing procedure of VE, the acrylate or methacrylate reacts slightly faster than styrene and ceases before VE fully cures. Meanwhile, styrene continues polymerizing during the entire curing process. The amount of conversion of styrene determines the density of crosslinking of VE [32], which affects the glass transition temperature and the free volume expansion coefficient.

1.3.1. Resin System Manipulation

There are two categories of methods in resin modifications. The first type is focused on mixing certain compatibilizer with the resin to reduce the interfacial energy and improve the interfacial adhesion of multiphase polymer. The second type is focused on adding compounds or homopolymers into the resin system to change the route of the crosslinking to improve some mechanical properties of the final product, such as impact properties.

The immiscible polymers blending together have been investigated for many years. It can be immiscible binary blends of some compatibilizers (usually homopolymers) to certain block copolymers or branched copolymers, which consist the same repeat units as the compatibilizers [33]. It also can be blending with compatibilizers, which have some identical parts with the thermoset resin and the rest are different but still miscible with the resin. Moreover, it can be mixing two immiscible polymers (block or graft copolymers) having some miscible blocks on both. The existance of the small amount of compatibilizers may reduce the phase separation of thermoset system, which leads to changes of internal stresses in the bulk polymers and improves the mechanical performance of the bulk. The internal stresses, especially the thermal residual stresses may introduce shape distortions, warpage, or micro-cracks into the bulk [34].

The second type of the resin manipulation is adding homopolymers (usually thermoplastics with low unsaturated bonds) to modify the path of the copolymerization of the original resin system. It may change the thermal residual stresses of the polymer, such as epoxy modified by polyester [35]. The internal stresses of cured epoxy depend on the amount of additional polyester. With the addition of 16 phr polyester, the internal stress was almost absent without any sacrifice of mechanical properties and heat resistance. The changes of internal stresses are shown by the shrinkage of curing. The effects of the internal stresses depend on the application of the material. Thermosets, such as vinyl ester, are typically used

as the matrices for fiber reinforced composites. These stresses can introduce product failures to the composites or help to improve the mechanical performance of their composites. Moreover, the additives can change certain physical property of the polymer, such as hydrophilicity.

Acrylic resins (AR) are usually used as plasticizers in cellulose nitrate and chlorine-containing binders for coatings. They show good flexibility and excellent adhesion. AR used in this study is the copolymer from n-butyl acrylate and vinyl isobutyl ether. The ester groups in AR can introduce higher polarity to the resin, which increases the hydrophilicty of AR. The more hydrophilic resin system should help increase the interfacial adhesion between flax and VE. In the preliminary study, AR was used as a coating to coat flax fibers' surface and also mixed with VE resin to manipulate the resin system.

Figure 1.7 shows the comparisons of specific interlaminar shear strength of untreated and treated cellulosic fibers with neat VE and modified VE with 1% AR. These results lend credence to the necessity to further explore the factors affect the mechanical properties of cellulosic fibers reinforced VE composites. It was observed in the preliminary testing that the chemical treatments investigated on unidirectional flax improved the interfacial bonding between fibers and VE matrix to a certain degree. The cleanliness of unidirectional cellulosic fibers affects the interfacial bonding significantly. However, the chemical treatments on hemp mat did not show the similar results, which it is due to the geometry and the architecture of the hemp mat affect the dispersion of VE.

On the other hand, the resin manipulation showed the similar effects on both unidirectional flax and randomly-oriented hemp. The polarity of acrylic resin is in middle of cellulosic fibers and vinyl ester, which is the reason that acrylic resin was chosen as a compatibilizer to modify vinyl resin system. It means acrylic resin increases the interaction between the fibers and matrix.

However, if the polarity is the only reason acrylic resin improves the interfacial properties of the composites, 3% acrylic resin coating should increase the interfacial bonding, or at least showed similar performance as other treatments. However, the results of acrylic coating show the decreasing of the specific interlaminar shear strength for unidirectional flax composites. It indicates acrylic resin as a compatibilizer for vinyl ester may also change the residual stresses during the curing process, which affect the mechanical properties of the final product.

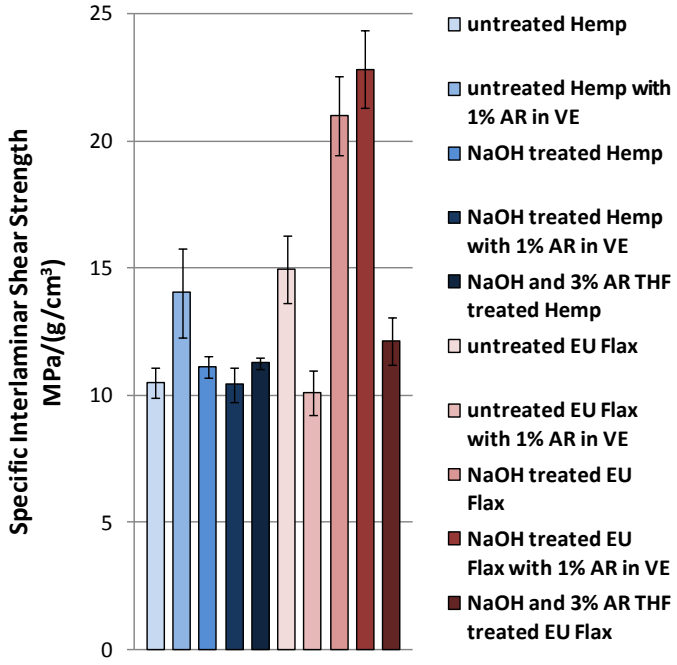

Figure 1.7 Comparisons of specific interlaminar shear strength among untreated and treated cellulosic fiber VE composites [22].

1.4. Thermal Residual Stresses

The thermal residual stresses at the interface between fibers and matrix and inside of the resin and fiber are the results of the chemical shrinkage and thermal cooling contraction [36,37]. There are two steps involved in the curing process of fiber reinforced thermoset composites. The first step is isothermal curing at a high temperature. During this step the

polymerization of the polymer matrix is the main chemical reaction, which causes the polymer to shrink and build up stiffness. Meanwhile, the fibers remain the same. The second step is thermal cooling from the curing temperature to room temperature. Due to the difference in thermal expansion coefficients of fibers and polymer matrix, polymer and fibers contract by different amounts. At the same time, the polymer may change its stiffness.

The residual stresses exist on both the macroscopic and microscopic scales. Tensile residual stresses from the matrix may significantly decrease the strength of the polymer and lead to premature fracture of a composite structure. Compressive residual stresses may increase the interfacial bonding between fibers and polymer matrix [38]. Residual stresses are also important at the free edge of a laminate. These stresses can create matrix cracking of delamination initiation if their values are high. It is important to predict and measure the residual stresses for production, design and performance of composites materials.

During polymerization, the chemical shrinkage stresses are introduced by the volume changes of polymer matrix. The chemical properties of the material and the procedure of curing determine the shrinkage stresses. There are two transitions, gelation and vitrification, which can be involved during the curing of the polymer matrix. Gelation is related with the formation of molecular networks. If the temperature of the isothermal curing is above the glass transition temperature, there will be only gelation for the polymer matrix. Gelation corresponds to the equilibrium elastic modulus. If the curing temperature is below the glass transition temperature, the polymer matrix will first gelate and then vitrify. Vitrification will occur when the curing temperature reaches the glass transition temperature, and it is related to the transition from a rubbery modulus to a glassy modulus [37].

The mismatch in the coefficients of thermal expansion (CTE) of the polymer and fibers can introduce thermal cooling stress. When the temperature of the system starts to decrease, both polymer and fiber start to contract. The contraction of polymer is restricted by

the bonded fibers, which leads the tension to the matrix. Meanwhile, the fibers are also compressed by the contraction of polymer matrix, which induces the compressive stress to the fibers. The properties of the fiber-polymer system, especially the interaction between fiber and matrix, decide the magnitude of these stresses [37]. These internal thermal residual stresses affect the quality of the interfacial adhesion of the fiber reinforced composites [39]. The interface condition can affect the toughness, stiffness and strength of the composites [40].

1.4.1. Measuring Methods

There are numerous methods that have been developed to determine the residual stresses in the fiber reinforced polymer composites, including experimental methods and analytical methods. These techniques estimate the magnitude of the thermal residual stresses on the three levels: the meso/micro-level (micro-mechanical level) [41,42], the macro-level (macro-mechanical level) [43], and a global laminate level [44].

There are two categories in experimental methods: destructive and non-destructive methods. As the name mentioned, the specimens for the destructive methods will be destroyed in the testing, such as hole-drilling [45], first-ply test [46], and sectioning [47]. During the specimens' preparation, the development of damage due to the cutting and drilling, which affect the performance of the composites, is still a challenge.

The second category is non-destructive methods, including warpage/curvature measurements [48], the cure-reference method [49], Photo-elasticity [50], micro-Raman spectroscopy [51], electrical conductivity [52], and embedded sensors [53]. Warpage and the cure-reference methods are based on in-plane and out-of-plane deformations. Under certain strains or stresses, some materials' properties change, such as the refraction of light, Raman peak position, and electrical conductivity. The thermal residual stresses of these materials can be measured by Photo-elasticity, micro-Raman spectroscopy, or electrical conductivity. For

those materials whose properties changes are hard to detect, embedded sensors can help to study the interlaminar or intralaminar stresses in the composites. Currently, strain gauges, fiber optic sensor, and embedded metallic particles are commonly used sensors. Strain gauges can provide accurate results during both heating and cooling process. Fiber optic sensors will not generate degradation of macro-level properties, but they can cause a stress concentration and affect the mechanical properties [54]. Embedded metallic particles usually combine with X-ray diffraction to measure the deformation induced by residual strains in the matrix.

For analytical methods, thermal residual stresses in the composites have been studied on the macro-level and meso/micro-levels. Classical laminate theory is used to predict at the ply level. The unit cell [41] or representative volume element approach [42] has been investigated on the micro-level. In order to simplify the procedure, most micromechanical models assume a periodic arrangement of fibers and can be isolated. The unit cell has the same elastic constants and fiber volume fraction as their composite. The square and hexagonal arrangements of the fibers are commonly applied.

1.4.2. X-ray Diffraction Stress Measurement

In the early 1950's, X-ray diffraction measurement was beginning to be applied in practical engineering problems, such as steels. With the development of techniques, diffractometers and the residual stress models, XRD measurements are now widely performed in any fine grained crystalline materials. However, thermoset matrices do not have a crystalline structure and do not show any diffraction from X-ray. So the method of embedded metallic particles in the thermoset matrix, combining with XRD, has been investigated in thermoset polymers and their composites. The embedded sensor can be aluminum, copper, silver, or nickel. Because the metal will be exposed to the thermal residual strains, it is important to select the metal which will not yield during the curing of polymer.

Aluminum particles, which are spherical or nearly spherical, can provide highest accuracy [55].

Embedded particles can show a change in the diffraction peak angle due to the residual strains in the polymer. The crystal lattice spacing d_0 can be calculated using Bragg's law:

$$d_0 = \frac{\lambda}{2\sin\theta_{\text{Bragg}}} \tag{1-1}$$

where θ_{Bragg} is the measured peak position. There are two rectilinear coordinate systems used in x-ray diffraction stress measurements [56]. One is the laboratory coordinate system (principal system), which consists of the axes with respect to which diffraction measurements are made. The other one is the sample coordinate system (normal system). For an anisotropic elastic material stress can be calculated by Eqn. (1-2):

$$\sigma_{ij} = C_{ijkl}\,\varepsilon_{kl} \tag{1-2}$$

for i, j, k and l = 1, 2, or 3 and elastic constants matrix C_{ijkl}. Also, strain can be defined in terms of the stress components by Eqn. (1-3):

$$\varepsilon_{ij} = S_{ijkl}\,\sigma_{kl} \tag{1-3}$$

where S_{ijkl} is the elastic compliance matrix. For an isotropic elastic material, the elastic constants E and v relate the stress and strain tensors by Eqn. (1-4)

$$\varepsilon_{ij} = \frac{1+\nu}{E}\sigma_{ij} - \delta_{ij}\frac{\nu}{E}\sigma_{kk} \tag{1-4}$$

To relate strain in one coordinate system to that in another system, this is done through direction cosines a_{mi} and a_{nj}, and

$$\varepsilon_{mn} = a_{mi}\,a_{nj}\,\varepsilon_{ij} \tag{1-5}$$

where a_{mi} defines the consine of the angle between x_i in the old coordinate system and x_m in the new coordinate system. Thus the relationship between strain ε_{33} in the principal coordinate system and ε_{kl} in the normal system is calculated by Eqn. (1-6)

$$\varepsilon_{33}=a_{3k}\,a_{3l}\,\varepsilon_{kl} \tag{1-6}$$

with

$$a_{ik}=\begin{bmatrix} cos\varphi\ cos\psi & sin\varphi\ cos\psi & -sin\psi \\ -sin\varphi & cos\varphi & 0 \\ cos\varphi\ sin\psi & sin\varphi sin\psi & cos\psi \end{bmatrix} \tag{1-7}$$

for the angle φ and ψ defined in Fig. 1.9. After substituting for a_{3k} and a_{3l}, the result is

$$\begin{aligned}\varepsilon_{\varphi\psi}=&\varepsilon_{11}cos^2\varphi\ sin^2\psi+\varepsilon_{12}sin2\varphi sin^2\psi+\varepsilon_{22}sin^2\varphi sin^2\psi+\varepsilon_{33}cos^2\psi\\&+\varepsilon_{13}cos\varphi sin2\psi+\varepsilon_{23}sin\varphi sin2\psi\end{aligned} \tag{1-8}$$

$\varepsilon_{\varphi\psi}$ is measured at angles φ and ψ in Fig. 1.8 by XRD. The difference between $d_{\varphi\psi}$, the value of d in the stressed sample and measured for the plane whose normal is at angle φ and ψ and the value of d_0 for the unstressed state is related by Eqn. (1-9):

$$\varepsilon_{\varphi\psi}=\frac{d_{\varphi\psi}-d_0}{d_0} \tag{1-9}$$

V. Hauk [57] provides formulas for determining the principal stresses σ_{11}, σ_{22}, σ_{33} in polycrystal specimens while neglecting the shear stresses σ_{12}, σ_{23}, σ_{31}. Application of these formulae to the present research is justifiable because of the low magnitude of the shear stresses in the specimens tested in this study. Here 11, 22, and 33 correspond to the directions (inside the inclusion) x, y and z. Knowing the X-ray elastic constant (XEC) S_1^{hkl} and $\frac{1}{2}S_2^{hkl}$ and the stress-free lattice spacing d_0 (which is measured on the filler powder), the strain measured in the direction by φ and ψ is given, in terms of the principal stresses by Eqn. (1-10)

$$\begin{aligned}\varepsilon_{\varphi\psi}=\frac{d_{\varphi\psi}-d_0}{d_0}=&\frac{1}{2}S_2^{hkl}(\sigma_{11}cos^2\varphi sin^2\psi+\sigma_{22}sin^2\varphi sin^2\psi+\varepsilon_{33}cos^2\psi)+\\&S_1^{hkl}(\sigma_{11}+\sigma_{22}+\sigma_{33})\end{aligned} \tag{1-10}$$

Dőlle [58] describes a method to calculate XEC using single crystal elastic constants S_{11}, S_{12}, and S_{66} for cubic symmetry. By using the Voigt and Reuss models, Dragoi [59] calculated the average XEC values (Voigt and Reuss) for Al (422).

The lattice spacings $d_{\varphi\psi}$ are obtained by changing the direction of the X-ray beam. The strain components ε_{ij} (i, j = 1, 2, 3) in the specimen coordinate system can be calculated by Eqn. (1-11):

$$\begin{aligned}\varepsilon_{\varphi\psi} &= \frac{d_{\varphi\psi} - d_0}{d_0} \\ &= \varepsilon_{11}cos^2\varphi sin^2\psi + \varepsilon_{12}sin2\varphi sin^2\psi + \varepsilon_{22}sin^2\varphi sin^2\psi \\ &\quad + \varepsilon_{33}cos^2\psi + \varepsilon_{13}cos\varphi sin2\psi + \varepsilon_{23}sin\varphi sin2\psi\end{aligned} \tag{1-11}$$

ε_{33} is calculated by Eqn. (1-12):

$$\varepsilon_{33} = \frac{\varepsilon_{\varphi=0,\psi=0} + \varepsilon_{\varphi=90,\psi=0}}{2} \tag{1-12}$$

ε_{11} and ε_{22} are obtained from the slopes of the $sin^2\psi$ plots at φ=0° and 90°. The stresses on the surface of aluminum particles can be calculated from the strain by using Hooke's law, assuming the system is isotropic. The residual stresses in unidirectional composites can be evaluated using the Eshelby approach and a linear visco-elastic model of the laminated plate [55]. However, this technique can only provide the properties on the surface of the composites. In addition, the concentration of the particles needs to be high enough to acquire diffraction, but low enough to minimize the effect on the stress inside the composites.

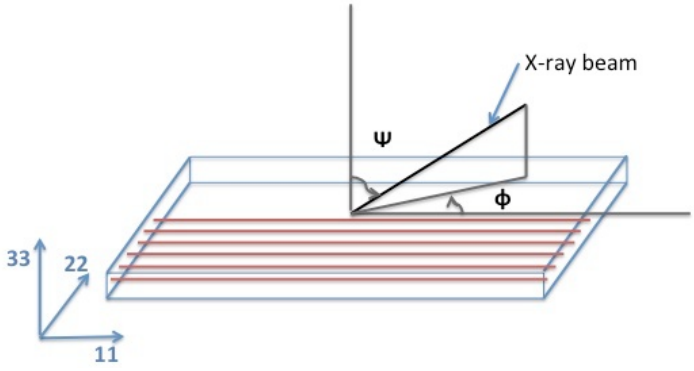

Figure 1.8 The diffraction plane and the coordinates of the specimen [55].

1.4.3. Eshelby Method

Eshelby developed a consistent theory of stresses and strains inside inclusions. Following the standard Eshelby procedure, the stresses inside an inclusion can be obtained [57] (Eqn. (1-13)):

$$\boldsymbol{\sigma}_{inclusion} = \boldsymbol{C}_{matrix}\,(\boldsymbol{S}-\boldsymbol{I})[(\boldsymbol{C}_{inclusion} - \boldsymbol{C}_{matrix})\boldsymbol{S} + \boldsymbol{C}_{matrix}]^{-1}\boldsymbol{C}_{inclusion}\,\boldsymbol{\varepsilon}^{T*} \tag{1-13}$$

where $\boldsymbol{\sigma}_{inclusion}$ is the stress inside the filler; $\boldsymbol{C}_{matrix}$ is the stiffness of the matrix; $\boldsymbol{S}$ is the Eshelby tensor; $\boldsymbol{I}$ is the identity matrix; $\boldsymbol{C}_{inclusion}$ is the stiffness of the inclusion; $\boldsymbol{\varepsilon}^{T*}$ is the differential thermal misfit. In addition, $\boldsymbol{\varepsilon}^{T*}$ can be calculated by Eqn. (1-14):

$$\boldsymbol{\varepsilon}^{T*} = (\boldsymbol{\alpha}_{matrix} - \boldsymbol{\alpha}_{inclusion})\Delta T \tag{1-14}$$

where $\boldsymbol{\alpha}_{matrix}$ is the CTE of the matrix; $\boldsymbol{\alpha}_{inclusion}$ is the CTE of the inclusion. The strain inside the inclusion is [59]:

$$\boldsymbol{\varepsilon}_{inclusion} = \{\boldsymbol{S}[(\boldsymbol{C}_{inclusion} - \boldsymbol{C}_{matrix})\boldsymbol{S} + \boldsymbol{C}_{matrix}]^{-1}\boldsymbol{C}_{inclusion} - \boldsymbol{I}\}\boldsymbol{\varepsilon}^{T*} \tag{1-15}$$

Eqn. (1-16) is the Eshelby tensor **S** for a spherical inclusion.

$$\boldsymbol{S}=\begin{bmatrix} \frac{7-5\nu_f}{15(1-\nu_f)} & \frac{-1+5\nu_f}{15(1-\nu_f)} & \frac{-1+5\nu_f}{15(1-\nu_f)} & 0 & 0 & 0 \\ \frac{-1+5\nu_f}{15(1-\nu_f)} & \frac{7-5\nu_f}{15(1-\nu_f)} & \frac{-1+5\nu_f}{15(1-\nu_f)} & 0 & 0 & 0 \\ \frac{-1+5\nu_f}{15(1-\nu_f)} & \frac{-1+5\nu_f}{15(1-\nu_f)} & \frac{7-5\nu_f}{15(1-\nu_f)} & 0 & 0 & 0 \\ 0 & 0 & 0 & \frac{4-5\nu_f}{15(1-\nu_f)} & 0 & 0 \\ 0 & 0 & 0 & 0 & \frac{4-5\nu_f}{15(1-\nu_f)} & 0 \\ 0 & 0 & 0 & 0 & 0 & \frac{4-5\nu_f}{15(1-\nu_f)} \end{bmatrix} \tag{1-16}$$

where ν_f is the Poisson ratio of the inclusion [60, 61].

1.5. Research Objectives

The interfacial properties of cellulosic fiber reinforced composites are essential rule to the mechanical performance of their composites. On the other hand, the mechanical properties of the composites indicate how good the interfacial adhesion between fibers and

matrices is. To accurately understand the interfacial behavior of the cellulosic fiber reinforced thermoset composites, all three aspects (fiber, resin and composites) should be studied on both chemical and physical/mechanical properties. From the chemical point, the interaction among the constituents of the cellulosic fibers as well as the interaction between these components and resin system should be assessed. Moreover, the interphase behavior of the modified resin system should be studied. On the physical/mechanical aspect, the thermal properties of the cellulosic fibers and resin system should be evaluated.

Using XRD technique on the amorphous polymer composites to study the changes of internal stresses has been applied on synthetic fiber reinforced composites. However, it is usually helpful to comprehend the fracture mechanics and fatigue behaviors in those composites. The effects of thermal residual stresses on interfacial properties of natural fiber reinforced amorphous polymer composites have not been studied. Due to the unique structure and properties of natural fibers, there are some challenges, in both the experimental parts and the theoretical parts, which need to be investigated.

The final composites will use the combination of chemical modification on fiber and resin system to provide better mechanical performance. The ideal chemical modification, either on cellulosic fibers or on the resin system, can reduce or eliminate the ineffective factors, as well as can effectively utilize all the components in the fiber-polymer system to achieve better mechanical performance. Moreover, the cost, time-efficiency, and environmental friendliness should be considered. With a full understanding of the factors (chemical and physical), which influence the interfacial properties of flax/VE composites, a general guide on how to improve the interfacial adhesion of flax/VE composites and their mechanical performance will be formed. In addition, based on the similarities of long cellulosic fibers, most of the physical and chemical factors and techniques studied on flax/VE composites can be applied on other unidirectional cellulosic fibers reinforced thermoset

composites, especially the thermal study on the interfacial properties of unidirectional cellulosic fiber composites. Changing the thermal residual stresses in cellulosic fiber composites to improve their interfacial properties and enhance their mechanical performance is a cost-saving, eco-friendly, straightforward method, which satisfies the demand of the natural fiber composites' manufacturing and their markets.

CHAPTER 2. RESEARCH METHODOLOGY

2.1. Test Matrix Development

To evaluate the interfacial properties of unidirectional fiber reinforced polymer composites, the strength and stiffness in the transverse direction of the composites are usually assessed, which are widely used in the studies of synthetic fiber reinforced composites. The failure in the transverse direction of the unidirectional composites is due to the stress concentration around the fiber. However, there are several differences between flax fibers and synthetic fibers. As mentioned in section 1.1.1, the cellulose fibrils are combined together by hemicellulose and lignin, and the interfacial bonding between cellulose fibrils and hemicellulose and lignin are weak. In addition, there is a hollow lumen in a single flax fiber, which is considered as a void in its composites. By applying transverse mechanical tests to evaluate the interfacial adhesion between flax and VE, the test results can be affected by the debonding between cellulose fibrils and non-cellulose chemicals. Thus, the transverse tests cannot to be used to evaluate the interfacial properties of flax composites.

On the other hand, the interfacial adhesion between flax and VE matrix is related to the chemical and physical properties of both flax fibers and VE matrix. Moreover, the mechanical performance of the flax/VE composites, such as tensile properties and flexural properties, are affected by their interfacial properties. In order to fully understand the interfacial properties of flax reinforced VE composites and estimate the ultimate properties of the composite, the physical and chemical properties of flax fiber, VE system and their composites should be studied. In addition, the effects of chemical modifications on both flax fiber and VE system need to be evaluated independently prior to creating a composite.

2.1.1. Analysis of Flax Fiber

In order to achieve the ideal interfacial bonding between the cellulosic fibers and polymer matrix, the chemical and physical properties of flax should be fully understood. As mentioned in Chapter 1, flax fibers need to be cleaned by chemical or physical methods. Understanding the effects of the chemical or physical modifications on the chemical components and structure of flax fibers can help to find the optimal treatment to improve the mechanical performances of flax composites. Alkaline treatment is a common method to clean the surface of cellulosic fibers with a reasonable cost and simple procedure. The changes of the chemical components and crystal structures in flax should be understood. Optimizing the surface modification procedure on the flax fiber will be investigated. Moreover, the mechanical performance of untreated and treated flax fibers need to be investigated and the ultimate properties of flax composites can be evaluated, which can provide a guide for the future work.

2.1.2. Analysis of VE Systems

In order to understand the interaction between flax fibers and VE matrix, the physical and chemical properties of VE system should be studied. The role VE plays in the cellulosic fiber reinforced composites is similar to the glue which bonds all the fiber bundles together. For the cellulosic fibers, pectin, lignin, and hemicellulose are the natural glues which hold the cellulose fibrils together, and the mechanical properties of non-cellulosic constituents are much lower than those of VE. However, the interactions among pectin, cellulose, hemicelluloses and lignin will provide a guide to modify VE resin system to achieve better interfacial bonding. The optimal chemical modification of the VE system will be developed to achieve the ideal bonding between fibers and polymer matrix. One direction of chemical modification in VE system is increasing the hydrophilicity of the whole system to increase

the interaction between cellulosic fibers and matrix. The other direction is modifying the microstructure of VE to increase the mechanical interlocking between fibers and matrix. Acrylic resin modification has shown significant improvement on the mechanical properties of the composites. The effect of AR on VE system is the combination of both directions and the optimized amount of AR added into VE resin will be studied. Meanwhile, the curing kinetics of modified resin system will be investigated using differential scanning calorimetry (DSC). The coefficients of linear thermal expansion of neat VE and modified VE will be tested by dynamic mechanical analysis. The shrinkage of neat VE and modified VE will be studied by post-cure shrinkage tests and the behavior of the different phases in the modified resin system during the curing procedure will be revealed. In addition, the mechanical properties of modified resin system will be investigated, including tensile properties, flexural properties and impact properties.

2.1.3. Analysis of Flax Composites

To evaluate the improvements on the interfacial properties of chemical modifications applied on both flax and VE system, the mechanical performance of untreated and treated flax/VE with/without AR need to be studied. There are two goals of this section. The first goal is to measure residual stresses in the cellulosic fiber reinforced composites. As mentioned in the last section, the chemical modifications in VE system will change the microstructure of VE, which is directly correlated with the changes of the thermal residual stresses. The changes of the internal thermal residual stresses of unmodified and modified composites will be evaluated by XRD using the aluminum particle "sensor", which will help explain the physical behavior of the interface between cellulosic fibers and polymer matrix. The thermal properties of cellulosic fibers and VE will be evaluated by dynamic mechanical analysis. The nominal particle concentration should be 4.6 mg/cm^2 [58], which can provide

enough diffraction signals with minimized effect on the properties of the composites. The calculations of the residual strains and stresses in the composites will be performed assuming room temperature elastic properties and the visco-elastic Eshelby model for multiple inclusions will be applied.

The second goal is to evaluate the effects of the thermal residual stresses on the interfacial adhesion between flax fibers and VE matrix. With the assistance of the properties of flax, VE and their composites, the relationship between thermal residual stresses and the interfacial properties of flax/VE composites will be builted.

2.2. Materials Used in Study

Unidirectional Chinese flax is water retted with the minimum mechanical handling from Harbin, China. The flax fiber was uncut, natural color, from the stalk with a density of approximately 1.42 g/cm^3. Three more different types of cellulosic fibers are also investigated to help analyze the factors affected the interfacial properties of cellulosic fiber reinforced composites. Unidirectional European flax is uncut, natural color, combed, top part of the flax stem from Holland through General Bailey Homestead Farm, Greenfield Center, NY. Unidirectional Canadian linseed stalks are supplied by Composite Innovation Centre, Winnipeg, Manitoba, Canada. Unidirectional North American hemp was bleached as received. The resin system used for all grades was a vinyl ester resin Hydropel® R037-YDF-40 from AOC resins, and 2-Butanone peroxide (Luperox® DDM-9) solution was used as the curing initiator, obtained from Sigma-Aldrich Co. Acronal® 700 L acrylic resin (AR) was obtained from BASF Aktiengesellschaft, Ludwigshafen, Germany, which is an acrylic resin (copolymer of n-butyl acrylate and vinyl isobutyl ether). THF (puriss. p.a., ≥99 % (GC)) and sodium chlorite (technical grade, 80%) were obtained from chemistry department, NDSU.

Aluminum powder (spherical, 99.9%) is purchased from Atlantic Equipment Engineers. The diameter of Al powder is between 1 μm and 3 μm.

2.3. Fiber Analysis

To accurately comprehend the effects of chemical treatments and the roles of different chemical constituents on the mechanical properties of the flax fibers, chemical analysis and tensile tests were performed on the untreated and NaOH/Ethanol treated flax fibers. In addition, the thermal properties of flax were evaluated.

Alkaline treatment: The loomed flax fibers were immersed into 500 mL of 10 g/L sodium hydroxide ethanol (95%) solution at 78 °C for 2 h. The treated fibers were washed with distilled water until no color was left in the water. Then the fibers were dried in an oven for 24 h at 80 °C.

VE resin solution treatments: two treatments were used, and in each case, the dried, NaOH treated flax fibers were manually separated and then immersed into either 3 wt.% VE/toluene solution and 3 wt.% VE/THF solution at room temperature for 1 h. The treated fibers were dried in an oven for 24 h at 80 °C.

3% acrylic resin solution treatment: flax fibers were dried after alkaline treatments, followed by hand–separation and immersion into 3 wt. % acrylic resin/THF solution for 1 h at room temperature (23 °C, 50 % RH). The AR treated fibers were dried in an oven for 24 h at 80 °C.

The purpose of the treatments used was to cause either a) dissolution or b) dissolution and coating. The alkaline treatment can reduce the proteins, waxes, ash, and minerals on the surface of fibers to improve the adhesion between the flax fiber and the vinyl ester matrix. In addition, alkaline treatment partially degrades lignin and helps the cellulose I lattice to partly transform into a cellulose II lattice when the concentration of the alkaline solution is higher

than 9 % (wt). Cellulose I can also be transformed by thermal treatment into cellulose II, which has a more stable crystalline structure [21].

VE treatment involves coating, with no chemical reactions between the vinyl ester resin and the flax fiber. For this treatment, toluene solution was chosen initially, as it is a common solvent. Afterward, toluene was replaced with THF as the solvent because of its lower polarity. In the THF solution, flax fiber and vinyl ester resin were expected to have a higher degree of contact than toluene. Often, this increased affinity causes the coated vinyl ester resin to cross-link with VE resin during composite processing. AR treatment is similar to a VE treatment that coats the surface of flax fibers with acrylic resin using THF as the solvent.

Bleaching is a conventional treatment for wood fibers that is used to reduce pectin and lignin. An often accepted theory [23] is that oxygen is the key to break down lignin. Another theory [23] is that Cl_2 oxidizes lignin. Hydrogen peroxide is the most effective agent for flax fiber bleaching. However, $NaClO_2$ is used predominantly because it is cost-effective over H_2O_2.

2.3.1. Chemical Analysis

Fiber composition was determined through a number of tests conducted by the Animal Sciences department at North Dakota State University. These included dry matter testing, neutral detergent solution and acid detergent solution characterization, and starch spectrophotometry. These allowed for the collection of percentage dry matter, as well as percentage cellulose, hemicellulose, lignin, starch, and ash. Dry matter determination was done according to AOAC standard 930.15, in samples were massed at room temperature, heated at 100 °C for 24 hours, cooled in a desiccator, and then massed a second time. Neutral detergent fiber, acid detergent fiber, and acid detergent lignin analysis were performed using

an ANKOM$^{200/220}$ Fiber Analyzer according to methods spelled out in USDA Agricultural Handbook No. 379 [62]. Determination of starch was performed after an acid and enzymatic isolation using a micro-titre reading with a SPECTRAmax 340 Microplate Reader, as specified in literature [63].

The cleanliness of the untreated and treated flax was observed by stereoscopy with an inverted light and optical microscopy. Images were taken of fibers from both microscopes and using a macro-lens of a digital camera (8 megapixels). Two different chemical solutions were prepared to coat the surface of the untreated and treated flax to identify the effects of chemical treatments. Oil red 0 (0.4% in carbon tetrachloride) was used as a histochemical stain for the cuticle residue on fibers. Phloroglucinol stain was prepared a saturated solution of phloroglucinol in 20% HCl, which can detect the structure of lignin [64]. The untreated and treated fibers were immersed into the stains for 10 min and then washed with water until there is no color left in the water. The cuticles on the surface of the fiber can show red color, the lignin from the shive can show light red and the clean fiber is the natural color of the fiber (light yellow). Fourier Transform Infrared Spectroscopy (FTIR) was used for studying the functional group modifications. Three mid-infrared spectroscopy systems were used to assess similar samples to those stained with oil red. These systems were: a Thermo Scientific Nicolet 6700 FT-IR equipped with a SensIR Dura Scope, a Thermo Scientific Nicolet 870 FT-IR integrated with a Continuum microscope, and a Smiths Detection IlluminatIR II attached to an Olympus BX51 microscope. FTIR spectra were obtained for all grades of flax fibers. A total of 32 scans were acquired at a resolution of 4 cm^{-1} between 4000 cm^{-1} and 650 cm^{-1}.

2.3.2. Thermal Properties

The coefficient of thermal expansion (CTE) of the treated flax was measured by the thermomechanical analyzer 2940 in the center for nanoscale science and engineering. Thermomechanical analysis (TMA) measured the displacement in the cross-section of the treated flax fibers as a function of temperature under a controlled atmosphere. A small bundle of fibers with combed line-up was placed on the tip of the probe and the temperature is raised from 25 °C to 150 °C by 10 °C/min. Three measurements were applied to calculated the average of the CTE of the cross-section area.

2.3.3. Mechanical Testing

The tensile properties of single flax fiber bundle were tested on a micro/nano-scale load frame. Single flax fiber bundle was selected by hands assisted with the optical magnifier and then glued on the paper frame (Fig. 2.1). The diameter of the fiber bundle was evaluated by an optical microscope to calculated the crossection area. The speciments were mounted on the load frame and the two edges of the paper frame is cut off before the testing starts. The step displacement of the load cell can reach 33.2nm in minimum and its precision is 5±0.003 lb. The testing strain rate is 0.001 and the test is stoped until the fiber bundle is failed. The elastic moduli and ultimate strengths of the flax bundles are calcuated according to the strain-stress curves. A minimun of ten specimens were tested.

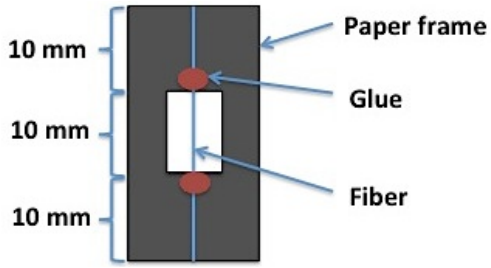

Figure 2.1 The schematic of tensile speciment.

2.4. Resin System in Study

2.4.1. System Manipulation

To improve the interfacial bonding between fibers and VE matrix, acrylic resin (AR) was added into VE resin. AR is a highly viscous liquid that is used particularly in combination with cellulose nitrate. It is a copolymer of n-butylacrylate ($C_7H_{12}O_2$) and vinyl isobutyl ether ($C_6H_{12}O$). 1% wt. and 1.5% wt. AR were added into VE resin and mixed before the peroxide initiator was added.

2.4.2. Resin System Characterization

The degree of cure or conversion in VE and AR modified VE were studied by differential scanning calorimetry (DSC). A DSC Q1000 from TA Instruments with an autosampler was used to measure the exothermic heat (heat per mass of material, J/g) when samples were subjected to a heat cycle from 0 to 180 °C by ramping at 10 °C/min. DSC was started just after preparing the mixture, which is because the total heat of reaction is measured from 0% to 100% conversion. The residual heat was measured after isothermally curing in an oven at 50 °C for 12 hrs and 48 hrs.

The glass transition temperatures (T_g) of VE and VE with AR were measured by the heat-cool-heat processurdes and the heat cycle from 30 to 180 °C, which the heating rate is 10 °C/min and the cooling rate is 5 °C/min. The second heating cycle was used to characterize the samples. Five measurements were applied to calculate the average changes. T_g of AR was measured by the heat-cool-heat processurdes from -80 to 100 °C. The heating rate and the cooling rate are same as the method for VE system.

The shrinkages after the curing of VE and modified VE with AR were evaluated by measuring the volume changes before and after the curing. The liquid VE resin mixture was put into a square aluminum mold and the width, length and height of the liquid were

measured. Then, the geometries of the cured VE were measured to calculate the volume changes after curing.

The cured VE and AR modified VE were analyzed by FT-IR spectrocopy with the same parameters of the fiber testings to detected the changes in the polymer structure of VE system. The contact angle measurements were conducted in a facility of the Department of Coatings and Polymeric Materials (First Ten Angstroms FTA 125). A water drop was introduced on the fiber surface through a syringe. A snap shot of the water drop on the fiber surface was captured immediately, and the contact angle was calculated from the water drop profile. Five measurements were taken from each cured resin sample. The moisture resistance properties of the two different resin systems were assessed through water absorption tests, according to the ASTM D570 and ASTM D5229. Four specimens for neat VE and VE with 1% AR were prepared according to the dimension requirement in the ASTM standards. These specimens were immersed in distilled water at room temperature. The weight of each specimen was measured once per 24 hrs. The average moisture content M (%) was calculated by Eqn. (2-1):

$$M\,(\%) = \frac{W - Wo}{Wo} \times 100 \qquad (2\text{-}1)$$

CTEs of VE and VE with AR were measured by a TA Q800 dynamic mechanical analyzer (DMA) using tension film fixture. Four rectangular specimens with dimensions of 15×7.8×2.69 mm for both neat VE and VE with 1% AR were prepared. The measurements were performed from 30 to 150 °C at a heating rate of 5 °C/min and a frequency of 1 Hz. In addition, the T_gs of both VE systems were evaluated by DMA with the dual cantilever fixtures. Four rectangular specimens (dimension: 46×10.6×3.71 mm) for each resin system were measured from 30 to 180 °C with a heating rate of 3 °C/min and a frequency of 1 Hz. The glass transition temperature was determined as the temperature at the maximum of the

tan δ vs. temperature curve. The storage modulus in the rubbery plateau region was determined at 30 °C above the glass transition temperature.

Moreover, the tensile properties VE and VE with AR were evaluated according to ASTM D3039 using an Instron 5567 load frame and five specimens were prepared. The speed of the cross-head was approximately 1 mm/min. The specimens were tested until tensile failure. The specific tensile strength and specific tensile modulus were calculated. The flexural properties of the cured resins were measured by three-point bending tests, as specified in Procedure A of ASTM D790, using an Instron 5567 load frame. The speed of the cross-head was dependent on sample thickness, and was on an average, approximately 1 mm/min. Five specimens were tested for each sample. The flexural strength and flexural modulus were calculated for each sample set.

2.5. Composite Processing

2.5.1. Composite Panels for Mechanical Testings

Composite panels of untreated and treated flax/VE (with/without AR) were fabricated using a modified form of vacuum assisted resin transfer molding (VARTM). A caul plate was used underneath the vacuum bag to provide a uniform cross sectional area. This also created a test part with a smooth surface finish on both sides. In order to obtain similar fiber volume fractions, the VARTM process was aided by compressing the vacuumed flax with 2 metric ton. The processing setup is shown in Fig. 2.2. The manually aligned unidirectional fibers showed a deviation of 0° to 10° with respect to the lay-up direction.

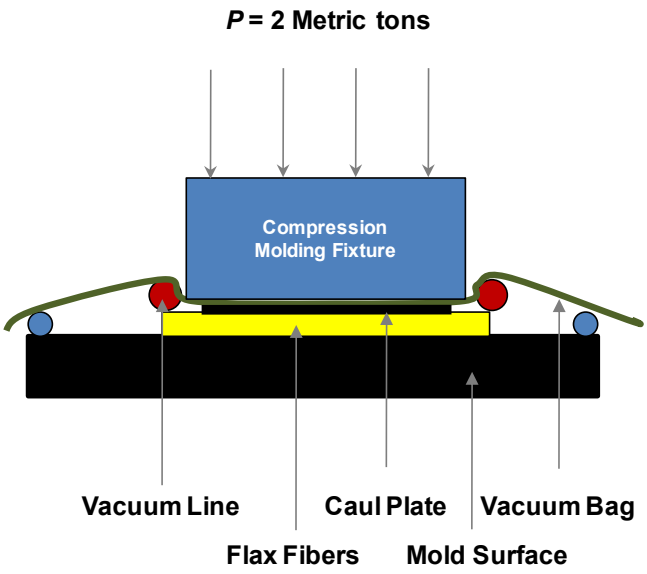

Figure 2.2. A schematic of compression-aided VARTM process.

2.5.2. Composite panels for X-ray diffraction

Aluminum powder was dispersed into absolute ethanol by the high shear stirring to form the homogenous slurry, which the concentration is 0.5% wt. 5~6 g NaOH/Ethanol treated flax was quickly put into the slurry and taken out under the nitrogen atmosphere and then the fiber was dried in the nitrogen atmosphere at room temperature for 24 h. The composite samples were manufactured by the modified VARTM under a nitrogen atmosphere.

2.6. Composites' Characterization

2.6.1. Chemical Analysis

The untreated and treated Canadian flax/VE (with/without AR) composites were analyzed by optical microscope and FTIR to study the chemical interaction between the fiber and VE matrix. 4% Oil red stain in CCl_4 was used to detect the ester group and FTIR spectra were obtained for all grades of composite materials processed.

2.6.2. Mechanical Testing

Interlaminar shear strengths were assessed using short beam strength tests, according to ASTM D2344. Short beam shear tests were carried out in displacement control at a rate of approximate 1 mm/min on an Instron 5567 load frame. Five specimens for each sample were tested. Interfacial shear strengths between fibers and surrounding matrix were evaluated by fiber bundle pull-out tests [65]. Tests were conducted using an Instron 5567 load frame with a 2 kN load cell at a rate of 0.5 mm/min. The interfacial areas of the pulled fiber bundle were measured by an optical microscope. With pull-out perimeter, a modified Kelly-Tyson equation [22] is applied to calculate the interfacial shear strength τ_i (Eqn. 2-2)

$$\tau_i = \frac{F_{\max}}{CL_e + A} \tag{2-2}$$

where F_{max} is the max load at pull-out, C is the fiber bundle perimeter, L_e is the fiber embedded length, and A is the area of the top surface of the fibers, which is encapsulated in resin and must be included in the surface area calculations. In addition, the flexural analysis and the tensile mechanical testing were performed according the to the same testing parameters as in resin tests.

Flexural properties were evaluated through three-point bending tests, according to the Procedure A of ASTM D790, on an Instron 5567 load frame. The speed of the crosshead was approximately 1.5 mm/min, which was determined by the dimension of the specimen. Five specimens were measured for every flax/VE composites.

Tensile testing was performed according to ASTM D3039 with a five-specimen sample set using an Instron 5567 load frame. The speed of the crosshead was 1.0 mm/min. Each test was performed until tensile failure occurred. The tensile modulus of each specimen was re-calculated by the slop of stress-strain plot in the linear region where the displacement is measured by the extensometer.

2.6.3. Moisture Resistance

The moisture resistant properties were assessed through water absorption tests, according to ASTM Standard D570 and ASTM D5229. Three specimens for untreated, treated cellulosic fiber/VE with 1% AR were prepared. The dimension of specimens were prepared according to ASTM D790 for three-point bend testing. The specimens were immersed in distilled water at room temperature. The weight of each specimen was measured once per 24 hrs.

Flexural analysis of the composites with 0 and 4%~5% (wt) water uptaking was performed through three-point bend testing as specified in Procedure A of ASTM Standard D790, using an Instron model 5567 load frame. The speed of the cross-head was 1.55 mm/min. Three specimens were measured for each sample. The mean value and standard deviation of specific flexural strength and specific flexural modulus was calculated for each sample set.

2.6.4. X-ray Diffraction

The treated flax/VE (with/without AR) with Al powder composites were marked six angles (0°, 30°, 45°, 90°, 120° and 135°), which the longitudinal directional of the fiber is the direction of 0°. XRD spectra of different angles were taken using a Philips X'per MPD X-ray Powder Diffractometer. The XRD diffraction conditions are shown in Table 2.1. The radiation is generated from Cu-K_{α}, and λ of K-α1 is 1.54060 Å and λ of K-α2 is 1.54443 Å. The scan is started at the position (2θ) of 136.01° and stopped at the position (2θ) of 138.99° at room temperature, which the step (2θ) size is 0.0200°. Peak separation of aluminum at (422) was carried out by least-square fitting by assigning Gaussian functions. The original aluminum powder was scanned using the same procedure.

Table 2.1 X-ray Diffraction Conditions

Radiation	Cu $K_{\alpha 1}$, λ=1.54060 Å
Reflection (hkl)	422
2θ range (°)	136~139
Step size (°)	0.0200

2.7. The Relationship Among All Characterization

The Figure 2.3 list the test methods applied on flax fiber, VE resin systems and their composites in this study. All these tests used on flax, VE and their composites cover most physical and chemical factors related to the mechanical performance of the flax/VE composites and explain the functions of every factor and how to improve the quality of the flax/VE compostes by adjusting these factors.

In the flax fiber section, chemical analysis, chemical stains and FT-IR are applied on untreated and treated flax to examine the effects of different chemical modifications on the fiber surface, such as the changes of chemical structure and crystallinity. TMA is used to obtain the coefficient of thermal expansion of flax, which helps to evaluate the thermal residual stresses in the composites and assess the effects of thermal residual stresses on the interfacial properties of flax/VE composites. The elastic properties of flax fiber are obtained by tensile tests, which also help to predict the elastic properties of the optimal flax/VE composites.

In the VE resin part, DSC, shrinkage during the curing and DMA are investigated to evaluate the kinetics of the curing with and without modification. The glass transition temperatures of the different VE systems are assessed by DMA and DSC to evaluate the crosslink densities of these VE system. CTEs of different VE systems are obtained by DMA, which help to evaluate the thermal residual stresses in the flax/VE composites. FT-IR spectra examine the chemical structural changes in modified VE system. Contact angle tests and moisture absorption tests are applied to evaluated the wettability between flax and VE matrix.

The results of tensile tests and flexural tests are used to confirm the changes in the crosslink densities of modified VE systems.

In the composites' section, chemical stains and FT-IR are used to check the chemical bonds between flax and VE matrix, which help to eliminate the possibility that AR forms chemical between flax fiber and VE matrix to increase the interfacial properties. The mechanical tests, including short beam shear tests, fiber bundle pull-out tests, flexural tests and tensile tests, evaluate the mechanical performance of flax/VE composites and assess the effects of chemical modification on both flax and VE resin. XRD measurements can determine the thermal residual stresses in the composites, which help to evaluate the effects of thermal residual stresses on the interfacial properties of flax.

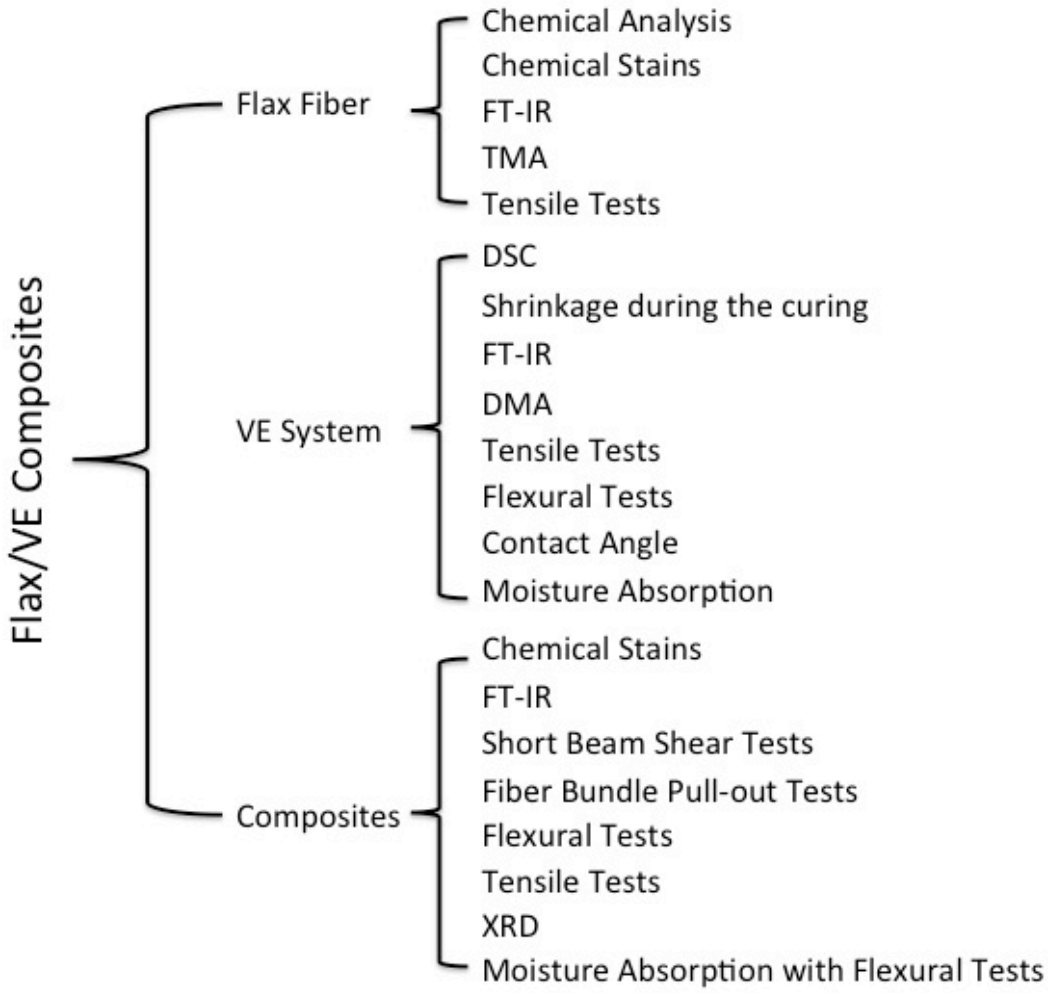

Figure 2.3 The chart of the test methods used in the study.

CHAPTER 3. CHEMICAL AND PHYSICAL PROPERTIES OF CHINESE FLAX

3.1. Chemical Analysis and Thermal Properties

The chemical contents of untreated and NaOH/Ethanol treated Chinese flax, bleached North American hemp and shive are shown in Table 3.1. There are higher amounts of ash, protein, lignin and fat substances in the untreated Chinese flax, which the content of cellulose is similar with other untreated linen flax from the literatures [66-68]. After the alkaline treatment, the amounts of the non-cellulose chemicals are decreased, which is because of the effects of alkaline treatment. During NaOH/Ethanol treatment the large fiber bundles are separated to smaller fiber bundles or even single fibers, which is due to the hydrolysis of pectin and degradiation of lignin. In addition, some non-cellulose substances are washed away, which provides cleaner and rougher fiber surface. The content of cellulose in bleached North American flax is 92.12%, which is higher than flax fibers and untreated hemp is typically between 70.2% and 74.4% by weight [66-68]. The bleaching treatment can efficiently remove lignin than other treatments. Shive is the residual small parts from the shell of the stem after the mechanical separations and it is usually considered as the weak bonding point in the composites. There is a fairly small amount of shive in the untreated Chinese flax and the content of cellulose in shive is only less than half of that in flax and hemp. Constituent contents of European and Canadian flax are presented in Appendix A-1.

The chemical constituents and the structure in Chinese, European, and Canadian flax and hemp are similar. The cellulose contents in Chinese and European flax are slightly higher than Canadian flax, which indicate that the mechanical properties of Chinese and European flax are superior than Canadian flax. Canadian flax is a linseed flax, which the length of the fiber is shorter than Chinese and European flax, which both are linen flax. On the other hand,

the spiril angle in flax is about 10 °, which is larger than that of hemp. The spiril angle of hemp is approximately 6~8 °, which implys that the mechanical properties of hemp is higher than flax. Due to the shortage of European and Canadian flax and adequate amount of Chinese flax, the majority of this study is based on Chinese flax.

Table 3.1 Constituent Content of Chinese flax, North American Hemp and Shive

Sample	Dry Matter %	Ash %	Crude Protein %	Cellulose %	Hemi--cellulose %	Lignin %	Crude Fat %
Untreated CHN Flax	94.21	1.93	5.33	72.00	8.15	6.52	1.04
NaOH/Ethanol treated CHN Flax	96.63	1.17	1.27	89.22	4.93	2.94	0.37
Bleached NA Hemp	95.35	0.3	0.42	92.12	3.61	2.11	0.19
Fine Shive	90.84	9.35	7.83	30.53	12.34	2.05	0.29

The results of the histochemical stains with oil red and phloroglucinol, which stain the flax cuticle and lignin but not the fiber, are shown in Fig. 3.1. The stereoscopy image of the untreated flax (Fig. 3.1 a) shows a lot of red stain staying on the flax and the cuticle on the fiber surface is clearly observed in the closer image (Fig. 3.1 b). The stereoscopy image of treated flax (Fig. 3.1 c) has several big pieces of oil red stain. However, there is no evidence shown that any lipid on the surface of flax from the closer view (Fig. 3.1 d). The red stains in the stereoscopy image are possibly from the plastic plate and are attached on the fibers. Moreover, the fiber bundle size of alkaline treated flax (Fig. 3.1 d) is smaller than that of the untreated fiber (Fig. 3.1 b), which indicates that the alkaline treatment can separate large fiber bundles into small fiber bundle or single fibers. In Figure B-1 the similar phenomenon is observed for Canadian linseed flax. Microscopic results confirmed the removal of the lipid-containing cuticle and showed the effectiveness of the treatment, as hardly any cuticle was observed associated with the fibers after treatment.

The non-cellulosic substances, such as pectin, was, ash, dye and so on, on the surface of flax can reduce the interfacial bonding between flax and VE. In addition, these non-

cellulosic substances are very weak, which reduce the mechanical properties of flax/VE composites. Thus, a clean surface of flax can improve the interfacial adhesion between flax and VE and enhance the mechanical performance of flax/VE composites. Moreover, the smaller fiber bundle size can increase the contact area between flax and VE, which leads to a better interfacial bonding. The chemical analysis and oil red stain study can explain the chemical effects of surface treatments on flax and help to predict the interfacial properties of flax/VE composites.

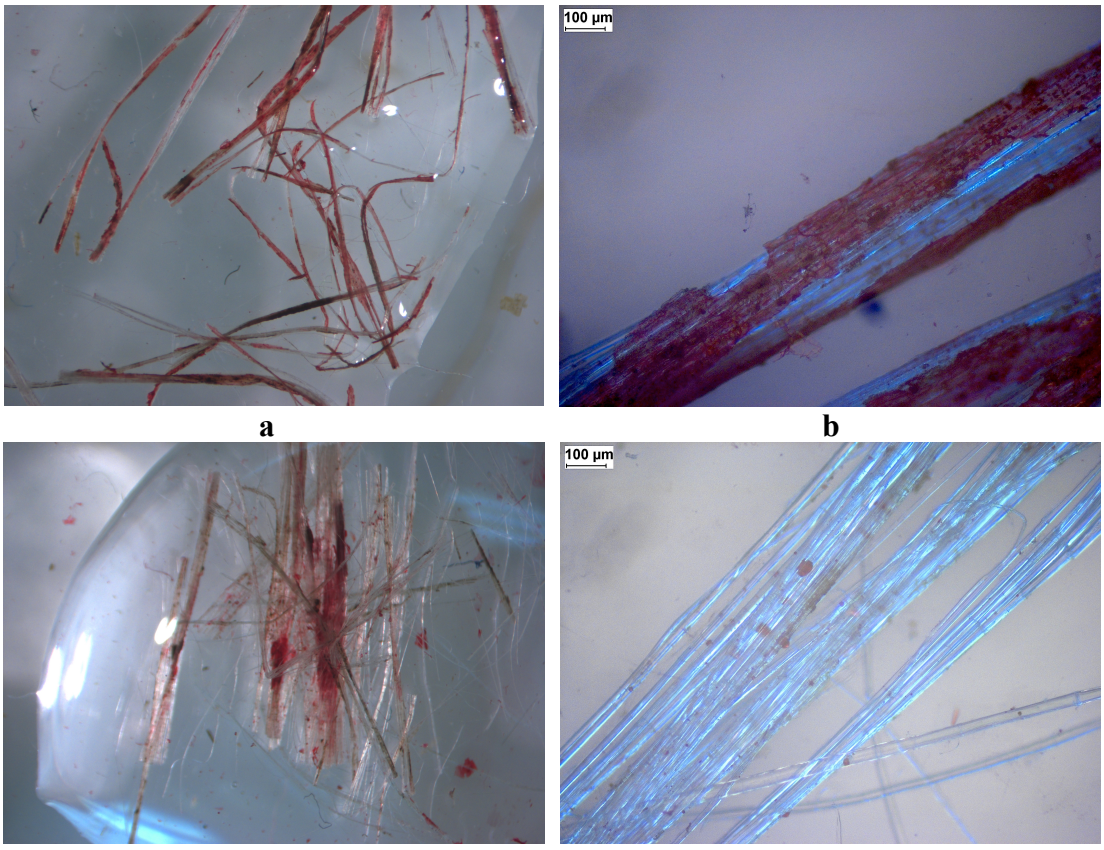

Figure 3.1 Chinese flax stained with oil red O for cuticle: a) stereoscope image of untreated; b) optical microscope image of untreated; c) stereoscope image of NaOH/Ethanol treated; d) optical microscope image of NaOH/Ethanol treated.

The FTIR spectra of untreated and treated flax fiber are presented in Fig. 3.2. The spectrum of untreated flax fiber showed characteristic bands for cellulose. These bands

included a hydrogen bonded –OH stretching [24] at 3600 cm^{-1} to 2995 cm^{-1}, the –CH stretching at 2906 cm^{-1} and 2844 cm^{-1}, the –OH bending [24] at 1575 cm^{-1}, the $–CH_2$ bending at 1409 cm^{-1}, the –CH bending at 1377 cm^{-1}, and the C–O stretching at 1018 cm^{-1}. The spectrum of all specimens showed the bands for cellulose.

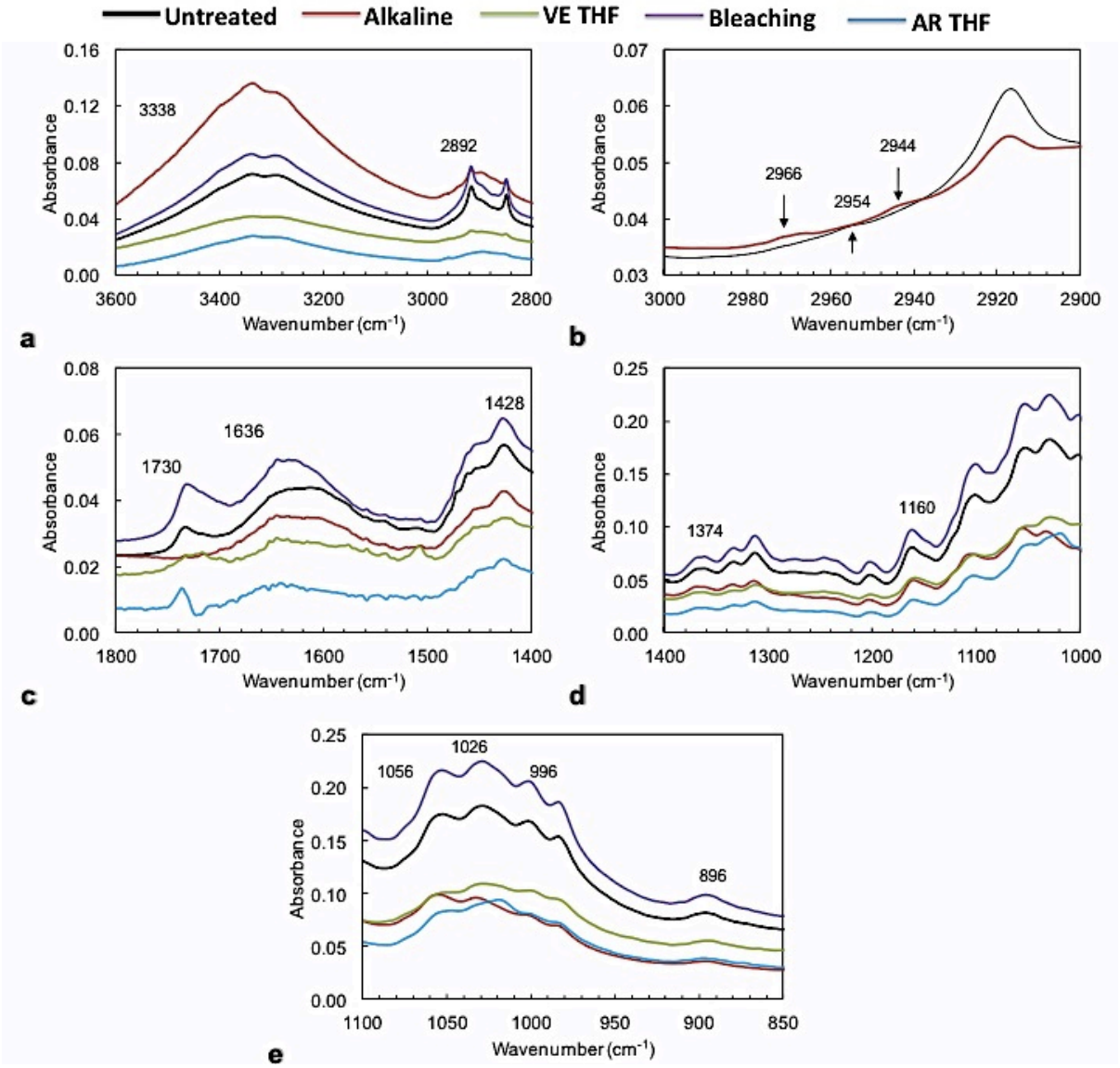

Figure 3.2 FTIR spectra of untreated and treated flax fiber showing (a) hydroxyl region, (b) –CH stretching, functional groups of (c) carbonyl region, (d) cellulose II and (e) microcrystalline cellulose.

The hydroxyl region is detailed in Fig. 3.2 a, showing the characteristic bands at 3340 cm^{-1} which is from intramolecular hydrogen bond in cellulose. The spectra for the

untreated flax and bleached flax show prominent methylene stretching at the 2850 cm^{-1} and 2920 cm^{-1} that represent the presence of waxy constituents [23]. Weak presence of these bands was observed in the NaOH/Ethanol treated, 3% VE THF treated, and 3% AR THF treated flax fiber spectra, showing the effectiveness of these treatments in eliminating waxes from the flax fiber structure. The spectra of 3% VE THF treated flax showed wide, low-absorbance peaks from 3573 cm^{-1} to 2973 cm^{-1}, which indicated a decrease in H-bonded –OH. However, the 3340 cm^{-1} band showed a decrease in absorbance with VE THF and AR treatments and VE-N showed a broad peak for –OH stretching at 3600 cm^{-1} to 2995 cm^{-1}. These spectral characteristics support alkaline treatment exhibiting a strong effect on the functional groups of cellulose [69]. The spectra in the 3000 cm^{-1} to 2900 cm^{-1} range obtained from untreated- and NaOH/Ethanol-treated flax are shown in Fig. 3.2 b. The band observed at 2954 cm^{-1} in the untreated fiber spectra can be attributed to the –CH stretching in cellulose I [70]. The bands at 2966 cm^{-1} and 2944 cm^{-1} in NaOH/Ethanol treated flax are illustrative of –CH stretching in cellulose II [68]. Hence, these distinct differences in spectra support the formation of cellulose II from cellulose I using the NaOH/Ethanol treatment in the flax fiber.

The FTIR spectra representing bands from transient products of the surface treatments are shown in Fig. 3.2 c. As shown, the band at 1730 cm^{-1} exhibits an oxidation product that was absent in alkaline, 3% VE THF, and 3% AR THF treatments when compared with the untreated flax. This band signifies a C=O stretching in unconjugated ketones, carbonyls, or esters [71,72]. However, in bleaching treatment, the 1730 cm^{-1} band was present with a significant intensity. The spectrum of bleached fiber shows a peak at 1685 cm^{-1}, which is illustrative of C=O stretching [72]. The presence of carbonyl group peak supported sodium chlorite oxidizing the hydroxyl groups in lignin to form carbonyl groups and reducing the color of flax fiber. A minor peak was observed at 1677 cm^{-1} that resulted from the C=O group of vinyl ester [70]. The 1636 cm^{-1} (adsorbed water) band was seen in the untreated and

bleached flax, but to a lower degree in alkaline treatment and other treatments used in this study. CH_2 scissoring in cellulose II is a representative of cellulose II and amorphous cellulose and often detected in the spectra at about 1430 cm^{-1}, was present in all treated and untreated fibers with a varying degree of absorbance. This band is exhibited by the crystalline region of the fiber.

The bands at 1374 cm^{-1} (C–H deformation in cellulose II) and 1160 cm^{-1} (C–O–C vibration from β-glycosidic link in cellulose II [72]) are shown in Fig. 3.2 d. These bands are understood to be representative of cellulose II. The spectra in Fig. 3.2 d showed the presence of these bands in all treated/untreated fiber, with bleaching treatment exhibiting higher absorbance over the other treatments. The representative microcrystalline cellulose bands are shown in Fig. 3.2 e. The bands of interest in this region are 896 cm^{-1} showing a C–O–C valence vibration of β-glycosidic link or deformation in cellulose II [72]. This band is exhibited by the amorphous region of the fiber. The 896 cm^{-1} band showed the lowest absorbance in treatments other than the baseline and bleaching, hence was supporting of the utilization of the surface treatments in increasing the overall crystallinity of the fibers.

The analysis of FTIR spectra confirms the chemical effects of different surface modifications on flax. It also presents the chemical structure on the surface of flax, which can help to analyze the chemical interaction between flax and VE to determine the chemical structure on the interface between flax and VE. It will be discussed in section 5.1.

CTE of flax fiber measured by TMA is the CTE of the cross section area α_T. Figure 3.3 is the test curve of the treated flax. The contraction in the region lower than 100 °C in the curve is close to linear and the region above 110 °C drop dramatically. However, the temperature during the curing of the composite is normally below 100 °C in this study, so the region from 40 °C to 80 ° is used to calculate α_T of the treated flax. CTE α_T of the treated flax is $-29.91\times10^{-5} \pm 8.71\times10^{-5}$ /°C. The mismatching of CTEs between flax and VE system can

introduce the thermal residual stresses to the composites during the curing, which can influence the interfacial properties of the composites. CTE of flax in the transverse direction will be used to calculate the thermal residual stresses in the composites in Chapter 6.

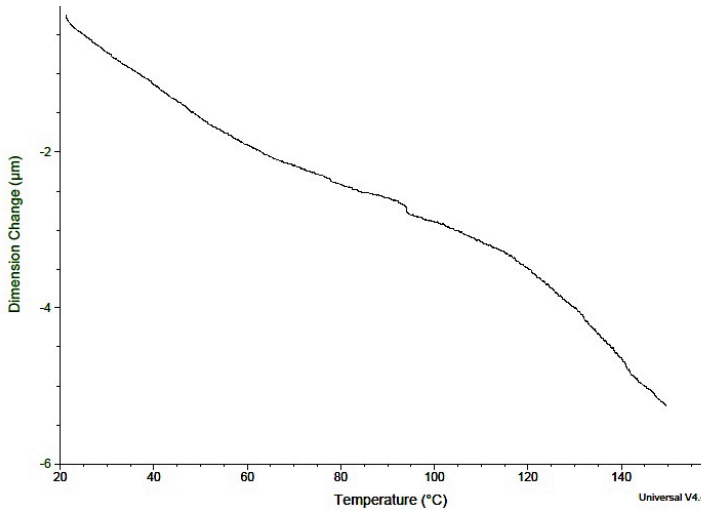

Figure 3.3 The CTE curve of the treated flax measured by TMA.

3.2. Elastic Properties

3.2.1. Estimation of the Elastic Properties of the Flax Fiber Bundle

Flax fiber is made up by several different natural polymers, which is similar to the polymer composites. Cellulose fibrils are the reinforcement, which govern the merchanical properties of the flax fiber, and other constituents are the polymer matrices to hold the fibrils together. The elastic properties of pure cellulose fiber are reported in Table 3.2. For the unidirectional composites, the elastic modulus in longitudinal direction can be calculated by the Eqn. (3-1),

$$E_c = E_f V_f + E_m V_m \tag{3-1}$$

However, flax fiber is the composite with a hollow center and a 10° spiral angle. The reinforcement - cellulose fibrils are fairly short, which can be considered as short fibers aligned to the same direction (Fig. 3.4). These factors should be taken into account to

calculate the elastic properties of flax fiber and therefore the equations above are not valid. The hollow center can be treated as the void in the composite. Halpin and Tsai [73] have developed a generalized equations to calculate the elasticity for micromechanics analysis, which is quite accurate. The Halpin-Tsai equation can be written as

$$\frac{M}{M_m} = \frac{1 + \xi\eta V_f}{1 - \eta V_f} \tag{3-2}$$

where

$$\eta = \frac{\left(\frac{M_f}{M_m}\right) - 1}{\left(\frac{M_f}{M_m}\right) + \xi} \tag{3-3}$$

ξ is the shape factor, as the fiber with circular cross section the value of ξ is 2 for transverse modulus and ξ is 1 for shear modulus. M can be E_L, E_T or G_{LT}; M_f represents E_f or G_f; and M_m stands for E_m or G_m. Poisson raito is calculated by Eqn. (3-4)

$$\nu_{LT} = \nu_f V_f + \nu_m V_m \tag{3-4}$$

To consider the effect of the spiral angle θ the state of stress on a unidirectional flax fiber is shown in Fig. 3.4, where x is the longitudinal direction and also the test direction. The elastic modulus on the test direction can be calculated by the following:

$$\frac{1}{E_x} = \frac{\cos^4\theta}{E_L} + \frac{\sin^4\theta}{E_T} + \frac{1}{4}\left(\frac{1}{G_{LT}} - \frac{2\nu_{LT}}{E_L}\right)\sin^2 2\theta \tag{3-5}$$

Moreover, there should have some voids in the fiber "composite" and it introduces V_0 to the calculations and $V_f + V_m + V_0 = 1$. In this way, the matrix volume fraction can be obtained by $V_m' = V_m + V_0$. Thus, the correct elastic modulus of the matrix is

$$E'_m = \frac{E_m V_m}{V_m + V_0} \tag{3-6}$$

$$\nu'_m = \frac{\upsilon_m V_m}{V_m + V_0} \tag{3-7}$$

The hemicellulose-lignin matrix can also be assumed as randomly-orientated short fiber "composite" and its elastic properties (hemicellulose-lignin "composite") are obtained by the following equations:

$$E_m = \frac{3}{8}E_L + \frac{5}{8}E_T \tag{3-8}$$

$$G_m = \frac{1}{8}E_L + \frac{1}{4}E_T \tag{3-9}$$

The density of flax fiber is close to the density of cellulose. In the following calculation the fiber volume fraction is assumed it is equivlent the content of cellulose. Thus, the fiber volume fraction of untreated flax is 72% and 89.22% for NaOH/Ethanol treated flax. The spiral angles of 0° and 10° are both taken into account because the alignment of fibrils is changed into parallel to the load direction, which the spiral angle is 0°. In addition, there are two cases are considered: 1) There are some voids and defects in the untreated flax and it is assumed about 5%; 2) There are no voids in the untreated and treated flax fiber, which means there are no pores or defects in the fiber.

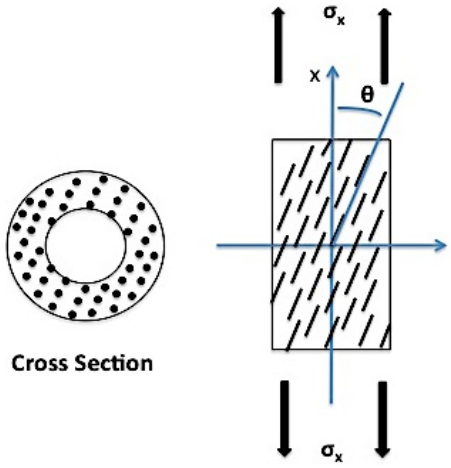

Figure 3.4 The cross section area of a flax fiber (left) and state of stress on a flax fiber (right).

Table 3.2 Elastic Properties of Cellulose, Hemicellulose and Lignin[8,74]

Sample	E_L (GPa)	E_T (GPa)	G_{LT} (GPa)	ν_{LT}
Cellulose	134.00	27.20	4.40	0.1
Hemicellulose	8.00	4.00	2.00	0.2
Lignin	4.00	4.00	1.50	0.33

The estimated elastic properties of untreated and treated flax calculated according to Halpin-Tsai equations are presented in Table 3.3. The elastic modulus of untreated flax in the literature is generally between 27.6 GPa and 38 GPa [66,75-78], which is lower than the theoretical elastic modulus of untreated flax with voids. The content of voids in the theoretical result is only 5%. However, the content of voids in untreated flax in practice may be higher than 5%. In addition, the growing defects (kinks) in the tested flax fiber can reduce the elastic modulus. In this theoretical results, it is assumed alkaline treatment will not affect the properties of the flax "composite". However, alkaline treatment can only remove partial of lignin and hemicellulose and open the fiber bundles. Thus, the elastic properties of treated flax in practice should be lower than the theoretical results. However, the highest elastic modulus of treated flax is approximate 85 GPa [8]. It is because the elastic modulus of tested flax fiber can be increased in the longitudinal direction during a tensile test. The spiral angle is reduced to 0° in a tensile test and the tested results can be close to the elastic modulus of the longitudinal direction (E_L in Table 3.3).

As mention in Chapter 2, the transverse properties of flax/VE composites are difficult to evaluate accurately and the mechanical performance of their composites are related to load transfer through the interface. Thus, the mechanical properties can indicate the quality of interfacial adhesion between flax and VE. The theoretical elastic properties of flax will be used in Chapter 6 to obtain the optimal elastic properties of flax/VE composite, which assumes perfect interfacial adhesion between flax and VE and there are no voids and

misalignment of flax. These optimal elastic properties will assist in evaluating the effects of thermal residual stresses on the interfacial properties of flax composites.

Table 3.3 The Estimated Elastic Properties of Flax

	Untreated Flax with Voids	Untreated Flax without Voids	NaOH/Ethanol Treated Flax with Voids	NaOH/Ethanol Treated Flax without Voids
V_f (%)	72.00	72.00	89.22	89.22
V_m (%)	23.00	28.00	5.78	10.78
V_0 (%)	5.00	0	5.00	0
E'_m (GPa)	3.97	4.83	2.65	4.94
G'_m (GPa)	1.46	1.78	0.97	1.81
ν'_m	0.21	0.26	0.13	0.25
E (θ=10°, GPa)	49.91	51.73	59.02	62.39
E_L (θ=0°, GPa)	97.59	97.83	119.84	120.09
E_T (GPa)	14.79	16.08	19.08	22.03
G_{LT} (GPa)	3.11	3.34	3.54	3.96
ν_{LT}	0.13	0.14	0.10	0.12

3.2.2. Experimental results of tension testing

It has been observed that the alkaline treatment can remove the pectin and separate the fiber bundles. The imges of the fibers for the tensile tests (Fig. 3.5) confirmed the changes of the fiber bundle: the average diameter of untreated flax is around 150 μm and the diameter of NaOH/Ethanol treated flax is between 50 μm and 100 μm. The wide range of the treated fiber's diameter indicates that the removal of lignin and hemicellulose from flax is uneven during alkaline treatment, which leads to the testing results falling in quite a wide range.

The experimental elastic moduli of untreated and treated flax are shown in Fig. 3.6. The tensile moduli are calculated from the region before the fibers were broken. It is observed that the Young's modulus is increased with the decreasing of the fiber cross-section area. It is because there are more non-cellulose components to bind cellulose fibrils together in the flax with the large cross-section area, which reduce the elastic properties of flax.

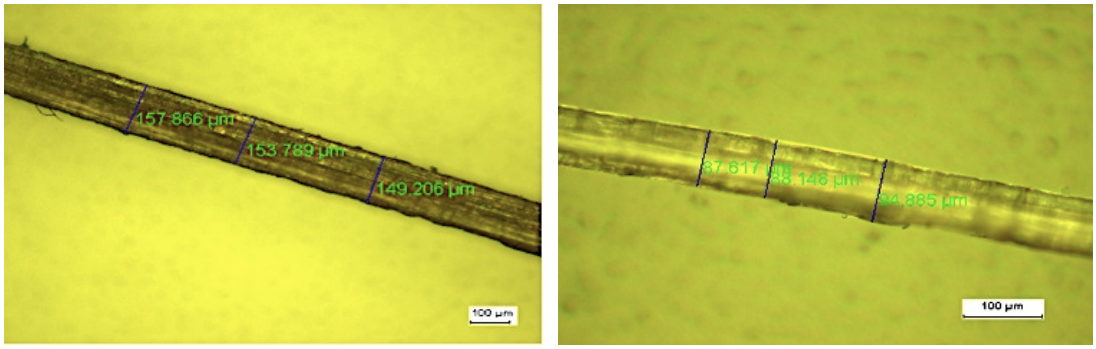

a **b**

Figure 3.5 Optical microscopy images from the fibers for the tension: (a) untreated flax; (b) NaOH/Ethanol treated flax.

The elastic moduli of treated flax are higher than those of untreated fibers, but not significant. The amount of tested fibers is not large enough to show a clear trend. The lowest elastic modulus of untreated flax is 6.12 GPa, which is less than half of the theoretical transverse modulus of untreated flax with 5% void. There are several factors caused the low performance. The tested fiber with lower modulus may contain a larger amount of non-cellulose components or voids than others. There are some growing defects on the tested region. In addition, the fibers were glued on the paper frames, which can reduce the test results. During a tensile testing, the glue, which is also a type of polymer, has some elastic and plastic deformation/elongation. It was taken as a part of the total deformatiom/elongation of flax fiber during the elastic modulus calculation. Thus, the tested results are lower than the real elastic modulus. However, the highest tensile modulus of untreated flax is 39.21 GPa, which is only 10 GPa lower than the theoretical results. The highest tensile modulus of treated flax measured is 42.45 GPa, which is only 68% of the theoretical result. This is mostly due to the affect of alkaline treatment. Alkaline treatment cleans the flax fibers and separate the large fiber bundles into smaller bundles. Meanwhile, the treatment introduces some voids to the fiber bundle and leave some loose fiber bundles, which have lower tensile properties.

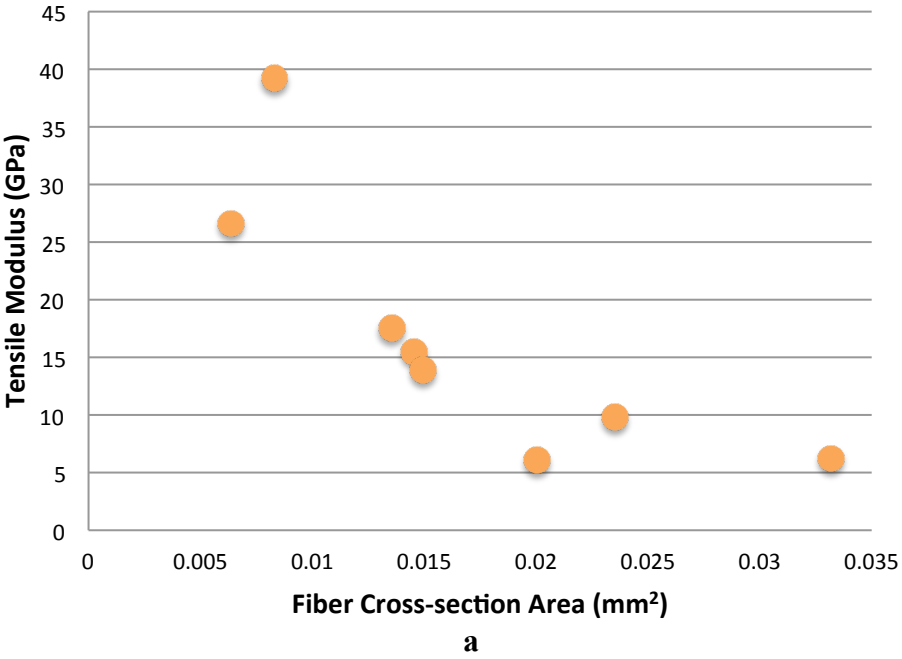

a

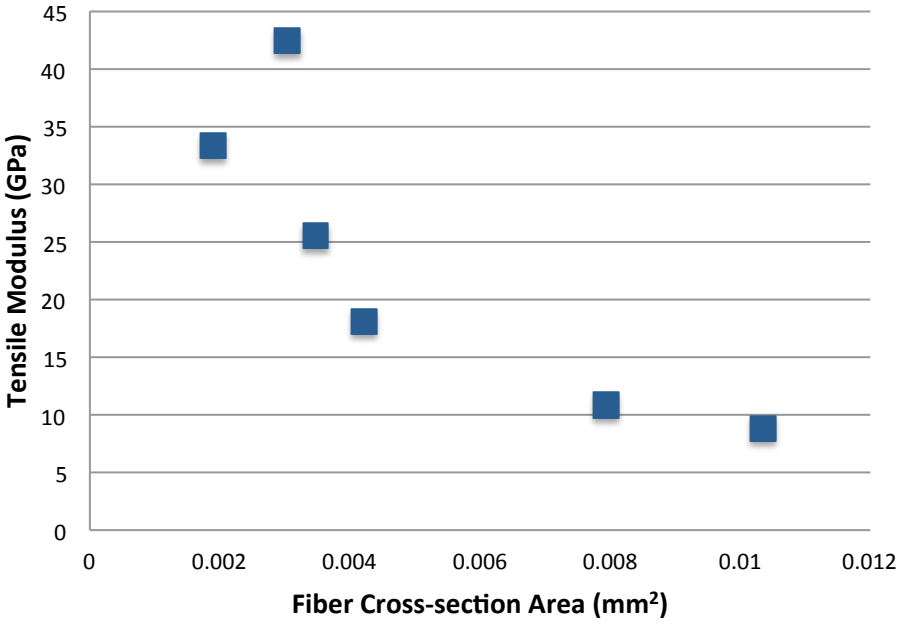

b

Figure 3.6 Experimental elastic moduli of flax: a) untreated flax, b) NaOH/Ethanol treated flax.

CHAPTER 4. CHEMICAL AND PHYSICAL PROPERTIES OF VE SYSTEMS

Resin system manipulations show some effects on cured resin, such glass transition temperature, crosslink density, CTE, hydrophilicity and elastic properties. These factors also affect the final properties of flax composites, especially the interfacial properties. The hydrophilicity of VE affects the wettability between flax and VE, which directly relates to the interfacial adhesion of flax composites. CTEs of VE and flax are used to evaluate the thermal residual stresses in flax composites, which can increase or decrease the mechanical interlocking between flax and VE. The changes of CTE are related to the changes of T_g and crosslink density in VE systems. The elastic properties of VE influence the mechanical properties of flax/VE composites. Thus, the study of different VE systems can help to evaluate the interfacial properties of flax/VE composites.

4.1. Curing Kinetics of VE Systems

The degree of cure or coversion of VE system can be calculated by Eqn. (4-1):

$$\alpha_t = \frac{\Delta H_{rxn} - \Delta H_{res}}{\Delta H_{rxn}} \equiv \frac{\Delta H_t}{\Delta H_{rxn}} \tag{4-1}$$

where α_t is denotes the degree of cure at curing time t (hr), ΔH_t is the liberated heat during time t, ΔH_{res} is the residual heat after time t, and ΔH_{rxn} is the total heat of reaction. Figure 4.1 shows the typical DSC temperature scans of unmodified and modified VE systems, which were uncured or isothermally cured at 50 °C for 12 and 48 hours. The integrated area of the exothermic peak was determined as the liberated heat in the DSC scan. The total heat of reaction (ΔH_{rxn}) and the residual heat after curing (ΔH_{res}) were obtained. With 48 hours of curing at 50 °C, unmodified and modified VE systems had achieved 100% curing. Table 4.1 presents the degree of cure or conversion of neat VE, VE with 1% AR and VE with 1.5% AR

at 50 °C for 12 hours. The degree of cure in VE system increases with the increasing of AR added into VE resin. It indicates AR additive can improve the mobility of carbon chain in VE in the vitrification, which leads to modified VE systems have higher curing degree.

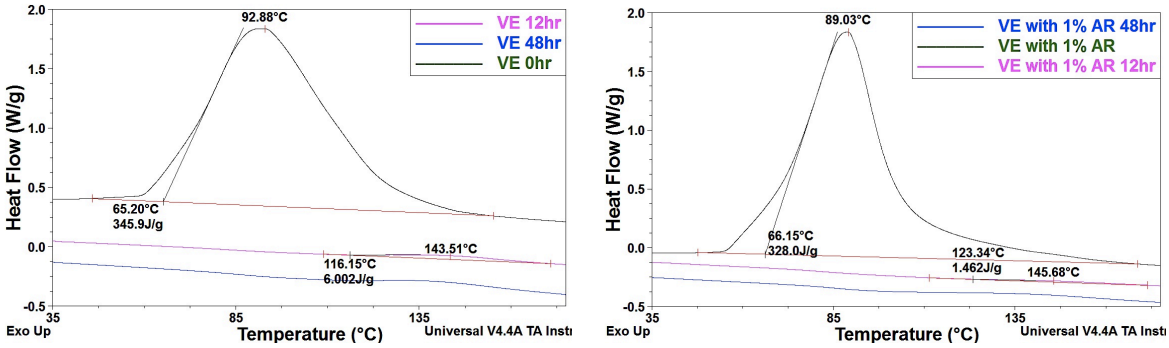

a **b**

Figure 4.1 DSC curves at 10 °C/min of neat VE system curing (a) and VE with 1% AR system (b) that have been cured at 50 °C for 0 hour, 12 hours and 48 hours.

Table 4.1 The Degree of Cure or Conversion of Unmodified and Modified VE Systems at 50 °C

Sample	Curing time t (hr)	ΔH_{res} (J/g)	ΔH_{rxn} (J/g)	The degree of cure
Neat VE	12	6.59	353.00	98.13
VE with 1% AR	12	1.46	328.00	99.55
VE with 1.5% AR	12	0.09	291.50	99.97

DSC describes the thermal equilibrium thermodynamics in the form of energy transfer—heat, throughout a process occuring at constant pressure. Table 4.2 lists the DSC curves of AR, neat VE, VE with 1% AR and VE with 1.5% AR. The absence of crystalline melting transitions indicates that these compounds are amorphous and not prone to crystallize. The jump in the $C_p = f(T)$ DCS curve indicates a second-order transition as the glass transition, in which there is no heat of transition. Thus, T_g is characterized by the heat capacity jump or heat capacity increase at the glass transition (ΔC_p). The glass transition temperature of VE with 1 % AR shows 10 °C increasing compared to the neat VE system. In addition, T_g of VE with 1.5 % is slightly increase than the neat VE system. The higher glass transition temperatures in modified VE systems usually indicates modified VE systems have

higher crosslink density. The crosslink densities of different VE systems will be discussed in section 4.3. The curing reaction of VE system is a copolymerization of styrene and vinyl ester (divinyl/vinyl monomers) and vinyl ester acts like the crosslinking reagent. Thus, the amount of vinyl ester in VE system is determined by the crosslink density of cured VE. Acrylic resin can increase the mobility of carbon chain of VE resin, which may lead to higher crosslink density in the cured VE, which results higher glass transition temperature of modified VE system. The higher T_g and higher crosslink density can increase the elastic modulus of cured VE resin. Thus, the elastic properties of flax/VE with AR should be higher than unmodified composites.

Table 4.2 The Glass Transition Temperatures of AR and VE Systems

Sample	AR	Neat VE	VE with 1% AR	VE with 1.5% AR
T_g (°C)	-35.82	121.85	131.24	125.63

The shrinkages after curing of neat VE, VE with 1% AR and VE with 1.5% AR are presented in Table 4.3. The shrinkage of neat VE is the lowest and its volume after curing decreases approximately 10%. On the other hand, the shrinkage of VE with 1% AR has highest volume change after curing. After the amount of AR added into VE resin increases to up 1.5% wt, the change of volume is reduced to 10.91%, which is close to the neat VE system. The shrinkages after curing are related to the thermal expansion of VE system and the thermal residual stresses generated by curing in the matrix. The difference of the shrinkages among the three VE systems indicates that AR additive changes CTEs of the VE systems, which will be discussed more in Chapter 6.

Table 4.3 The Shrinkages after Curing of Different VE Systems

Sample	Volume before Curing (mm^3)	Volume after Curing (mm^3)	Shrinkage (%)
Neat VE	142912.73	128563.86	10.04±0.37
VE with 1% AR	146178.24	127575.88	12.73±0.17
VE with 1.5% AR	144433.99	128669.81	10.91±0.65

4.2. FT-IR Spectroscopy

The FTIR spectrum of AR is shown in Fig. 4.2. The two small peaks at 2930 cm^{-1} and 2860 cm^{-1} are from C–H stretching and the sharp peak at 1730 cm^{-1} comes from C=O group. There is no evidence showing there is C=C bond existing in AR. The FTIR spectra of neat VE and VE with 1% AR are shown in Fig. 4.3. In the neat VE spectrum, C–H stretching (2899 cm^{-1}, 2807 cm^{-1}), carbonyl group (1706 cm^{-1}), C–H bending of CH_2 group (1450 cm^{-1}), and C–O (1114 cm^{-1}) were observed. The comparison of these two spectra indicated the presence of common chemical groups, e.g., the peaks from 2954 cm^{-1} and 2869 cm^{-1} are from C–H stretching, the peak at 1731 cm^{-1} is from carbonyl group, the peak at 1479 cm^{-1} is from C–H bending of CH_2, and the peak at 1160 cm^{-1} is from C–O. All these peaks showed a shift to a higher wavenumber and with a higher absorbance in the spectrum of VE with 1% AR. The peak shift can be caused by the similarity in functional groups of VE and AR and because of the modification of carboxyl and carbonyl behavior of AR by other functional groups present. A sharp peak was also observed at about 1444 cm^{-1} in the spectrum of VE with 1% AR, which is representative of C–H bending of CH_3 from AR. These FT-IR spectra prove that AR participates the polymerization of VE resin, which confirms the results from DSC. In addition, AR introduces more ester groups to the network of VE, which can increase the hydrophilicity of the VE system and improve the wettability between flax and VE resin. Thus, the existing of AR can improve the interfacial bonding between flax and VE, which is confirmed by the interfacial study of flax/VE composites in Chapter 5. However, the changes in the structure of the VE polymer chain cannot be predicted by FT-IR spectra.

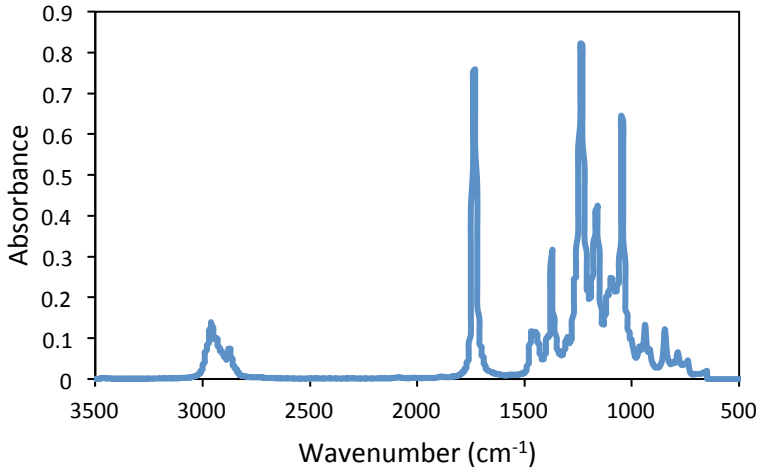

Figure 4.2 FT-IR spectrum of AR.

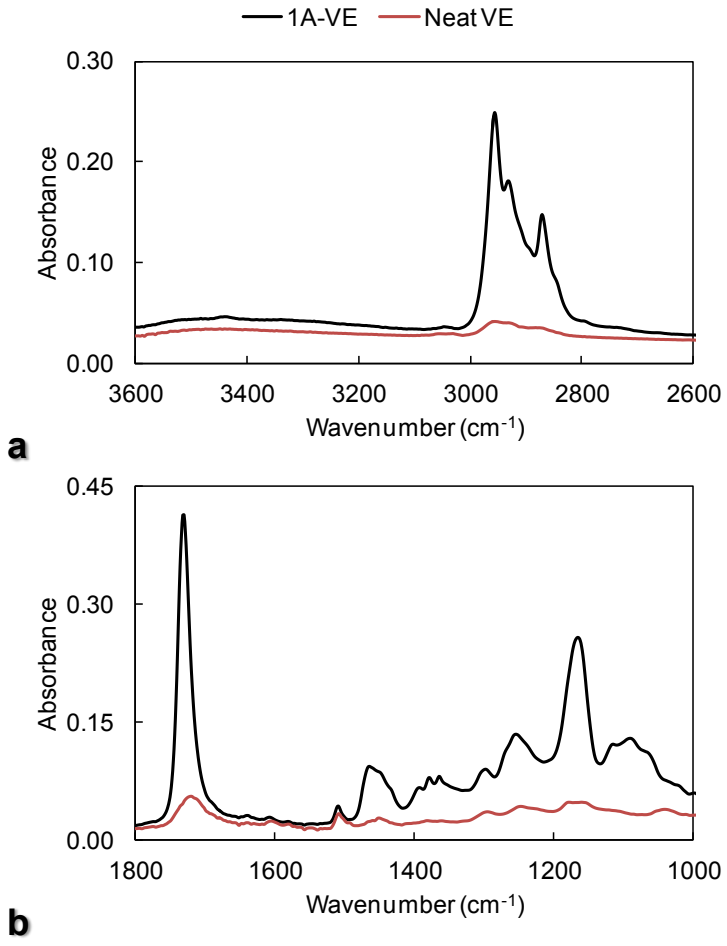

Figure 4.3 FT-IR spectra of neat VE and VE with 1% AR (1A-VE).

4.3. Thermal Properties of VE Systems

The coefficients of linear thermal expansion (CLTE) of neat VE, VE with 1% AR and VE with 1.5% AR in the region between 40 °C to 80 °C are listed in Table 4.4 measured by DMA. The thermal expansion of VE is not linear because there are two phases in the VE structure, which have different CTE. In this study, the composites are cured at room temperature and during the curing, the temperature of the panel raises a little. However, the temperature of the curing panel is lower than 80 °C. Thus, CLTEs of VE systems are evaluated from the region under 80 °C. CLTE of modified VE system are both higher than neat VE, which indicates AR added into VE system increase the sensitivity to the temperature. Meanwhile, DMA plot of modified system is more linear than neat VE, which is because AR reduces the separation of the two phases in VE and help two regions mix together. The effects of CTEs of different VE systems on the interfacial properties of flax/VE composites are discussed in Chapter 6.

Table 4.4 The Linear Coefficients of Thermal Expansion of VE Systems

Sample	CLTE (40 °C to 80 °C) μm/m•°C
Neat VE	19.66±0.89
VE with 1% AR	21.46±0.16
VE with 1.5% AR	22.65±0.12

DSC and DMA measure the glass transition temperature using different principles and T_g measured by DMA are more than 10 °C higher than those using DSC (Table 4.5). The peak position and transition breadth of the tan δ of each resin were determined using the crosslink density [79] in DMA and DSC measures the changes in heat flow in the transition region. The difference of glass transition temperature between neat VE and VE with 1% AR is smaller than DSC results. However, both measurements show the same trend of T_g values relating to AR ratios.

The crosslink density is an important factor related to the physical properties of cured VE, which higher crosslink density indicates higher elastic modulus. The crosslink density (ν_e) is calculated by Eqn. (4-2), which is derived from the theory of rubber elasticity:

$$E' = 3\nu_e RT \tag{4-2}$$

where *E'* is the storage modulus of thermoset in the rubbery plateau region, *R* is the gas constant, and *T* is the absolute temperature. The storage modulus in the rubbery plateau region is changed slightly with the temperature changes. The rubbery plateau region is approximate 30 °C above T_g. The storage modulus (E') and tan δ curves of the cured neat VE and VE with 1.5% AR are presented in Fig. 4.4. There are two phases in neat VE system, but there is only one phase shown in VE with 1.5% AR. With the increase of AR, the two phases' separation is decreased until disappeared. Crosslink densities of neat VE, VE with 1% AR and VE with 1.5% AR are presented in Table 4.5. It is observed that crosslink densities of modified VE systems are higher than that of neat VE, which indicates that acrylic resin also serves as the crosslinking reagent and leads to higher crosslinking during the curing of VE. In addition, higher crosslink density indicates higher elastic modulus of VE, which is confirmed in next section 4.4. On the other hand, AR additive does not show negative effects on the mechanical performance of VE resin and flax/VE composites.

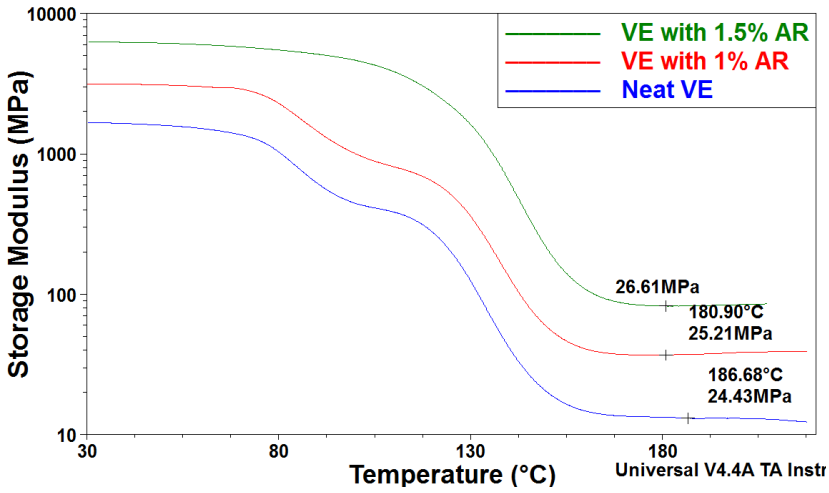

(a)

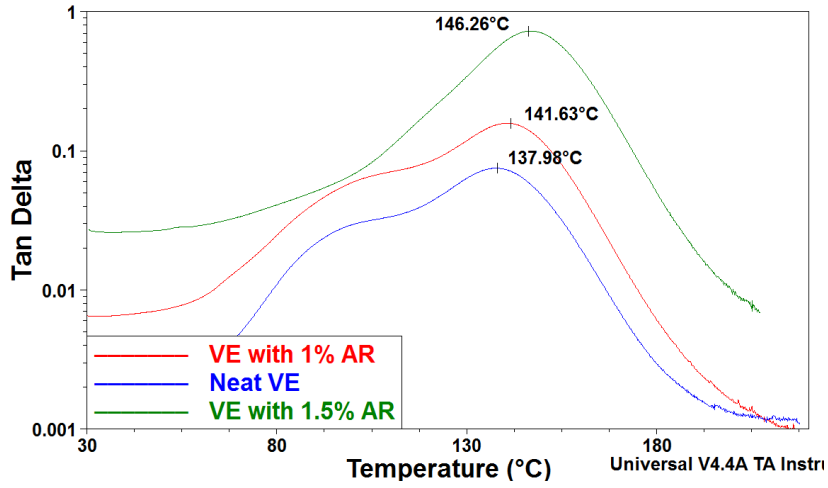

(b)

Figure 4.4 Storage modulus and tan δ versus temperature for neat VE and VE with 1% AR: a) storage modulus; b) tan δ.

Table 4.5 Dynamic Mechanical Properties and Crosslink Densities of Different VE Systems

Sample	T_g (°C)	E' (MPa) at 30 °C	E' (MPa) at T_g+30°C	v_e ($\times 10^{-3}$ mol/cm^3)
Neat VE	144.84±4.60	4221.50±248.19	18.45±4.69	1.69±0.43
VE with 1% AR	145.45±3.89	3891.00±281.21	25.34±0.83	2.26±0.07
VE with 1.5% AR	147.25±0.43	4497.67±41.40	26.63±0.31	2.36±0.03

4.4. Mechanical Performances of VE Systems

The results of the tensile tests of neat VE and VE with 1% AR are shown in Fig. 4.5. The tensile modulus of neat VE is 1.06±0.07 GPa and the tensile modulus of modified VE is 1.27±0.20 GPa. The additive AR increases the tensile modulus of VE system slightly, which agrees with the results of DMA. Higher crosslink density leads to higher elastic modulus. In addition, the increasing in their tensile strength is much clear, which the tensile strength of modified VE (42.97±2.87 MPa) is about 40% higher than that of neat VE (30.85±3.05 MPa). From the plots of tensile tests (Fig. 4.6), the neat VE system exhibited a clear ductile behavior. The specimens failed in plastic deformation after a short linear elastic portion. Neat VE is more plastic and shows a lower modulus than modified VE. The significant changes in the tensile properties were observed in VE with 1% AR system. The stress-strain curves still exhibited yielding and plastic deformation. However, there was a distinct transition from ductile to brittle behavior as a result of adding AR, as shown by the shape of the stress-strain curves.

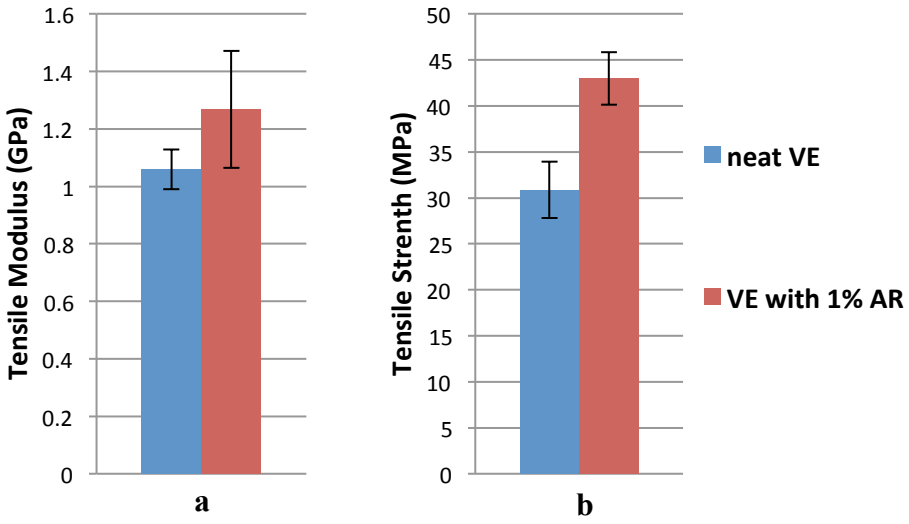

Figure 4.5 Comparisons of tensile properties of neat VE and modified VE: a) tensile modulus; b) tensile stregnth.

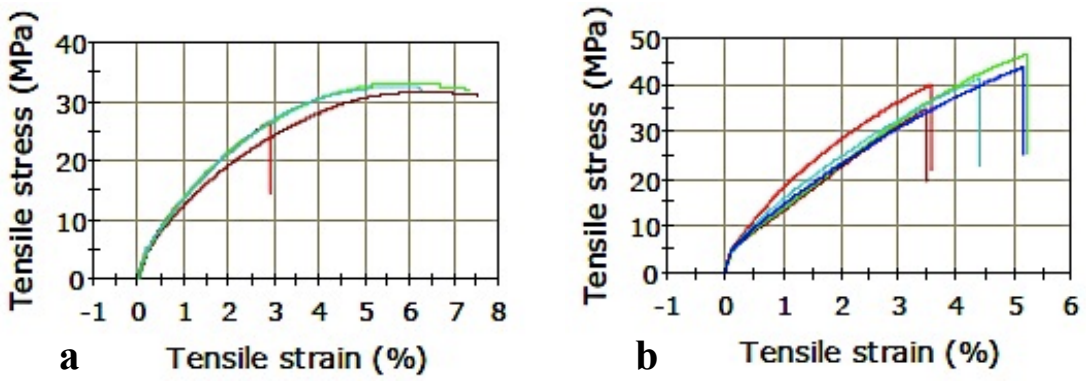

a b

Figure 4.6 Stress-Strain curves of VE systems: a) neat VE, and b) VE with 1% AR.

The flexural properties of both VE systems are presented in Figure 4.7. The flexural modulus of modified VE resin (1.40±0.02 GPa) is slightly higher than that of neat VE (1.32±0.04 GPa). AR additive changes the behavior of VE from more ductile into more brittle, which has been confirmed by the results of tensile tests. Thus, the flexural modulus of modified VE performs higher than that of neat VE. However, the flexural strength of both VE systems are similar with each other, which are around 47 MPa. In the flexural testing, the compressive load generated by bending leads to the fracture in VE. Thus, the changes in crosslink density of VE does not show significant improvement on the flexural strength of VE with 1% AR.

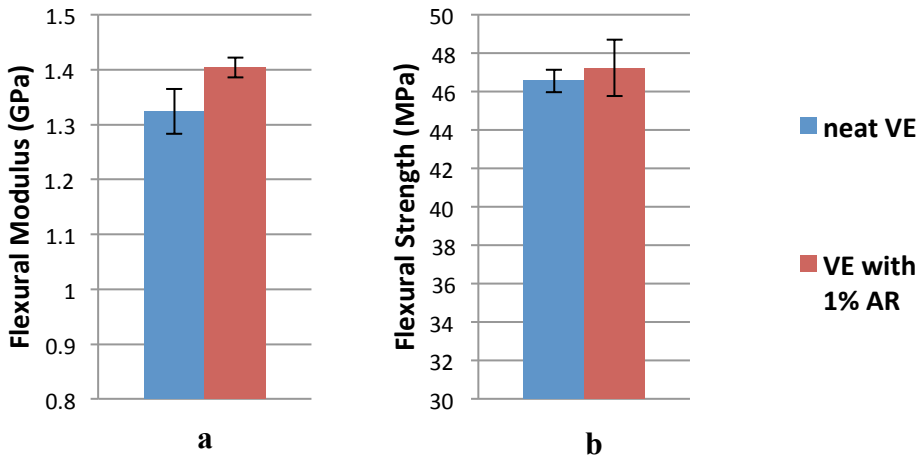

Figure 4.7 Comparison of flexural properties of neat VE and VE with 1% AR: a) flexural modulus; b) flexural strength.

4.5. Moisture Resistance of VE Systems

Figure 4.8 is a captured image by the camera to evaluate the water drop angle attached on the surface. The angle is formed by the tangent of the water drop and the resin surface. There is approximate 2 degree difference between neat VE and VE with 1% AR (Fig. 5.9). It indicates that the additive AR slightly increases the hydrophilicity of VE system, which improves the wettability between flax and VE matrix. In the chemical structure of AR there are large amounts of ester groups and carbonyl groups, which increase the hydrophilicity of the whole VE system. It is confirmed by their FT-IR spectra. Thus, AR additive improves the interfacial bonding between flax and VE matrix, which is confirmed by the study of interlaminar properties of flax/VE composites in Chapter 5.

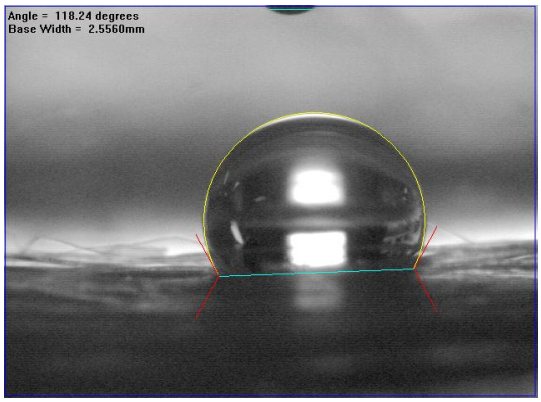

Figure 4.8 The image of the contact angle test.

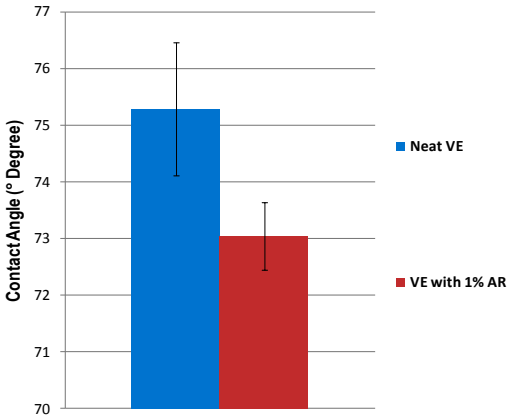

Figure 4.9 The contact angle comparison of neat VE and VE with 1% AR.

The moisture resistant properties of neat VE and modified VE systems are presented in Fig. 4.10. The moisture uptaking of VE with 1% AR is about 0.1% higher than neat VE after 10,000 hrs testing. The evidence proves that AR increases the hydrophilicity of VE system, which could increase the adhesion between flax and VE. The testing environment, such as temperature and humidity, can significantly affect the moisture absorption of the specimens, which led to a dramatic change in the results. However, this change did not affect the trend of the results.

Although water absorption profiles present a clear trend, it is interesting to determine and compare the values of water diffusivity in both systems. Table 4.6 is the water diffusivity of neat VE and VE with 1% AR. Water diffusivity *D* was calculated from the initial slope of the water absorption profiles shown in Fig. 4.10 using Eqn. (4-3):

$$D = \frac{\pi}{16}\left(\frac{h}{M_m}\right)^2\left(\frac{M_{t_2}-M_{t_1}}{\sqrt{t_2}-\sqrt{t_1}}\right)^2 \quad (4\text{-}3)$$

where *h* is the thickness of the specimen, M_m is the maximum water uptake of the specimen, M_{t_1} *and* M_{t_2} are the weights of the specimen at time t_1 and t_2, respectively. The value of t_1 and t_2 were chosen in the linear regime in Fig. 4.10. Water diffusivity of neat VE is smaller than that of VE with 1% AR. This can be attributed to the effect of AR.

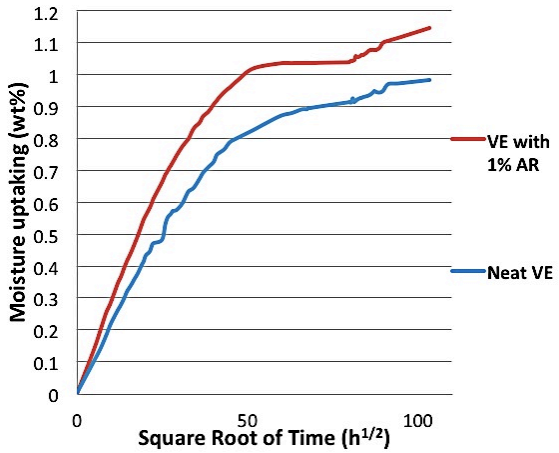

Figure 4.10 Moisture absorption of neat VE and VE with 1% AR.

Table 4.6 Water Diffusivity in neat VE and VE with 1% AR

Sample	M_m (%) (10,733 hrs)	D ($\times 10^{-6}$ mm^2/s)
Neat VE	0.9829	3.8558
VE with 1% AR	1.1470	5.3814

CHAPTER 5. CHEMICAL AND PHYSICAL PROPERTIES OF FLAX/VE COMPOSITES

5.1. Chemical Anaylsis

The steroscopy images of untreated and alkaline treated Canadian flax VE composites with oil red stain are presented in Fig. 5.1 a) and b). The oil red stain, which stained the vinyl ester material, indicated that the fibers became impregnated with vinyl ester resin even at a considerable distance from the resin and the movement of resin along the fibers. This movement prevented a pure source of fiber from being present for infrared analysis. Another attempt was made to look at isolated but resin-impregnated fibers stretched across and stretched over a circular opening of a microscope stage mount and secured at the ends with tab (Fig. 5.1 c) and d)). In this case, the total reflection mode was attempted. Spectra obtained in this way had very poor signal/noise and were not usable.

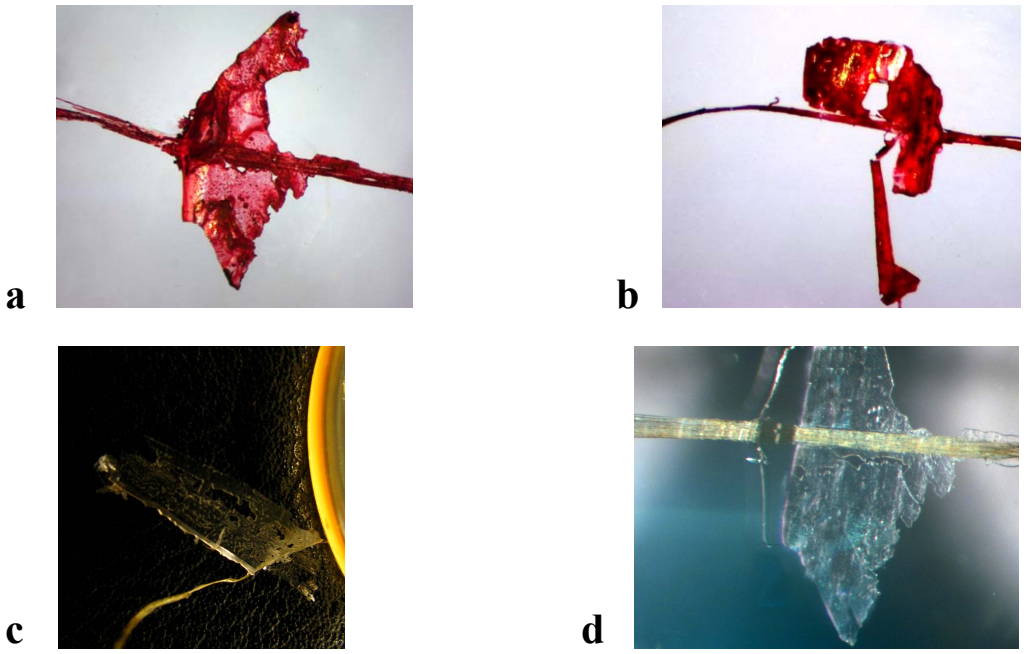

Figure 5.1 Canadian linseed flax in vinyl ester resin: a) stereoscope image of untreated flax/VE with oil red O; b) stereoscope image of NaOH/Ethanol treated flax/VE with oil red O; c) digital camera image of a fiber bundle prepared in resin

for IR; d) optical microscope image of fiber bundle with attached resin for IR.

The spectra in Fig. 5.2 were taken using a DuraScope ATR device, which shows neat VE, alkaline treated Canadian flax/ VE and alkaline treated Canadian flax/VE with 1% AR. All of the strong major band positions are marked. The spectra are dominated by bands from the two resins masking those of the flax fiber except in the O-H stretch region around 3371 cm^{-1}. The spectra in Fig. 5.3 were taken using a dedicated ATR microscope with samples positioned on IR reflecting slides. A stacked plot of infrared spectra is from alkaline treated Canadian linseed flax fiber in VE with 1% AR that was obtained with the IllminatIR II system. These spectral data were collected using a 25 µm x 25 µm aperture, which permitted analysis of fibers with less associated resin.

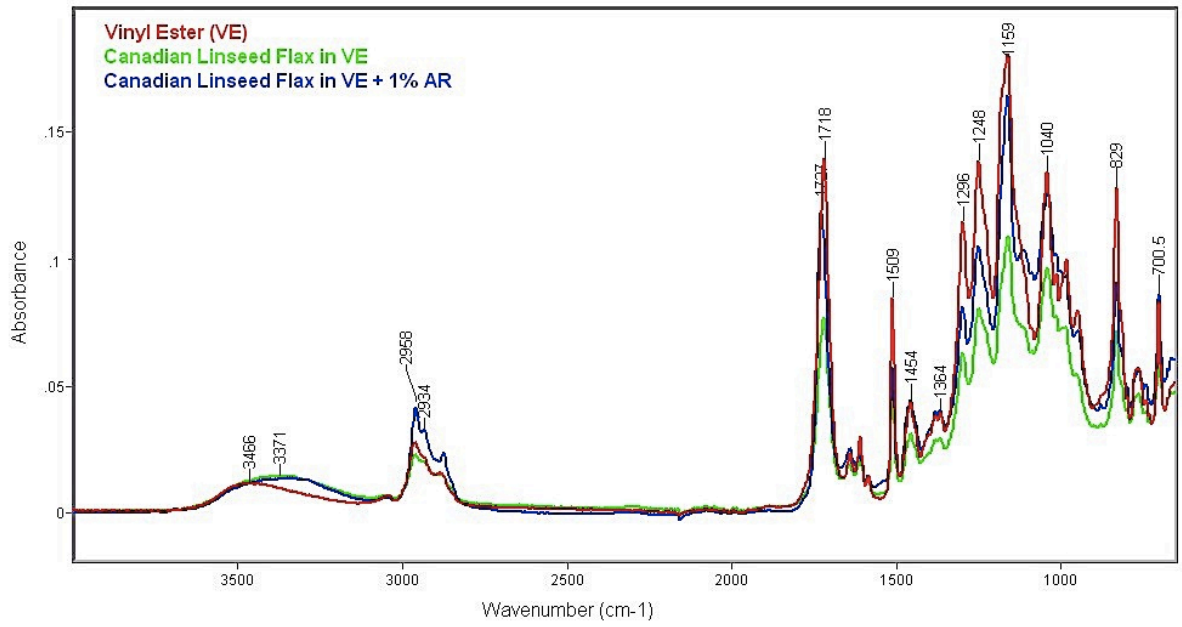

Figure 5.2 Infrared spectra comparison of neat VE, NaOH/Ethanol treated flax/VE and NaOH/Ethanol treated flax/VE with 1% AR.

In Figure 5.3 the comparison is among that of untreated clean isolated Canadian linseed fiber, without any evidence of waxes or aromatics, to that of isolated NaOH/Ethanol treated fibers in VE with 1% AR. The latter spectrum appears to indicate about equal portions of the resin to cellulosic fiber. The spectrum of the treated fiber imbedded in VE

with 1 % AR takes on the look of that of the resin by itself. The largest change in going from untreated clean flax fiber to resin-imbedded fiber appears to be the loss of O-H stretch vibrations. This finding might indicate just the suppression of hydrogen bonding or could indicate the formation of covalent bonding between cellulose and the resin.

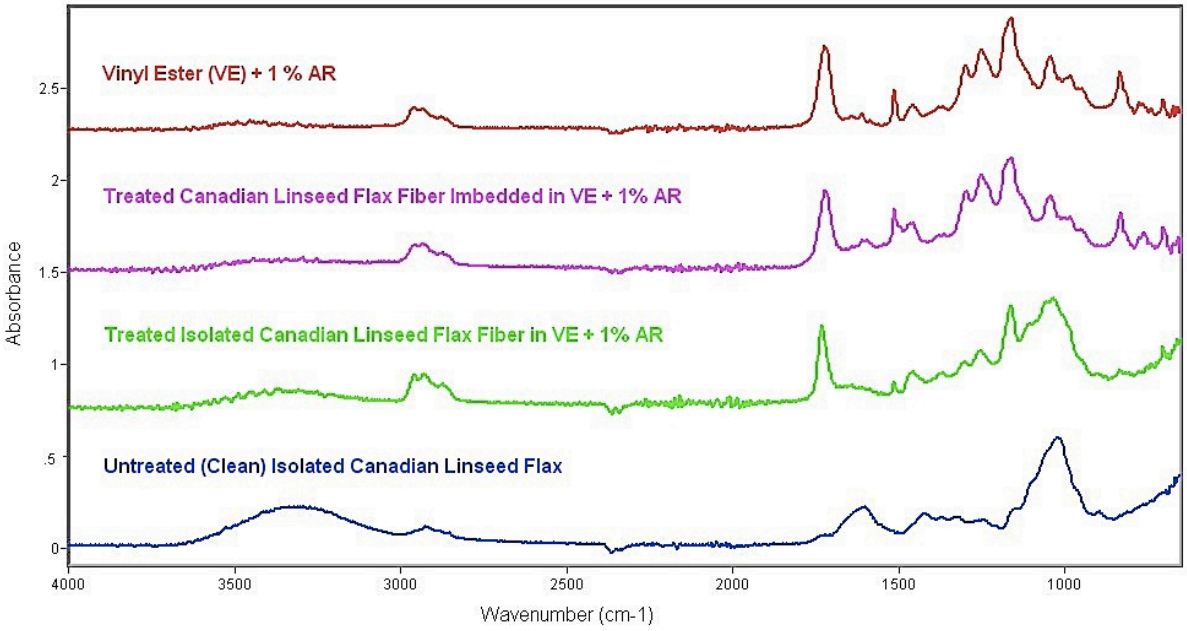

Figure 5.3 Stacked plot of infrared spectra of untreated flax, treated flax/VE with 1% AR and VE with 1% AR.

5.2. Mechanical Properties

In this section, the results of different mechanical tests are presented by the specific results, which are normalized the densities of flax/VE composites. The density of flax changes before and after the chemical modification. In addition, the fiber volume fraction of different composite panels is varied. The range of the fiber volume fraction of flex/VE composites is between 45% and 50%. The density of different composite panels is changed with their fiber volume fraction. Thus, the specific results reduce the effects of the density change in untreated and treated fiber and take the variation of fiber volume fraction into

account. The densities and fiber volume fraction of different flax/VE composites are presented in Appendix C.

5.2.1. Interfacial Properties

The interfacial properties of flax/VE composites are evaluated by short beam shear tests and fiber bundle pull-out tests. The results of short beam shear tests of flax/VE composites are presented in Fig. 5.4 and Table 5.1 to compare the interlaminar properties of the flax/VE composites. Interlaminar shear strength (ILSS) is a function of fiber to matrix bonding. Higher ILSS values indicates better interfacial adhesion between fiber and matrix. A successful short beam test is in which the failure initiates at the interface between fiber and matrix. And the tight tolerances should be maintained in the specimen dimensions. There is barely any clear failure on the surface of the specimens observed. Comparing the untreated and treated flax composites, it is observed that both surface treatments on flax and resin manipulations improved the interlaminar shear strength. This implies that all treatments enhance the adhesion between fiber and matrix.

It is observed that the interlaminar shear strength of treated flax/VE is 226% higher than that of untreated flax/VE and the specific ILSS of treated flax/VE is 216% higher than that of untreated flax/VE. The differences between untreated and treated flax composites are due to the effect of alkaline treatment. Alkaline treatment removes the non-cellulosic chemicals, which provides rough surface of flax, and sparates the big fiber bundles into smaller fiber bundles, which increases the contact area between fiber and matrix. All these effects increase the mechanical interlocking between flax and VE. In addition, alkaline treatment exposes more cellulose molecules on the fiber surface, which increases the chances to form hydrogen bonds between cellulose and VE. Both mechanical interlocking and hydrogen bonds can increase the interlaminar shear strength of the composites.

The interlaminar shear strengths of treated flax/VE with 1% wt. AR and treated flax/VE with 1.5% wt. AR both show slightly increasing than treated flax/VE. AR as an additive increases the hydrophilicity of VE system according to the results of moisture absorption and contact angle tests, which can reduce the repulsion between flax and VE. However, there is no evidence that there is any type chemical bonds existing between flax and VE with AR from the spectra of FT-IR of flax composites. Thus, AR does not introduce or form any chemical bonds with flax to increase the interfacial properties of the composites. The misalignment of fiber bundles in the composites can increase the standard deviation of the tests' results. Moreover, the variation of the fiber volume fraction in different composites introduces some differences in the final results.

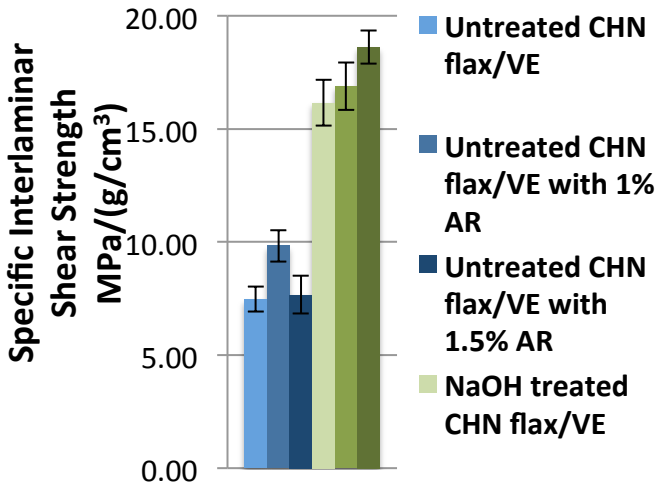

Figure 5.4 Comparison of specific interfacial shear strength of different types of flax/VE composites.

Fiber bundle pull-out tests were also performed to assess the quality of interfacial bonding between fiber and matrix. The results of the fiber bundle pull-out tests of flax/VE are shown in Table 5.1 and Fig. 5.5. The interfacial shear strength of treated flax/VE is slightly higher than untreated flax/VE and the similar situation for the results with AR additive. However, the trend is not as clear as the results of ILSS of their composites. The fiber bundles used for the pull-out tests were selected carefully and most

of the fiber bundles are very clean. Thus, the treatment does not show significant effects on the interfacial shear strength. In addition, only limited amount of fiber bundles were surrounded by abundance of resin, which reduces the possibility to form voids. On the other hand, the errors generated during the microscopy measurements can introduce larger standard deviation to the final results. However, without considering the standard deviations, the trend of the interfacial shear strength is similar to that of the interlaminar shear strength.

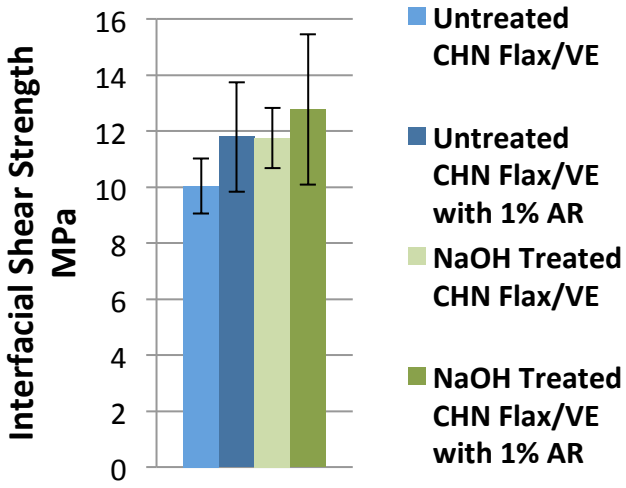

Figure 5.5 Comparison of interfacial shear stength of Chinese flax/VE composites.

Table 5.1 Interfacial Properties Comparison of Chinese Flax/VE Composites

Sample	Interlaminar Shear Strength (MPa)	Density (g/cm^3)	Fiber Volume Fraction (%)	Interfacial Shear Strength (MPa)
Untreated CHN Flax/VE	9.46±0.69	1.27±0.01	41.72	10.04±0.98
Untreated CHN Flax/VE with 1% AR	12.63±0.90	1.28±0.02	44.00	11.79±1.96
Untreated CHN Flax/VE with 1.5% AR	9.27±1.01	1.21±0.04	39.18	-
EtO^-Na^+ treated CHN Flax/VE	21.44±1.35	1.33±0.03	44.28	11.75±1.08
EtO^-Na^+ treated CHN Flax/VE with 1% AR	22.30±1.39	1.32±0.02	44.65	12.77±2.68
EtO^-Na^+ treated CHN Flax/VE with 1.5% AR	24.28±0.96	1.30±0.01	40.24	-

5.2.2. Flexural Properties

Flexural properties of composites are functions of fiber strength, matrix strength and the efficiency of load transfer. The correct failure should take place by breaking of fibers and not by interlaminar shear (which is discussed in the 5.2.1). The compression failure is the main failure mode observed on the surface of the specimens. The debonding failure is also detected on some specimens. The specific flexural properties of untreated and treated flax/VE with/without AR are presented in Fig. 5.6 and the actual values are shown in Table 5.2, measured by three-point bending tests.

The actual and specific flexural moduli of the flax composites are similar to the results of fiber bundle pull-out tests and the trend is not significant. The flexural moduli of the composites are related to the structural variation in the flax fiber cells. The swelling and partial removal of non-cellulosic chemicals in flax fibers decrease the resistance of microfibrils to stretching [78]. NaOH/Ethanol treated flax/VE with AR (1% and 1.5%) perform the best in specific flexural modulus and the composites with 1% AR shows the highest, which indicates AR increases the interfacial bonding between fiber and matrix.

The trend of flexural strength of flax/VE composites is very clear, which is similar to the results of short beam shear tests. The treated flax composites perform much better than untreated flax composites, which is because of the effects of alkaline treatment. Untreated flax/VE with AR composites show slightly increasing in the flexural strength, which is because AR additive increases the wettability between fiber and matrix. However, there is no increasing in flexural strength of treated flax/VE with AR. The interface between flax fiber and orientation of microfibrils plays an important role. Some coiled fibrils in flax fibers are loosened [17] during the alkaline treatment and these fibrils can contribute to uncoiling when a bending force is applied, which leads to the reduction in interfacial stress transfer. On the other hand, compression failure dominates in the flexural tests. The local microbuckling of

fibers would be the same amount in modified or unmodified flax/VE composites. Thus, the improvement in flexural strength is not significant in treated flax/VE with AR.

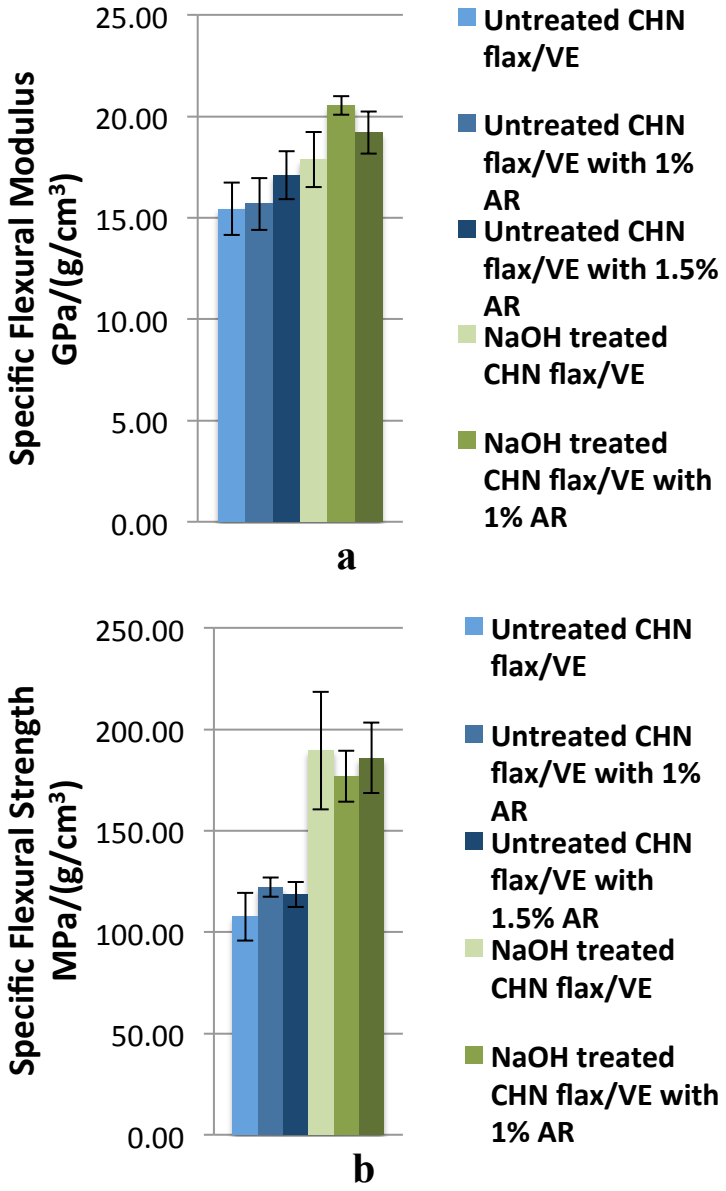

Figure 5.6 Comparison of specific flexural properties of Chinese flax/VE composites: a) specific flexural modulus; b) specific flexural strength.

Table 5.2 Flexural Properties Comparison of Chines Flax/VE Composites

Sample	Flexural Modulus (GPa)	Flexural Strength (MPa)	Density (g/cm^3)	Fiber Volume Fraction (%)
Untreated CHN Flax/VE	19.89±1.66	138.61±15.20	1.29±0.02	45.12
Untreated CHN Flax/VE with 1% AR	20.13±1.64	156.76±6.08	1.28±0.02	44.00
Untreated CHN Flax/VE with 1.5% AR	20.67±1.43	143.36±7.51	1.21±0.04	39.18
EtO^-Na^+ treated CHN Flax/VE	23.51±1.43	249.38±38.06	1.32±0.03	40.91
EtO^-Na^+ treated CHN Flax/VE with 1% AR	27.11±0.61	233.62±16.67	1.32±0.02	44.65
EtO^-Na^+ treated CHN Flax/VE with 1.5% AR	25.02±1.95	242.32±22.59	1.30±0.01	40.24

5.2.3. Tensile Properties

Tensile properties are analyzed to correlate the effects of both fiber loading and processing methodology upon unidirectional flax fiber composites. The results of tensile tests of flax composites are presented in Fig. 5.7 and Table 5.3. The specific tensile modulus of untreated flax/VE is the lowest, which is similar to its specific tensile strength. It means all the surface treatments and modifications improve the tensile performance of flax/VE composites.

Untreated flax/VE with AR composites perform better than untreated flax/VE in tensile modulus and specific tensile modulus. The specific tensile modulus of untreated flax/VE with 1% AR shows approximate 24% higher than that of untreated flax/VE. It indicates AR additive helps the load transfer between matrix and fiber by increasing the interfacial adhesion between fiber and matrix, which is confirmed by the results of ILSS that AR improves the interfacial properties of flax composites. Moreover, AR additive increases the elastic modulus of VE according to the results from the study of resin system. Thus, the tensile modulus of flax/VE with AR composites can be increased with AR. However, treated flax/VE with 1% AR composites show the similar specific tensile modulus to that of treated

flax/VE, which all are close to the specific tensile modulus of untreated flax/VE with AR composites. In tensile tests, the properties of flax fiber dominate the tensile performance of their composites. The chemical treatment applied in this study has minimum effects on the properties of flax. The flax fiber bundle structure is varied during the alkaline treatment [80]. Some chemical modifications on the surface of flax can damage fibers, such as the hydrolysation of cellulose during the treatment, which have been proved in the previous work [65]. The similarity in specific tensile modulus of modified composited is because of the minimum changes in the flax properties. In addition, the variation of fiber orientation in different composites' panel can affect their mechanical performance. The standard deviation of treated flax/VE with 1% AR is quite large, which indicates the existance of misalignment of flax or voids in their composites. On the other hand, the specific tensile modulus of treated flax/VE with 1.5% AR shows the best performance, which is about 30% higher than other modified flax composites. This increase confirms the effect of AR on the mechanical properties of VE.

The trend of the specific tensile strengths of flax composites is similar to the trend of their ILSS and specific flexural modulus. The specific tensile strengths of treated flax composites are higher than those of untreated flax composites. NaOH/Ethanol treated flax/VE performs 67% higher than untreated flax/VE in specific tensile modulus. In addition, The specific tensile strength of NaOH/Ethanol flax/VE with 1% AR shows approximate 135% increasing compared to that of untreated flax/VE with 1% AR. These significant increase in specific tensile strength is because alkaline treamtent can change the crystallinity of cellulose [19]. The crystal structure changes of cellulose during alkaline treatment has been proved by the FT-IR spectra. The specific tensile stength of treated flax/VE with 1.5% AR shows slightly decrease compared to treated flax/VE with 1% AR. However, the standard deviations of tensile results are in a wide range. The misorientation of flax fiber during

composites' processing can increase the variation of the tests' results. In addition, the fiber volume fraction of different flax composites varied and some of the changes in the composites' density are inconsistent with their fiber volume fraction, which is due to the changes of the voids in the composites.

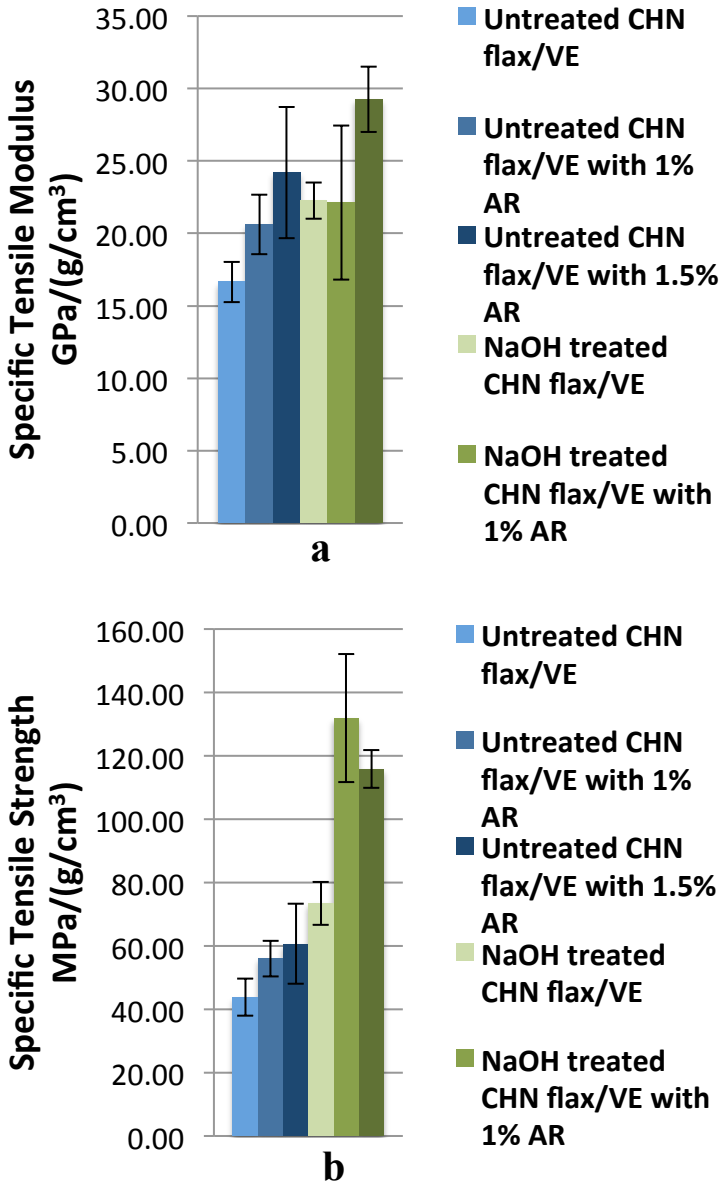

Figure 5.7 Comparison of specific tensile properties of Chines flax/VE composites: a) specific tensile modulus; b) specific tensile strength.

Table 5.3 Tensile Properties Comparison of Chinese Flax/VE Composites

Sample	Tensile Modulus (GPa)	Tensile Strength (MPa)	Density (g/cm^3)	Fiber Volume Fraction (%)
Untreated CHN Flax/VE	21.13±1.77	55.69±7.48	1.27±0.05	50.34
Untreated CHN Flax/VE with 1% AR	26.14±2.61	71.01±7.18	1.27±0.03	45.71
Untreated CHN Flax/VE with 1.5% AR	30.63±5.74	76.80±16.07	1.27±0.04	46.82
EtO^-Na^+ treated CHN Flax/VE	28.63±1.61	94.39±8.74	1.29±0.07	45.59
EtO^-Na^+ treated CHN Flax/VE with 1% AR	29.46±7.09	175.71±26.98	1.33±0.01	46.40
EtO^-Na^+ treated CHN Flax/VE with 1.5% AR	38.61±2.97	115.86±7.89	1.32±0.02	45.13

5.3. XRD Results

Flax/VE (unmodified and modified) composites containing isolated small spherical filler particles (Al powders) were prepared. The concentration of Al powder ethanol solution was selected after preliminary experiments. In the preliminary study, 0.1%, 0.3% and 0.5% Al/ethanol slurries were prepared to distribute Al uniformly into alkaline treated flax. The treated flax fibers with Al powder were processed into composites panels, which were used for X-ray diffraction. A 0.5% Al ethanol slurry provided XRD signals, which the intensity was strong enough to distinguish the small changes of X-ray diffraction angles. On the other hand, the small spherical Al particles in the composites were very small amounts, so the Al powder's contribution to the stress state of the specimen can be neglected. The spherical Al particles were evenly distributed in the flax/VE composites to form the intralaminar composite architecture. The XRD spectra of Al powder in treated flax/VE with 1% AR from different angles (φ and ψ) are presented in Fig. 5.8. The direction φ=0° was chosen parallel to the fibers' direction and φ=90° was the transverse direction. Three ψ angles were selected between 0° to 45° for each φ angle. It is observed that the differences of 2θ from (422) plan from different measured angles (φ and ψ) are fairly small and the peak separation was carried

out by least-squares fitting by Gaussian functions. The lattice spacing d_0 for different angles are listed in Table 5.4, which the lattice spacings d_0 were calculated using Bragg's law.

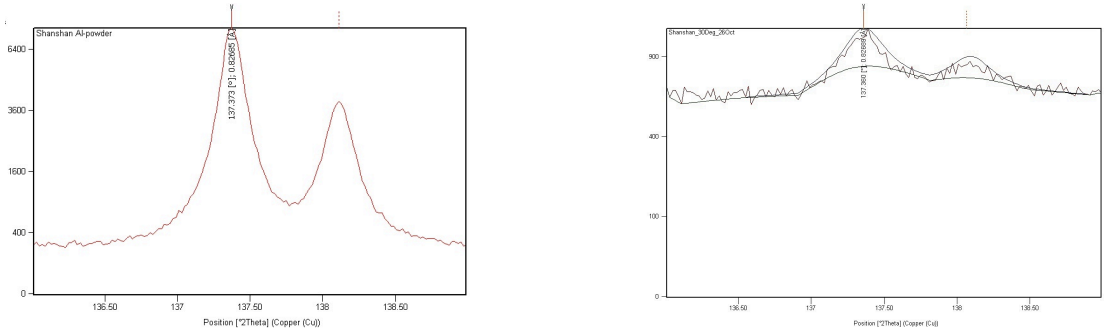

a **b**

Figure 5.8 X-ray diffraction spectra of pure Al powder (a) and treated flax/VE at φ=0° and ψ=30° (b).

Table 5.4 The Lattice Spacings of Flax/VE Composites at Different Angles for Al

Sample	$Sin^2\psi$	d_0 (Å) φ=0°	d_0 (Å) φ=90°
Flax/VE	0.00	0.8269	0.8269
	0.25	0.8268	0.8269
	0.50	0.8268	0.8270
Flax/VE with 1% AR	0.00	0.8270	0.8267
	0.25	0.8269	0.8269
	0.50	0.8268	0.8270

5.3.1. Sine Squared Psi Method

Hauk [81] gives formulas to determine the principal stresses σ_1, σ_2 and σ_3 in polycrystalline specimens and the shear stresses σ_{12}, σ_{23} and σ_{31} are neglected. In this study, 11, 22 and 33 correspond to the direction inside the inclusion x, y and z respectively. The strain measured in the direction defined by φ and ψ is given by Eqn (1-8) and (1-10). Eqn. (1-10) can be written as:

$$\sigma_{11} - \sigma_{22} = \frac{1}{\frac{1}{2}s_2^{hkl}} \frac{\partial \varepsilon_{\varphi=0,\psi}}{\partial sin^2\psi} \tag{5-1}$$

where $\frac{\partial \varepsilon_{\varphi=0,\psi}}{\partial sin^2\psi}$ is the slope of the $\varepsilon_{\varphi=0,\psi}$ vs. $sin^2\psi$ plot.When φ=0 and ψ were varied, Eqn. (1-10) can be written as:

$$\sigma_{22} - \sigma_{33} = \frac{1}{\frac{1}{2}S_2^{hkl}} \frac{\partial \varepsilon_{\varphi=90,\psi}}{\partial sin^2\psi} \tag{5-2}$$

where $\frac{\partial \varepsilon_{\varphi=90,\psi}}{\partial sin^2\psi}$ is the slope of the $\varepsilon_{\varphi=90,\psi}$ vs. $sin^2\psi$ plot. In addition, σ_{33} can be written as:

$$\sigma_{33} = \frac{\frac{d_{\varphi=0,\psi=0} - d_0}{d_0} - S_1^{hkl}(\sigma_1 + \sigma_2)}{S_1^{hkl} + \frac{1}{2}S_2^{hkl}} \tag{5-3}$$

The principal strains and principal stresses can be calculated by equations (5-1)-(5.3). But this method is not valid if the $\varepsilon_{\varphi,\psi}$ vs. $sin^2\psi$ plots are oscillatory.

5.3.1.1 X-ray elastic constants

X-ray elastic constants (XEC) can be obtained using single crystal elastic constants S_{11}, S_{12} and S_{66} for cubic symmetry. The following equations can be obtained for the Voigt and Reuss models [54]:

Voigt:

$$S_1^V = \frac{(2S_{11} - 2S_{12} - S_{44})(S_{11} + 2S_{12}) + 5S_{12}S_{44}}{2(3S_{11} - 3S_{12} + S_{44})} \tag{5-4}$$

$$\frac{1}{2}S_2^V = \frac{5(S_{11} - S_{12})S_{44}}{2(3S_{11} - 3S_{12} + S_{44})} \tag{5-5}$$

Reuss:

$$S_1^R(hkl) = S_{12} + (S_{11} - S_{12} - \frac{S_{44}}{2}) \frac{h^2k^2 + k^2l^2 + l^2h^2}{(h^2 + k^2 + l^2)^2} \tag{5-6}$$

$$\frac{1}{2}S_2^R(hkl) = S_{11} - S_{12} - 3(S_{11} - S_{12} - \frac{S_{44}}{2}) \frac{h^2k^2 + k^2l^2 + l^2h^2}{(h^2 + k^2 + l^2)^2} \tag{5-7}$$

where h, k and l are Miller's indices. The single crystal elastic constants S_{11}, S_{12} and S_{44} [77] and the average XEC calcuated by Voigt and Reuss models and for Al are presented in Table 5.5.

Table 5.5 Single Crystal Elastic Constants and XEC for Al powder

Inclusion	S_{11} (10^{-3} GPa^{-1})	S_{12} (10^{-3} GPa^{-1})	S_{44} (10^{-3} GPa^{-1})	S_1(hkl) (10^{-3} GPa^{-1})	$\frac{1}{2}S_2$(hkl) (10^{-3} GPa^{-1})
Al (422)	15.8	-5.8	35.8	-4.9	19.0

The stress and the strain measured at φψ direction can be calculated by Eqn (5-8) and (5-9):

$$\sigma_{\varphi\psi} = \sigma_{11}cos^2\varphi sin^2\psi + \sigma_{22}sin^2\varphi sin^2\psi + \sigma_{33}cos^2\psi \tag{5-8}$$

$$\varepsilon_{\varphi\psi} = \varepsilon_{11}cos^2\varphi sin^2\psi + \varepsilon_{22}sin^2\varphi sin^2\psi + \varepsilon_{33}cos^2\psi \quad (5\text{-}9)$$

5.3.2. Least Squares Method

The least squares method can be applied to Eqn. (1-8) and (1-10) to obtain least squares values of the principal stresses and principal strains. If there are shear stresses and strains existing in the system, the least squares method can be applied. If there are no shear stresses and strains, the linear squares method can be used. The $\varepsilon_{\varphi\psi}$ vs. $\sin^2\psi$ plots should be non-oscillatory when this method is appled.

5.3.3. Aluminum Filler

The normal strain ε_{33} was obtained from the average between $\varepsilon_{\varphi=0,\ \psi=0}$ and $\varepsilon_{\varphi=0,\ \psi=90}$. The least squares method was applied to determine the slope of the line on $\varepsilon_{\varphi\psi}$ vs. $\sin^2\psi$ plot. ε_{11} and ε_{22} were calcuated from the slopes of $\varepsilon_{\varphi\psi}$ vs. $\sin^2\psi$ plot at φ=0° and 90° respectively. Figure 5.9 presents the plots of $\varepsilon_{\varphi\psi}$ vs. $\sin^2\psi$ of differen flax/VE composites.

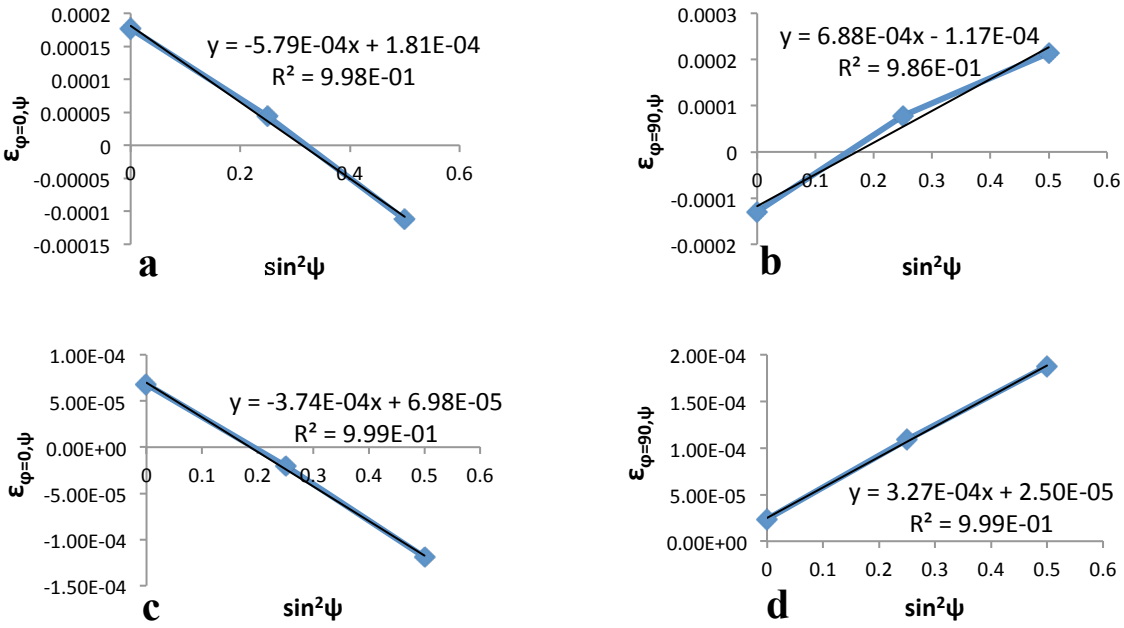

Figure 5.9 Plots of $\varepsilon_{\varphi\psi}$ vs. $\sin^2\psi$ of different flax/VE composites: a) φ=0° and b) φ=90° are from flax/VE; c) φ=0° and d) φ=90° are from flax/VE with 1% AR.

X-ray elastic constants at (422) plan obtained in 5.3.1 are used to calculate Young's modulus *E* and Poisson ratio ν values of Al by Eqn. (5-10) and (5-11):

$$S_1 = -\frac{\nu}{E} \tag{5-10}$$

$$\tfrac{1}{2}S_2 = \frac{1+\upsilon}{E} \tag{5-11}$$

As a result, *E* is 71 GPa and ν is 0.351. Assuming the material is isotropic, the stresses were calucated from the strains by generalized Hooke's law. Table 5.6 presents the strains and stresses inside Al inclusions.

Table 5.6 Strains and Stresses inside Al Powders

Sample	ε_{11} (10^{-6})	ε_{22} (10^{-6})	ε_{33} (10^{-6})	σ_{11} (MPa)	σ_{22} (MPa)	σ_{33} (MPa)
Al in Flax/VE	719.86	-547.12	31.85	50.50	-16.09	14.34
Al in Flax/VE with 1% AR	374.54	-327.06	47.38	25.56	-11.31	8.36

5.3.4. Stresses from Matrix

There are no external stresses applied on the composite, so the stresses inside the Al inclusion are related to the thermal residual stresses generated by the matrix. It can be seen that the residual stress $\sigma_{residual}$ depends on both matrix and the inclusion properties and the residual strain due to the thermal expansion misfitting can be expressed as:

$$\varepsilon^T = (\alpha_M - \alpha_I)\Delta T \tag{5.14}$$

where α_M stands for the coefficient of thermal expansion of the matrix, α_I is the coefficient of thermal expansion of the inclusion, and $(\alpha_M - \alpha_I)$ denpends on the direction.

After obtaining the stress state inside the Al inclusion, the stresses in matrix can be assessed. Eshelby's inclusion theory is one of the most often applied theorical methods to evaluate the stresses in matrix. In Eshelby model, the ellipsoidal inclusions are randomly distributed within the matrix and the stress in the inclusion is uniform. Using the condition of microstress balance expressed in Eqn. (5.15),

$$(1-f) < \sigma_M > + f < \sigma_I >= 0 \tag{5.15}$$

where *f* is the fraction of inclusion I in a matrix M. Using the principal of equivalent inclusion and traction forces at the interfaces, the stresses generated from matrix can be calculated. The stress transfer factors as a matrix with three components along the first diagonal should be considered.

$$\sigma_{AI} = k\sigma_M \tag{5.16}$$

where

$$k = \begin{bmatrix} k_{11} & 0 & 0 \\ 0 & k_{22} & 0 \\ 0 & 0 & k_{33} \end{bmatrix} \tag{5.17}$$

The stress transfer factors are related to the properties of matrice and inclusions. Assuming the matrix is homogeneous and isotropic, Hauk [81] gave the figures which provide the relation between stress transfer factor vs. logarithm of ratio Young's moduli $\log(E_{matrix}/E_{inclusion})$. According to the figures, k_{11} is 1.9, k_{22} *and* k_{33} are -0.3. The stresses from VE matrices can be calculated by Eqn. (5.16). The strains in matrix were calculated by generalized Hooke's law. Table 5.7 is listed the stresses and strains from both VE and VE with 1% AR. In the next chapter, the effects of these stresses and strains in the matrix will be discussed.

Table 5.7 Stresses and Stains from VE and VE with 1% AR

Sample	σ_{11} (MPa)	σ_{22} (MPa)	σ_{33} (MPa)	ε_{11} (10^{-6})	ε_{22} (10^{-6})	ε_{33} (10^{-6})
VE in Flax/VE	26.58	53.63	-47.79	0.023	0.058	-0.075
VE in Flax/VE with 1% AR	13.45	37.72	-27.87	0.0075	0.034	-0.038

5.4. Moisture Resistance

The results of the moisture absorption study in Chapter 4 show that AR increases the moisture uptake of VE system. The moisture resistance of natural fiber composites is important for their application and degradation. Thus, the moisture absorption of flax/VE

composites needs to be investigated in future studies. The following section discusses the moisture resistance of flax/VE composites and their flexural behaviors with small amount of moisture uptake.

5.4.1. Moisture Absorption

Water absorption profiles for the untreated and treated flax/VE with 1% AR composites are presented in Fig. 5.10 and the immersed time is 1896 hrs. The fiber volume fraction of flax/VE with 1% AR composites was controlled about 47%. The water uptake of untreated flax composites is approximate 6% more than alkaline treated flax composites. NaOH treatment cleans the surface of fibers, which leads to better adhesion between fiber and matrix and better water resistance for the composites. Table 5.8 is the water diffusivity of untreated and treated flax fiber reinforced composites. Water diffusivity of NaOH treated flax composites was lower than those of untreated flax composites. This can be attributed to the good adhesion between fiber and matrix and the lower fiber volume fraction.

Table 5.8 Water Diffusivity in European Flax/VE Composites

Sample	M_m (%) (1896 hrs)	D ($\times 10^{-6}$ mm^2/s)	V_f (%)
Untreated EU flax/VE with 1% AR	20.60	4.66	47.44
EtO^-Na^+ treated EU flax/VE with 1% AR	14.99	3.02	46.97

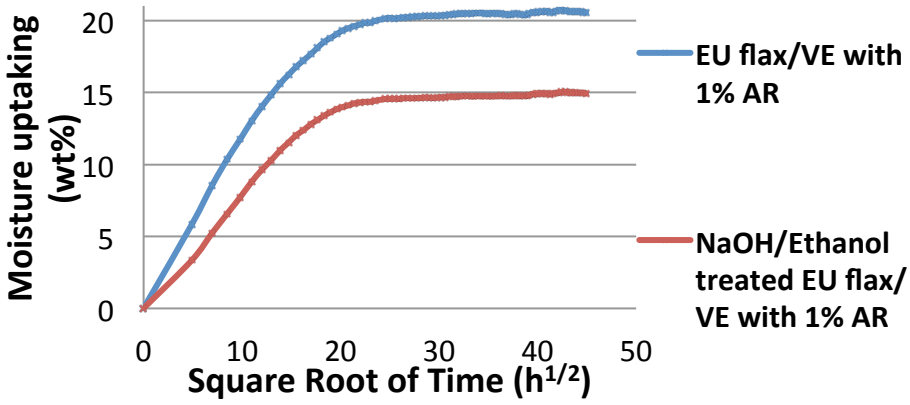

Figure 5.10 Water uptake with time of EU flax/VE with 1% AR composites.

5.4.2. Water Desorption of Composites

Figure 5.11 shows the results of water desorption of untreated and NaOH treated flax/VE with 1% AR composites, which are consistent with the results of water absorption. Untreated flax composites lost the largest amount of moisture during the testing, which is about 20.08%. NaOH treated flax composites lost about 15.23%. The trend of the water desorption results is consistent with the results of the moisture absorption tests.

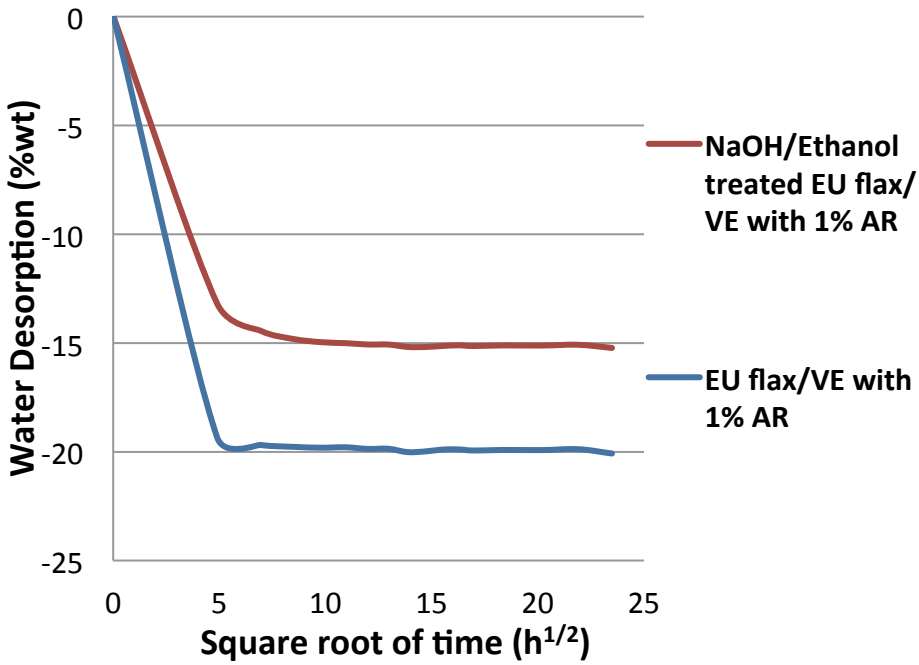

Figure 5.11 Water desorption with time of untreated, NaOH treated EU flax/VE with 1% AR.

5.4.3. Flexural Properties with Moisture Absorption

Table 5.9 and Fig 5.12 show the specific flexural properties of untreated, treated flax composites with different amount of water absorption. All the flexural properties of all fiber reinforced composites show decreasing with certain amount of water absorption. All the flexural strength and modulus of flax/VE composites after moisture absorption show a dramatic decrease. The moisture resistance for the flax composites treated will limited their application.

The specific modulus of flax composites with 4~5% water uptake shows approximate 75% decreasing than the original dry flax/VE. The specific modulus of NaOH/Ethanol treated flax/VE-AR with 4~5% water uptake reduces about 77% than the dry samples. The reduction of treated flax composites is slightly higher than untreated flax composite. Alkaline treatment increases the contact area between fiber and matrix, which provide good interfacial bonding in the composite. However, the fiber is highly hydrophilic, especially after the hydrophobic substances, such as wax, has been removed by alkaline treatment. With the same amount of water absorption, the damage on the fiber and interface is higher than untreated flax composites.

The drop in flexural strength of the flax composites after moisture absorption is smaller than flexural modulus of the composites. The specific flexural strength of untreated flax composites with 4~5% water uptake is 46% lower than the original ones and NaOH treated flax composites with 4~5% water uptake shows about 43% decreasing compared to the dry samples. However, with approximate 5% water uptake the flexural properties of flax composites are reduced at least close to 50%. The dramatic drop of the flexural properties with 4~5% water uptake can limit the application of flax/VE composites. In the future study, the improvement of moisture resistance should be investigated.

Table 5.9 Comparison of Flexural Properties of flax/VE Composites with Moisture Uptake

Sample	Original			4%~5% Water Uptake		
	Specific Flexural Strength MPa/(g/cm^3)	Specific Flexural Strength GPa/(g/cm^3)	V_f 100%	Specific Flexural Strength MPa/(g/cm^3)	Specific Flexural Strength GPa/(g/cm^3)	V_f 100%
Flax/VE with 1% AR	216.98±19.75	28.75±1.23	49.10	116.92±9.61	7.17±0.22	47.44
NaOH/Ethanol treated Flax/VE with 1% AR	264.32±14.12	26.95±1.98	47.06	149.15±6.12	8.73±0.46	46.94

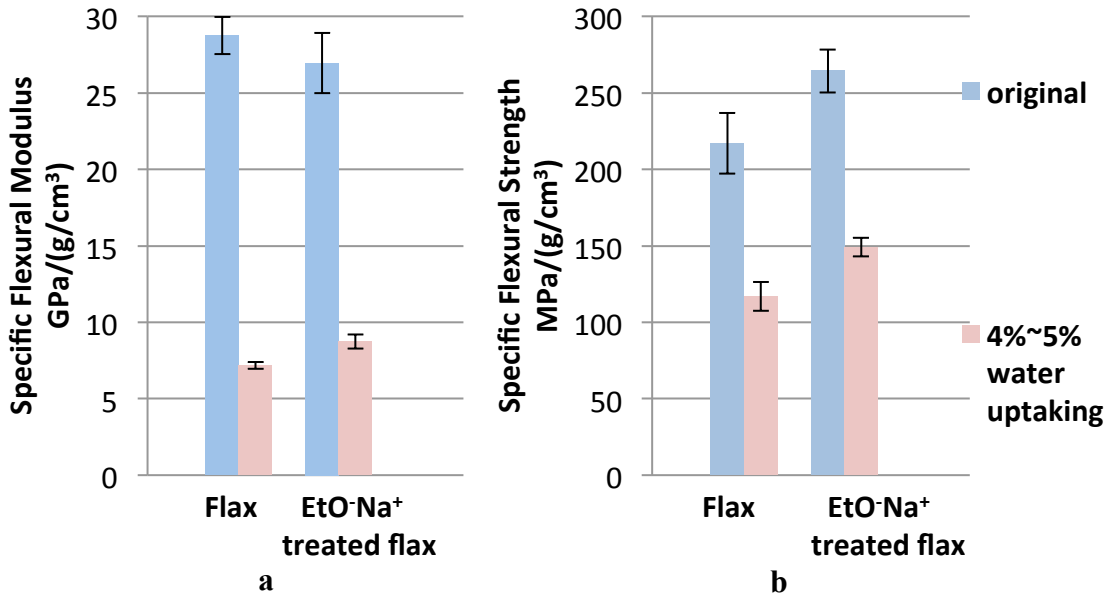

Figure 5.12 Specific flexural properties of flax composites with different amount of water absorption: a) specific flexural modulus; b) specific flexural strength.

CHAPTER 6. EFFECTS OF THERMAL RESIDUAL STRESSES ON THE INTERFACIAL PROPERTIES OF COMPOSITES

6.1. Optimal Elastic Properties of Flax/VE Composites

In Chapter 3, the theoretical longitudinal elastic modulo of untreated and treated flax with/without voids have been calculated. The Young's modulus of neat VE is 3.66 GPa according to the information from AOC resins. The fiber volume fraction of flax/VE composites for tensile tests in this study is listed in Appendix C. Thus, assuming the interfacial bonding between flax and VE is perfect and there are no voids or misalignment of flax, the optimal/ultimate elastic modulus of flax/VE composites can be calculated using Eqn. (6-1). The theoretical longitudinal elastic moduli of different flax/VE composites are presented in Table 6.1.

$$E_c = E_f V_f + E_m V_m \tag{6-1}$$

Table 6.1 Theoretical Elastic Moduli of Flax/VE Composites with Different Fiber Volume Fraction

Sample	Elastic Modulus (GPa)	Fiber Volume Fraction (%)
Untreated flax with voids	49.91	-
Untreated flax without voids	51.73	-
NaOH/Ethanol treated flax with voids	59.02	-
NaOH/Ethanol treated flax without voids	62.39	-
Neat VE	3.66	-
Untreated flax with voids/VE	24.80	45.71
Untreated flax without voids/VE	25.63	45.71
Untreated flax with voids/VE	25.31	46.82
Untreated flax without voids/VE	26.17	46.82
Untreated flax with voids/VE	26.94	50.34
Untreated flax without voids/VE	27.86	50.34
NaOH/Ethanol treated flax with voids/VE	28.64	45.13
NaON/Ethanol treated flax without voids/VE	30.16	45.13
NaOH/Ethanol treated flax with voids/VE	28.90	45.59
NaON/Ethanol treated flax without voids/VE	30.44	45.59
NaOH/Ethanol treated flax with voids/VE	29.35	46.40
NaON/Ethanol treated flax without voids/VE	30.91	46.40

The experimental results of elastic modulus of flax/VE are list in Table 6.2. The elastic modulus of untreated flax/VE is about 21% lower than the theoretical result of untreated flax with voids/VE composites and 24% lower than the theoretical results of untreated flax without voids/ VE composites. However, the tested elastic modulus of untreated flax/VE with 1% AR is approximately 2% higher than the theoretical result of untreated flax without voids/VE composites. For alkaline treated flax composites, the experimental results of elastic modulus of NaOH/Ethanol treated flax/VE are lower than the theoretical results. The tested tensile modulus of NaOH/Ethanol treated flax/VE with 1% AR is equivalent to the theorectical result of alkaline treated flax with voids/VE composites and only about 5% lower than the theorectical elastic modulus of alkaline treated flax without voids/VE composites. Moreover, the longitudinal Young's moduli of alkaline treated flax/VE with 1.5% AR composites is approximately 28% higher than the theroretical result alkaline treated flax without voids/VE composites. AR additive can increase the crosslink density and the elastic modulus of VE resin, which has been confirmed by the results of DMA and tensile tests in Chapter 4. However, if the increase in elastic modulus in NaOH/Ethanol treated CHN Flax/VE with 1% AR is because that AR improves the elastic modulus of VE resin, Young's modulus of VE with 1.5% AR should be 18.02 GPa, which is more than five times increase compared to the elastic modulus of VE. Moreover, the increase in elastic modulus is limited by chemical components in VE resin, which has been confirmed by other researchers [80]. On the other hand, the interfacial properties of alkaline treated flax/VE with 1.5% AR shows better performance than other composites (Chapter 5). Therefore, the effects of AR additive in the composites are not only increasing the elastic properties of VE and the wettability between flax and VE (proved in Chapter 4), but improving the interfacial bonding, especially the mechanical interlocking between flax and VE matrix, by changing the thermal residual stresses in the composites.

Table 6.2 Experimental Elastic Moduli of Flax/VE Composites

Sample	Elastic Modulus (GPa)	Fiber Volume Fraction (%)
Untreated CHN Flax/VE	21.13±1.77	50.34
Untreated CHN Flax/VE with 1% AR	26.14±2.61	45.71
Untreated CHN Flax/VE with 1.5% AR	30.63±5.74	46.82
NaOH/Ethanol treated CHN Flax/VE	28.63±1.61	45.59
NaOH/Ethanol treated CHN Flax/VE with 1% AR	29.46±7.09	46.40
NaOH/Ethanol treated CHN Flax/VE with 1.5% AR	38.61±2.97	45.13

6.2. Residual Stresses in Flax/VE Composites

The stresses calculated in the Al powder are assumed to be equivalent to the residual stresses in the matrix generated by the curing (Eqn. (6-2)), which are equivalent to the results in Table 5.7.

$$\sigma_{Al}^{Residual} = k\sigma_{M}^{Residual} \tag{6-2}$$

The thermal strains generated from the matrices are calculated by generalized Hooke's law, which are also equivalent to the results in the Table 5.8. Coefficients of thermal expansion of VE and VE with 1% AR have been measured by DMA in Chapter 4. The principal residual stresses and strains in different VE systems and their CTEs are presented in Table 6.3. It is observed that the residual stresses σ_{11}^{R} and σ_{22}^{R} in VE with 1% AR show decrease compared to those residual stresses in neat VE system. σ_{11}^{R} is parallel to the longitudinal direction of the flax fiber, which is not related to the interface between fibers and matrix. σ_{22}^{R} is one of the transverse directions, which is related to the misfitting of thermal expansion between flax and VE matrix. σ_{33}^{R} is not only generated by the thermal expansion in the composites, but related the external loading during the processing of the composites panels. Moreover, the external force applied on 33 direction is about 1 metric ton, which introduces a large influence on σ_{33}^{R}. Thus, σ_{22}^{R} is the one which can explain the relationship between thermal residual stresses and interfacial adhesion in the flax/VE composites. These residual stresses are related to the interaction between VE and Al inclusions and are the local stresses around

Al. Accordingly, the residual stresses around flax fiber are determined by the interaction between flax and VE.

AR additive increase the coefficient of thermal expansion of cured VE system, which is 21.46 μm/m•°C. CTE of Al inclusion is 22.4 μm/m•°C and is close to CTE of modified VE system. It is known that the thermal residual stresses are generated by the mismatching of CTEs of VE and Al inclusion. The increase in CTE of modified VE reduces the difference in thermal expansion/contract between VE and Al inclusion. Thus, both residual stresses σ_{11}^{R} and σ_{22}^{R} in VE with 1% AR show decrease compared to neat VE system.

Table 6.3 Coefficients of Thermal Expansion in the Flax/VE composites

Sample	α_M (μm/m•°C)	σ_{11}^{R} (MPa)	σ_{22}^{R} (MPa)	σ_{33}^{R} (MPa)	ε_{11}^{R} (10^{-6})	ε_{22}^{R} (10^{-6})	ε_{33}^{R} (10^{-6})
VE in Flax/VE	19.66	26.58	53.63	-47.79	0.023	0.058	-0.075
VE in Flax/VE with 1% AR	21.46	13.45	37.72	-27.87	0.0075	0.034	-0.038

6.3. Effects of Thermal Residual Stresses on the Interfacial Properties in Composites

CTE of treated flax in transverse direction is -299.1 μm/m•°C, which was measured by TMA in Chapter 3. Flax fibers shrink in transverse direction when the temperature raise, which is opposite to VE resin and Al inclusion. Thus, AR additive actually enlarge the difference of CTE between VE and flax in transverse direction. There are three steps in the curing process of VE system. In the first step, the initiator (peroxide) generates the free radicals to start the polymerization in VE resin. The second step is the growth of the polymer chains, which the temperature of the system starts to raise because this chemical reaction is an exothermic process. The third step is the termination of the chains' growth and the temperature of VE system is still much higher than room temperature. After VE cured, the temperature of the composite panel starts to decrease to the room temperature. During the cooling process, VE matrix starts to shrink in all directions and flax fiber begins to expand in transverse directions. The thermal behaviors of flax fiber and VE on the interface during the

cooling are sketched in Fig. 6.1. The blue arrows indicate the direction of the expansion of flax fiber during the cooling and the red arrows stand for the direction of the contraction of VE.

In the section 6.2, the changes of residual stresses in unmodified and modified VE at the local area surround Al inclusion were discussed. AR additive increases the CTE of modified VE system and reduces the mismatching between VE and Al inclusion, which causes the reduction of residual stresses in the matrix. It helps to predict that the residual stresses in the matrix around flax fibers increases in the modified VE. As Fig. 6.1 shown, the local stresses on the interface of flax VE should be compressive stresses, generated by the thermal expansion/contraction behavior. These thermal residual compressive stresses push flax fibers and VE matrix towards each other and increase the mechanical interlocking, which improves the interfacial adhesion between flax and VE.

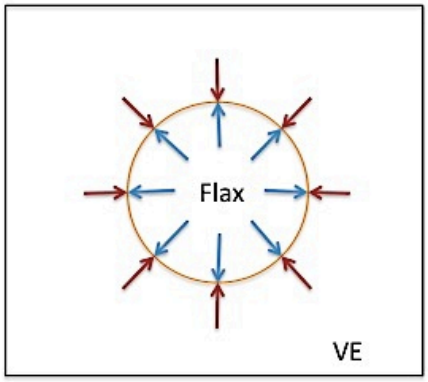

Figure 6.1 The thermal behaviors of flax and VE on the interface.

AR additive increases the coefficient of thermal expasion of VE, which enlarges the thermal contraction of VE system during the cooling. The compressive stresses on the interface of flax/VE with AR composites can also increase, which causes stronger mechanical interlocking between flax and VE. The interlaminar shear strength and elastic moduli of flax/VE with AR composites are higher than others confirms the improvement on the

interfacial adhesion between flax and VE (Chapter5). However, the interfacial properties of flax/VE composites in this study are discussed at room temperature. If the specimens are tested at an elevated temperature, the interfacial properties of flax/VE composites should decrease because of the decrease of thermal residual stresses in transverse direction.

Considering the effects of the coefficients of thermal expansion of flax and VE system, it is easy to predict the mechanical interaction between flax and VE on the interface of their composites. By changing CTE of VE can simply improve the interfacial adhesion of flax/VE composites. There are several methods to measure the coefficient of thermal expansion of VE system and they are simple and cost saving. It provides a direction from mechanical aspect to manipulate resin system to enhance the interfacial properties of the flax composites.

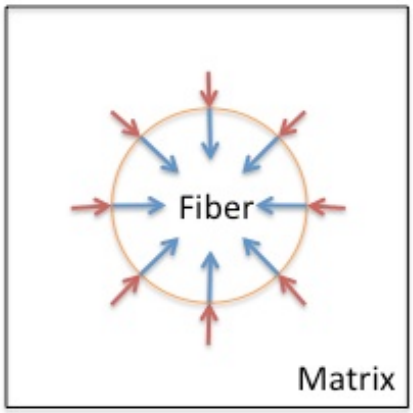

Figure 6.2 The thermal behaviors of fiber and polymer matrix on the interface.

On the other hand, if both the reinforced fiber and polymer matrix contract with the decrease of temperature (Fig. 6.2), increasing the coefficient of thermal expansion of polymer matrix to generate compressive thermal residual stresses can also improve the interfacial properties of their composites. If both the reinforced fiber and polymer matrix expand with the decrease of temperature, reducing the CTE of polymer matrix to produce compressive

thermal residual stresses can improve the interfacial adhesion of its composites. However, this method is constricted by the application temperature of the composites.

CHAPTER 7. CONCLUSIONS AND RECOMMENDATIONS FOR FUTURE WORK

In this work, the physical and chemical properties of Chinese linen flax were assessed and the effects of different chemical modifications to the surface of flax on their composites were evaluated. A systematic profile of Chinese linen flax was provided. In addition, the techniques that can be applied to study cellulosic fibers for the purpose to use as reinforcement to composites was provided. A new method to manipulate the vinyl ester system with acrylic resin was developed, which can improve the mechanical properties of flax/VE composites, especially the interfacial properties. Moreover, the approach to manufacture flax/VE composites, which has high elastic properties and good interfacial properties, was invented. The combination of alkaline treamtent on flax fiber and AR manipulated VE have excellent interfacial properties and mechanical performance. The specific interlaminar shear strength of alkaline treated flax/VE with 1.5% AR shows approximately 149% increase than untreated flax/VE composites and about 15% higher than alkaline treated flax/VE composites. NaOH/Ethanol treated flax/VE with AR shows 33% higher in specific flexural modulus and 73% better in specific flexural strength than untreated flax/VE composites. In addition, AR modified alkaline treated flax composites performs approximately 75% better in specific tensile modulus and 201% higher in specific tensile strength than untreated flax/VE composites. The experimental elastic modulus of flax/VE with 1% AR was shown close to the theoretical elastic modulus of flax/VE composites. The tested elastic modulus of flax/VE with 1.5% AR is even higher than the theoretical results. Both types of flax/VE composites show better performance on the interfacial properties. Moreover, alkaline treatment, the chemical modification applied on flax surface, is a cost saving method and the VE manipulation is very easy to apply.

The study of residual stresses in the composites by X-ray diffraction technique provided a new method to evaluate the interfacial properties of cellulosic composites and show the effects of thermal expansion/contraction of both fiber and resin on their interfacial adhesion. There are plenty of studies which show how chemical bonding, wettability and processing methods influence the mechanical performance of cellulosic fibers. However, this is the first time the thermal properties of flax and VE were taken into account to analyze the interfacial properties. This provides a more comprehesive information about the physical and chemical factors, which can affect the interfacial properties of unidirectional cellulosic fiber reinforced thermoset composites.

The theory of changing (increase or reducing) the coefficient of thermal expansion of VE system by adding AR can be applied to other thermoset resin systems. With the knowledge of the thermal properties of cellulosic fiber and resin system, a cost, time-efficency modification method can be easily developed. However, the precondition of the resin manipultation is that the modification shows minimum affect on the mechanical properties of the resin system.

For the future work, the thermal properties study on other cellulosic composites should be investigated. With enough experimental results on thermal properties and interfacial properties, the theoretical model between the thermal properties and interfacial properties in the cellulosic fiber composites should be developed. Finally, the study of moisture resistantance of cellulosic composites should be investigated, which play an important rule on the application and service life of cellulosic composites.

REFERENCES

1. J. Holbery, D. Houston. Natural-Fiber-Reinforced Polymer Composites in Automotive Applications. *JOM* 58: 80-86, 2006
2. M. Carus. Bio-composites. Technologies and Applications. *Nova-Institute* 2010
3. A. K. Mohanty, M. Misra, L. T. Drzal, Natural Fibers, Biopolymers, and Biocomposites, CRC Taylor & Francis 2005
4. P. A. Fowler, J. M. Hughes, R. M. Elias. Review Biocomposites: technology, environmental credentials and market forces. *Journal of the Science of Food and Agriculture* 86: 1781-1789, 2006
5. B. Z. Jang. Advanced Polymer Composites: Principles and Applications. ASM International. Material Park 1994
6. K. K. Chawla. Composite Materials Science and Engineering. Springer-Verlag 2001 2nd Edition
7. E. Kvavadze, O. Bar-Yosef, A. Belfer-Cohen, E. Boaretto, N. Jakeli, Z. Matskevich, T. Meshveliani. 30,000-Year-Old Wild Flax Fibers. *Science* 325, 1359, 2009
8. C. Baley. Analysis of the Flax Fibres Tensile Behaviour and Analysis of the Tensile Stiffness Increase. *Composites: Part A* 33, 939-948, 2002
9. G. Bogoeva-Gaceva, M. Avella, M. Malinconico, A. Buzarovska, A. Grozdanov, G. Gentile, M.E. Errico. Natural Fiber Eco-Composites. *Polymer Composites* 28, 98-107, 2007
10. A. K. Bledzk, J. Gassan. Composites Reinforced with Cellulose Based Fibres. *Progress in Polymer Science* 24, 221-274, 1999
11. A. Mustata. Factors Influencing Fiber-Fiber Friction in the Case of Bleached Flax. *Cellulose Chemistry and Technology* 31, 405-413, 1997

12. T. P. Nevell, S. H. Zeronian. Cellulose Chemistry and its Applications. Ellis Harwood Limited, 1987

13. R. H. Atalla, D. L. Vander Hart. Native Cellulose. A Composites of Two Distinct Crystalline Forms. *Science* 223, 283-285, 1984

14. M. Wada, J. Sugiyama, T. Okano. Two Crystalline Phase (I_α/I_β) System of Native Cellulose in Relation to Plant Phylogenesis. *Journal of the Japan Wood Research Society* 41, 186-192, 1995

15. H. Yamaoto. Structural Changes of Native Cellulose Crystals Induced by Annealing in Aqueous and Acidic Solutions at High Temperatures. *Macromolecules* 22, 4130-4132, 1989

16. R. Hori, M. Wada. The Thermal Expansion of Cellulose II and Cellulose III_{II} Crystals. *Cellulose* 13, 281-290, 2006

17. Q. Zhang, V. Bulone, H. Agren. A Molecular Dynamics Study of the Thermal Response of Crystalline Cellulose I_β. *Cellulose* 18, 207-221, 2011

18. I. V. Weyenberg, T. H. Truong, B. Vangrimde, I. Verpoest. An Improving the Properties of UD Flax Fibre Reinforced Composites by Applying an Alkaline Fibre Treatment. *Composite Part A* 37, 1368-1376, 2006

19. M. Z. Rong, M. Q. Liu, Y. Liu, G. C. Yang, H. M. Zeng. The Effect of Fiber Treatment on the Mechanical Properties of Unidirectional Sisal-reinforced Epoxy Composites. *Composites Science and Technology* 61, 1437-1447, 2001

20. M. J. John, R. D. Anandjiwala. Recent Developments in Chemical Modification and Characterization of Natural Fiber-reinforced Composites. *Polymer Composites* 29, 187-207, 2008

21. S. Goutianos, T. Peijs, B. Nystrom, M. Skrifvars. Development of Flax Fibre based Textile Reinforcements for Composite Applications. *Applied Composite Material* 13, 199-215, 2006

22. Shanshan Huo. The Effects of Chemical Treatments on Interfacial Properties of Flax Fiber Reinforced Composites. MS Thesis. *North Dakota State University*, 2010

23. http://blog.sina.com.cn/s/blog_40b1323b0100buwm.html (Accessed September 9, 2009)

24. B. C. Barkakaty. Some Structural Aspects of Sisal Fibers. *Journal of Applied Polymer Science* 20, 2921-2940, 1976

25. George Marsh. Vinyl Ester–the Midway Boat Building Resin. *Reinforced Plastics*, Spetember:20-23, 2007

26. Sebastien Taillemite, Rick Pauer. Bright Future for Vinyl Ester Resins in Corrosion Application. *Reinforced Plastics*, May:34-37, 2009

27. Timothy F. Scott, Wayne D. Cook, John S. Forsythe. Kinetics and Network Structure of Thermally Cured Vinyl Ester Resins. *European Polymer Journal*, 38:705-716, 2002

28. X. Dirand, B. Hilaire, E. Lafontaine, B. Mortaigne, M. Nardin. Crosslinking of vinyl ester matrix in contact with different surfaces. *Composite*, 25 (7):645-652, 1994

29. Gaur B, Rai JSP. Curing and Decomposition Behavior of Vinyl Ester Resins. *Polymer,* 33(19):4210-4214, 1992

30. M. B. Launikitis. Vinylester Resin. *Handbook of Composites*, 3:38-49, 1982

31. K. S. Anseth, C. N. Bowman. Kinetic Gelation Predictions of Species Aggregation in Tertrafunctional Monomer Polymerization. *Journal of Polymer Science Part B: Polymer Physics*, 33:1769-1780, 1995

32. L. Rey, J. Duchet, J. Galy, H. Sautereau, D. Vouagner, L. Carrion. Structural Heterogeneities and Mechanical Properties of Vinyl/dimethacrylate Networks Synthesized by Thermal Free Radical Polymerisation. *Polymer*, 43:4375-4384, 2002

33. Timothy F. Scott, Wayne D. Cook, John S. Forsythe. Effect of the Degree of Cure on the Viscoelastic Properties of Vinyl Ester Resins. *European Polymer Jornal*, 44:3200-3212, 2008

34. L. A. Utracki. *Polymer Blends Handbook*, Kluwer Academic Publishers, 2002

35. V. Antonucci, A. Cusano, M. Giordano, J. Nasser, L. Nicolais. Cure-induced Residual Strain Build-up in a Thermoset Resin. *Composites: Part A* 37:592-601, 2006

36. Youming Cao, Dehong Yu, Liang Chen, Jun Sun. Internal Stress of Modified Epoxy Resins with Polyester. *Polymer Testing* 20:685-692, 2001

37. Zhang Boming, Yang Zhong, Sun Xinyuang. Measurement and Analysis of Residual Stresses in Single Fiber Composite. *Materials and Design*, 31:1237-1241, 2010

38. Jakob Lange Saffan Toll, Jan-Anders E. Manson. Residual Stress Build-up in Thermoset Films Cured above their Ultimate Glass Transition Temperature. *Polymer*, 36(16):3135-3141, 1995

39. Patricia P. Parlevliet, Harald E. N. Bersee, Adriaan Beukers. Residual Stresses in Thermoplastic Composites – A Study of the Literature – Part I: Formation of Residual Stresses, *Composites: Part A*, 37:1847-1857, 2006

40. Adriana Mustata. Factors Influencing Fiber-fiber Friction in the Case of Bleached Flax. *Cellulose chemistry and technology*, 31:405-413, 1997

41. Ronald P. Nimmer. Fiber-matrix Interface Effects in the Presence of Thermally Induced Residual Stresses. *Journal of composites technology and research*, 12, (2):65-75, 1990

42. Roderick D. Sweeting, Rodney S. Thomson. The Effect of Thermal Mismatch on Z-pinned Laminated Composite Structures. *Composite structures*, 66:189-195, 2004

43. Yunfa Zhang, Zihui Xia, Fernand Ellyin. Evolution and Influence of Residual Stresses/strains of Fiber Reinforced Laminates. *Composites science and technology*, 64:1613-1621, 2004

44. J.K. Kim, Y.W. Mai. Residual Stresses. In: Engineered Interfaces in Fiber Reinforced Composites. *Oxford: Elsevier Science Ltd.* 1998, 308-320

45. J. A. Barnes, G. E. Byerly. The Formation of Residual-stresses in Laminated Thermoplastic Composites. *Composites Science and Technology*, 51(4):479-494, 1994

46. N. J. Rendler, I. Vigness. Hole-drilling-strain Gage Method of Measuring Residual Stress. *Experimental mechanics*, 1966 SESA Spring Meeting :577-586, 1966

47. R. Y. Kim, H. T. Hahn. Effect of Curing Stresses on the First Ply-failure in Composite Laminates. *Journal of composite materials*, 13:2-16, 1979

48. Harold E. Gascoigne. Residual Surface Stresses in Laminated Cross-ply fiber-epoxy Composite Materials. *Experimental mechanics*, March:27-36, 1994

49. H. Dannenberg. Determination of Stresses in Cured Epoxy Resins. *SPE journal*, July: 669-675, 1965

50. P. G. Ifju, X. Niu, B. C. Kilday, S.-C. Liu, S. M. Ettinger. Residual Strain Measurement in Composites using the Cure-referencing Method. *Experimental mechanics*, 40(1):22-30, 2000

51. J. A. Nairn, P. Zoller. Matrix Solidification and the Resulting Residual Thermal-stresses in Composites. *Journal of Material Science*, 20(1):355-367, 1985

52. R. J. Young, R. J. Day. M. Zakikhani, I. M. Robinson. Fiber Deformation and Residual Thermal Stresses in Carbon Fibre Reinforced PEEK. *Composite Science and Technology*, 34(3):243-258, 1989

53. S. K. Wang, D. P. Kowalik, D. D. L. Chung. Self-sensing attained in Carbon-fiber-polymer-matrix Structural Composites by Using the Interlaminar Interface as a Sensor. *Smart Materials and Structures*, 13(3):570-592, 2004

54. Barrett CS, Predecki P. Stress Measurements in Graphite/epoxy Uniaxial Composites by X-rays. *Polymer composites,* 1:2-6, 1980

55. K. Shivakumar, A. Bhargava. Failure Mechanics of a Composite Laminate Embedded with a Fiber Optic Sensor. *Journal of Composite Materials*, 39(9):777-798, 2005

56. B. Benedikt, M. Kumosa, P. K. Predecki, L. Kumosa, M. G. Castelli, J. K. Sutter. An Analysis of Residual Thermal Stresses in a Unidirectional Graphite/PMR-15 Composite Based on X-ray Diffraction Measurements. *Composite Science and Technology*, 61(14):1977-1994, 2001

57. B. D. Cullity, S. R. Stock. Elements of X-ray Diffraction. *Prentice Hall.* Third Edition. 2001

58. V. Hauk. Structural and Residual Stress Analysis by X-ray Diffraction on Polymeric Materials and Composites. *Advances in X-ray Analysis*, 42:540-554, 2000

59. H. Dőlle. The Influence of Multiaxial Stress States, Stress Gradients and Elastic Anisotropy on the Evaluation of (Residual) Stresses by X-rays. *Journal of Applied Crystallography*,12:489-501, 1979

60. Danut Dragoi. Residual stress analysis of graphite/polyimide composites using the concept of metallic inclusions. *PhD Dissertation*. 1999

61. T. W. Clyne, P. J. Withers. An Introduction to Metal Matrix Composites. *Cambridge University Press*, 1992

62. Ján Široký, Richard S. Blackburn, Thomas Bechtold, Jim Taylor, Patrick White. Crystallinity Changes in Lyocell Following Continuous Treatment with Sodium Hydroxide. *Cellulose* 17,103-115, 2010

63. H.K. Goering and P.J. Van Soezt. Forage Fiber Analysis. *Agr. Handbook* 379, ARS, USDA 1970

64. R. Herrera-Saldana and J.T. Huber. J. Dairy Sci. 72, 1477, 1989

65. Jensen WA. Botanical Histochemistry – Principles and Practice. University of California, Barkeley. *W. H. Freeman and Company*. 1962

66. Jinyong Lee, Lawrence T. Drzal. Surface Characterization and Adhesion of Carbon Fibers to Epoxy and Polycarbonate. *International Journal of Adhesion and Adhesives* 25, 389-394, 2005

67. R. Malkapuram, V. Kumar. Recent Development in Natural Fiber Reinforced Polyporpylene Composits. *Journal of Reinforced Plastics and Composites* 28, 1169-1189, 2008

68. A. K. Bledzki, S. Reihmane, J. Gassan. Properties and Modification Methods for Vegetable Fibers for Natural Fiber Composites. *Journal of Applied Polymer Science* 50, 1329-1336, 1996

69. L. Y. Mwaikambo, M. P. Ansell. Chemical Modification of Hemp, Sisal, Jute, and Kapok Fibers by Alkalization. *Journal of Applied Polymer Sciences* 84, 2222-2234, 2002

70. D. L. Pavia. Introduction to Spectroscopy. *Brooks/Cole, Cengage Learning: Belmont*, CA, 2009

71. A. J. Michell. Second Derivative F.T.-I.R. Spectra of Cellulose I and II and Related Mono- and Oligo-Saccharides. *Carbohydrate Research* 173, 185-195, 1988

72. Jan B. Kristensen, Lisbeth G. Thygesen, Claus Felby, Henning Jørgensen, Thomas Elder. Cell-wall Structural Changes in Wheat Straw Pretreated for Bioethanol Production. *Biotechnology for Biofuels* 1, 1, 2008

73. Oh S.Y., Yoo D.I., Shin Y., Kim H.C., Kim H.Y., Chung Y.S., Park W.H., York J.H. Crystalline Structure Analysis of Cellulose Treated with Sodium Hydroxide and Carbon Dioxide by Means of X-ray Diffraction and FTIR Spectroscopy. *Carbohydrate Research* 340, 2376-2391, 2005

74. J. C. Halpin, S. W. Tsai. Effects of Environmental Factors on Composite Materials. AFML-TR 67-423, Dayton, OH, June 1969

75. Jochen Gassan, Andris Chate, Andrzel K Bledzki. Calculation of Elastic Properties of Natural Fibers. *Journal of Materials Science* 36, 3715-3720, 2001

76. R. Kessler, U. Becker, R. Kohler, B. Goth. Steam Explosion of Flax a Superior Technique for Upgrading Fibre Value. *Biomass and Bioenergy* 14, 237-249, 1998

77. P. Hornsby, E. Hinrichsen, K. Tarverdi. Preparation and Properties of Polypropylene Composites Reinforced with Wheat and Flax Straw Fibers. Part II: Analysis of Composite Microstructure and Mechanical Properties. *Journal of Materials Science* 32, 1009-1015, 1997

78. N. Barkoula, S. Garkhail, T. Peijs. Effect of Compounding and Injection Molding on the Mechanical Properties of Flax Fiber Polypropylene Composites. *Journal of Reinforced Plastics and Composites* 29, 1366-1385, 2009

79. A. Stamboulis, C. Bailie, T. Peijs. Effects of Environmental Conditions on Mechanical and Physical Properties of Flax Fibers. *Composites Part A: Applied Science and Manufacturing* 32, 1105-1115, 2001

80. Schwanninger, M.; Rodrigues, J. C.; Pereira, H.; Hinterstoisser, B. Short-time Vibratory Milling of Wood and Cellulose: Effects on the Shape of FT-IR Spectra. *Vibrational Spectroscopy* 36, 23-40, 2004

81. V. Hauk. Structural and Residual Stress Analysis by Nondestructive Methods. *Elsevier Science B. V.* 1997

82. H. Li. Synthesis, Characterization and Properties of Vinyl Ester Matrix Resin. *Virginia Polytechnic Institute and State University*. 1998

APPENDIX A

Table A-1 Constituent Content of European Flax and Canadian Flax

Sample	Dry Matter %	Ash %	Crude Protein %	Cellulose %	Hemi-cellulose %	Lignin %	Crude Fat %
Untreated European Flax	97.43	1.19	2.39	80.42	9.85	2.30	0.22
NaOH/Ethanol treated European Flax	95.85	0.62	0.70	90.37	5.63	0.79	0.09
Untreated Canadian Flax	93.30	2.36	4.08	66.99	10.29	6.13	2.44
NaOH/Ethanol treated Canadian Flax	95.77	1.38	1.53	84.19	4.99	6.15	0.50

Table A-2 Comparison of Mechanical Properties of Canadian Flax/VE Composites

Sample	Interlaminar Shear Strength (MPa)	Interfacial Shear Strength (MPa)	Flexural Modulus (GPa)	Flexural Strength (MPa)	Tensile Modulus (GPa)	Tensile Strength (MPa)	Density (g/cm^3)	Fiber Volume Fraction (%)
Untreated Canadian Flax/VE	9.02±1.53	11.81±0.73	15.16±0.38	141.69±7.76	27.75±2.41	70.61±10.34	ILSS, Flexural 1.12±0.04 Tensile 1.22±0.03	35.69 37.57
Untreated Canadian Flax/VE with 1% AR	10.14±1.57	12.22±1.27	13.19±1.07	127.43±5.86	27.18±0.80	80.20±6.76	ILSS, Flexural 1.19±0.01 Tensile 1.08±0.05	36.33 35.06
EtO^-Na^+ treated Canadian Flax/VE	11.38±2.29	20.74±2.89	17.41±1.72	173.83±17.47	38.23±6.70	101.74±9.57	ILSS, Flexural 1.19±0.04 Tensile 1.19±0.03	36.63 37.34
EtO^-Na^+ treated Canadian Flax/VE with 1% AR	15.50±5.47	17.67±1.18	15.28±1.09	162.57±11.44	35.79±4.90	104.71±10.47	ILSS, Flexural 1.12±0.01 Tensile 1.21±0.06	33.27 34.98

APPENDIX B

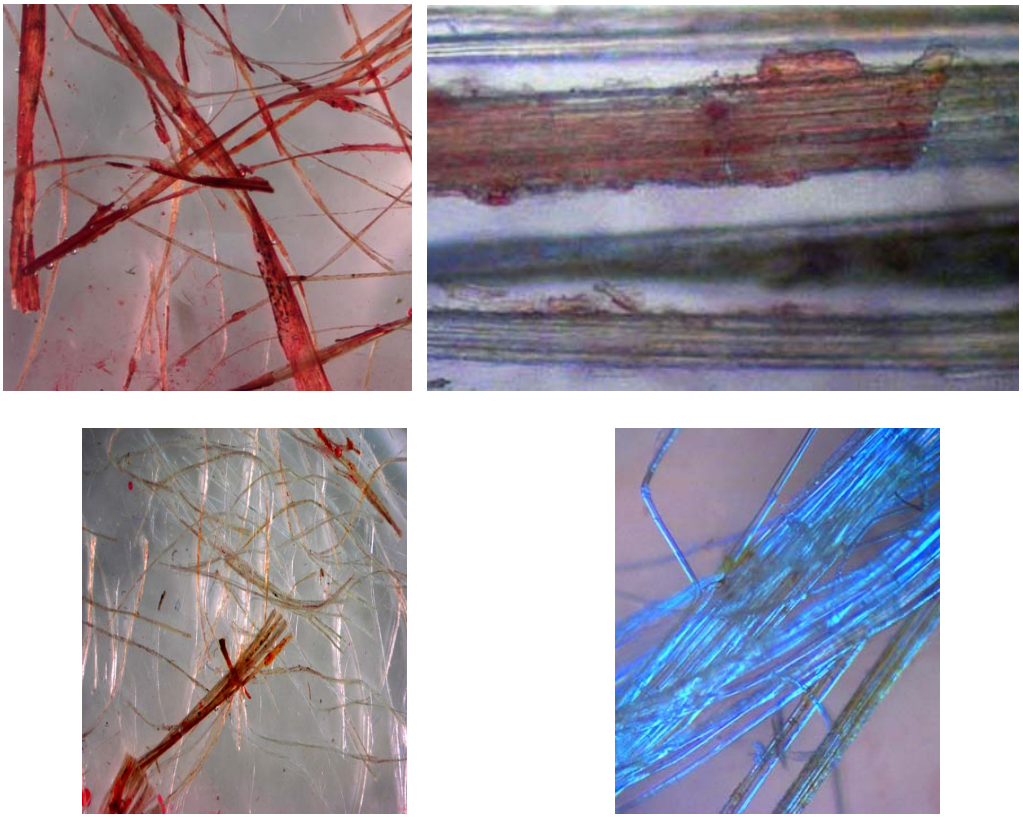

Figure B-1. Fiber from Canadian linseed flax stained with oil red O for cuticle. Upper left: stereoscope image of untreated; upper right: light microscope image of untreated; lower left: stereoscope image of NaOH-treated; lower right: light microscope image of NaOH-treated. The presence of red-stained cuticle covering bast fibers is prevalent on the untreated fibers, whereas NaOH removes most all the cuticle exposing fibers and fiber bundles. The red color in treated fibers in the stereoscope image is mostly oil red stain that has not washed out.

APPENDIX C

Table C-1 Density and Fiber Volume Fraction of Various Flax/VE Composites

Density test	Density (g/cm^3)	Fiber Volume Fraction
Untreated Flax fiber	1.42±0.02	
Untreated Flax/VE (ILSS)	1.27±0.01	41.72%
Untreated Flax/VE (tensile)	1.27±0.05	50.34%
Untreated Flax/VE (3-point bend)	1.29±0.02	45.12%
Untreated Flax/VE with 1% AR (ILSS, 3-point bend)	1.28±0.02	44.00%
Untreated Flax/VE with 1% AR (tensile)	1.27±0.03	45.71%
Untreated Flax/VE with 1.5% AR (ILSS, 3-point bend)	1.21±0.04	39.18%
Untreated Flax/VE with 1.5% AR (tensile)	1.27±0.04	46.82%
NaOH/Ethanol treated Flax/VE (ILSS)	1.33±0.03	44.28%
NaOH/Ethanol treated Flax/VE (tensile)	1.29±0.07	45.59%
NaOH/Ethanol treated Flax/VE (3-point bend)	1.32±0.03	40.91%
NaOH/Ethanol treated Flax/VE with 1% AR (ILSS, 3-point bend)	1.32±0.02	44.65%
NaOH/Ethanol treated Flax/VE with 1% AR (tensile)	1.33±0.01	46.40%
NaOH/Ethanol treated Flax/VE with 1.5% AR (ILSS, 3-point bend)	1.30±0.01	40.24%
NaOH/Ethanol treated Flax/VE with 1.5% AR (tensile)	1.32±0.02	45.13%
10% VE resin THF treated Flax/VE (ILSS)	1.32±0.04	45.34%
3% AR THF treated Flax/VE (ILSS)	1.26±0.01	50.89%